THE JOURNAL
OF
CHEMICAL PHYSICS

VOLUME 16, NUMBER 12 DECEMBER, 1948

Cation Arrangement in Spinels

E. J. W. VERWEY, F. DE BOER, AND J. H. VAN SANTEN
Natuurkundig Laboratorium der N. V. Philips' Gloeilampenfabrieken, Eindhoven, Nederland

(Received June 21, 1948)

RECENTLY values were given for the Madelung constant for various types of spinels,[1] this constant being determined by the expression for the total Coulomb energy of the ionic crystal per "molecule" XY_2O_4:

$$V = -\tfrac{1}{2}(e^2/a)(pM_{\text{tetr.}} + 2qM_{\text{oct.}} + 8M_0) = -M(e^2/a).$$

In this expression ep and eq are the ionic charges at tetrahedral and octahedral interstices and $M_{\text{tetr.}}$, $M_{\text{oct.}}$, and M_0 are the local Madelung constants determining the electrostatic potential at the tetrahedral and octahedral interstices and at the O^{2-} lattice points respectively. A recalculation of these M-values (owing to war conditions the details of the computations were completely lost) revealed that there had been an error in part of the calculations. The new values are given in Table I below. We also give now the values for the local Madelung constants.

Columns I contain the values according to the Evjen summation method (calculated earlier by E. L. Heilmann). As mentioned in our previous paper[1] these values contain a systematic error due to the circumstance that the outer face of the cube cut-out of the crystal carries an electric dipole layer. This electric double layer is caused by the fact that in the spinel crystal lattice successive atomic planes (100) contain alternatively an excess of positive and negative charges. The necessary correction can be estimated, however, by calculating the electrical

TABLE I.

Parameter	Charge		$M_{\text{tetr.}}$			$M_{\text{oct.}}$			M_0			M	
u	p	q	I	II	III	I	II	III	I	II	III	II	III
	4	2	28.07	24.94	25.01	11.86	15.00	14.98	17.69	14.55	14.55	138.1	138.2
0.375	2	3	19.10	17.53	17.57	16.42	17.99	17.97	15.84	14.27	14.27	128.6	128.6
	3	2½	23.59	21.23	21.29	14.14	16.49	16.47	16.76	14.41	14.41	130.7	130.8
	4	2	26.82	23.68		13.09	16.23		17.14	14.00		135.8	
0.380	2	3	17.84	16.27		17.66	19.23		15.92	14.35		131.4	
	3	2½	22.33	19.97		15.38	17.73		16.53	14.17		131.0	
	4	2	25.65	22.50		14.33	17.47		16.57	13.42		133.6	
0.385	2	3	16.67	15.10		18.90	20.47		15.94	14.37		134.0	
	3	2½	21.16	18.80		16.61	18.97		16.25	13.90		131.2	
	4	2	24.56	21.41		15.56	18.71		15.96	12.82		131.5	
0.390	2	3	15.58	14.01		20.13	21.70		15.92	14.35		136.5	
	3	2½	20.07	17.71		17.85	20.20		15.94	13.59		131.4	

[1] E. J. W. Verwey and E. L. Heilmann, J. Chem. Phys. **15**, 174 (1947).

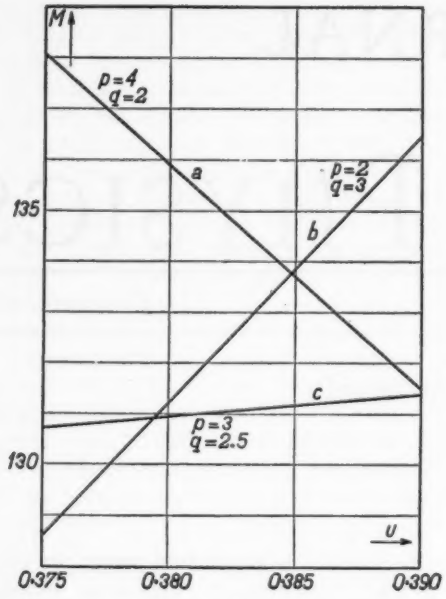

FIG. 1.

potential drop across this double layer for an infinitely large plane. Columns II contain the Evjen values corrected in this way.

Columns III contain, for the ideal case that the parameter is $u=0.375$, the values of $M_{\text{tetr.}}$, $M_{\text{oct.}}$, M_0, and of the total Madelung potential, calculated according to Ewald's method. It is seen that the agreement between the Ewald values (III) and the corrected Evjen values (II) is very satisfactory. This justifies the procedure used to calculate the values of columns II, also for other parameter values.

A discussion of the relative electrostatic stability of different spinel arrangements on the basis of the new M values is slightly more complicated because such a comparison cannot be given without a more careful consideration of the influence of the parameter values.

Most of the spinels investigated are of the 2–3 type. It appears that for this spinel type the conclusions concerning the relative stability of normal and inversed spinels remain the same as in our previous paper. Figure 1 shows the values of M as a function of the parameter u for different values of p and q. A comparison of the curves for $p=2$, $q=3$ (normal arrangement of the cations, curve b) with that for $p=3$, $q=2\frac{1}{2}$ (inversed arrangement of the cations, curve c) shows that for $u>0.379$ the electrostatic potential is largest for the normal arrangement. The experimental parameter values of all known normal spinels of the 2–3 type are within the region 0.380–0.390, for most of them even >0.385. Moreover we must consider that the parameter values of the normal spinels will generally be slightly larger than those of the corresponding inverse spinels, because in the first case a larger (divalent) ion occupies the tetrahedral interstice. Hence we may again conclude that 2–3 spinels have the highest electrostatic stability in the normal cation arrangement (X^{2+} in the tetrahedral position Y^{3+} in octahedral position).

For 4–2 spinels the available data are scanty. Moreover the lack of accuracy of these u-values does not permit definite conclusions. According to the new M values a relative stability of the inverse 4–2 spinel (curve a), on the basis of a purely electrostatic picture of the chemical bond, can only be expected if $u>0.385$.

THE JOURNAL OF CHEMICAL PHYSICS VOLUME 16, NUMBER 12 DECEMBER, 1948

The Scattering of Light and the Radial Distribution Function of High Polymer Solutions

BRUNO H. ZIMM
Department of Chemistry, University of California, Berkeley, California

(Received June 2, 1948)

A radial distribution function of polymer segments in a solution of a high polymer may be defined as a quantity proportional to the density of segments at a given distance from some given segment. An approximate expression is derived for this function for dilute solutions of chain molecules of moderate degrees of polymerization. By Fourier inversion a simple expression for the intensity of light scattering, as a function of angle and concentration, may be obtained.

I. INTRODUCTION

THE following work describes briefly the theoretical derivation of some equations connected with the phenomenon of light scattering from solutions of thread-like molecules.* The use of these equations in handling experimental data is described in a succeeding paper.

A radial distribution function, $\rho(r)$, for polymer segments in a polymer solution may be defined by the statement that $nN\rho(r)d\tau/V$ is the probability of finding the center of some segment within the volume element $d\tau$ at a distance r from some other arbitrarily chosen segment, given that there are N polymer molecules of n segments each in a total volume V. By "segment" is meant an arbitrary small portion of the chain of a thread-like molecule. In the ensuing discussion it will be assumed that all the segments in the solution have the same constitution and size, also that all molecules have the same degree of polymerization n.

When a dilute solution of such a nature is illuminated by a parallel beam of light, the excess scattering (over that of the solvent alone) will be given by the well-known formula,

$$I(\vartheta)=\frac{kn^2N^2}{V^2}\int\rho(r)\exp\left(\frac{2\pi i\mathbf{s}\cdot\mathbf{r}}{\lambda}\right)d\tau. \quad (1)$$

In this equation, $I(\vartheta)$ is the intensity of excess scattering per cubic centimeter, ϑ is the angle between the incident and scattered rays, $\mathbf{s}$ the vector difference between unit vectors in the directions of the incident and scattered rays, λ the wave-length. The integration goes over all orientations as well as magnitudes of $\mathbf{r}$ at constant $\mathbf{s}$. The magnitude of $\mathbf{s}$ is found to be $2\sin(\vartheta/2)$. The factor K contains the electromagnetic constants of the material and a function of the angle of scattering. If the incident light is unpolarized, K is proportional to $1+\cos^2\vartheta$. If the incident beam is plane-polarized, K is proportional to $\sin^2\varphi$, where φ is the angle between the direction of scattering and the normal to the direction of the incident beam in the plane of vibration of the electric vector.

Aside from its intrinsic interest as a property of the solution, the radial distribution function $\rho(r)$ has value, therefore, because of its connection with the light scattering phenomenon. A good approximation to $\rho(r)$, for an *isolated* chain molecule, Eq. (5) below, has been known for some time, and has been used to derive the expression for the light scattering from such a molecule.[1,2] In this paper we will attempt to extend the work to a pair of chain molecules, obtaining in this way an expression for light scattering applicable to polymer solutions at concentrations high enough to be accessible to direct experimental observation.

II. SEPARATION OF $\rho(r)$ INTO INTERNAL AND EXTERNAL PARTS

A segment in the vicinity of another reference segment may belong either to the same or to a different molecule. Accordingly, the probability of finding a segment, defined above as $nN\rho(r)d\tau/V$,

* A preliminary report of these results has already appeared in J. Phys. and Coll. Chem. 52, 260 (1948).

[1] P. Debye, J. Phys. and Coll. Chem. 51, 18 (1947).
[2] B. Zimm, R. S. Stein, and P. Doty, Polymer Bull. 1, 90 (1945).

may be divided into two parts, as follows:

$$\frac{nN\rho(r)d\tau}{V}=\left[\rho_1(r)+\frac{N\rho_2(r)}{V}\right]nd\tau. \quad (2)$$

The first term, the internal part of $\rho(r)$, denotes the probability of finding a segment of the same molecule as the reference segment; the second term, the external part, denotes the probability of finding a segment of a different molecule.

The first step in obtaining $\rho_1(r)$ is to define $W_{ij}(r)d\tau$ as the probability of finding the jth segment at distance r from the ith segment and in the volume element $d\tau$. The theory of random flights[3] gives for this probability the formula:

$$W_{ij}(r)d\tau=\left(\frac{3}{2\pi b^2(|i-j|)}\right)^{\frac{3}{2}} \times\exp\left(\frac{-3r^2}{2b^2(|i-j|)}\right)d\tau, \quad (3)$$

where b is a constant which depends on the architecture of the chain. By comparison of the definitions, it may be seen that $\rho_1(r)$ is related to $W_{ij}(r)$ by the summation:

$$n\rho_1(r)=\frac{2}{n}\sum_{i>j}\sum\left(\frac{3}{2\pi b^2(i-j)}\right)^{\frac{3}{2}} \times\exp\left(\frac{-3r^2}{2b^2(i-j)}\right). \quad (4a)$$

Replacing the summation by integration and substituting the variable $z=i-j$ leads by simple transformations to the following equation:

$$n\rho_1(r)=2\int_0^n\left(\frac{n-z}{n}\right)\left(\frac{3}{2\pi b^2 z}\right)^{\frac{3}{2}} \times\exp\left(\frac{-3r^2}{2b^2z}\right)dz. \quad (4b)$$

Placing this formula for $\rho_1(r)$ in Eq. (1) and integrating, the "internal" part of $I(\vartheta)$ may be obtained.[1,2] The function that is involved will be called $P(\vartheta)$ in this paper:

$$P(\vartheta)=\int\rho_1(r)\exp\left(\frac{2\pi i\mathbf{s}\cdot\mathbf{r}}{\lambda}\right)d\tau =\frac{2}{u^2}(e^{-u}-1+u), \quad (5)$$

where

$$u=\frac{8\pi^2}{3}\frac{b^2n}{\lambda^2}\sin^2\frac{\vartheta}{2}.^{**}$$

III. THE EXTERNAL PART OF $\rho(r)$

It is now proposed to investigate $\rho_2(r)$. We first define a function $F_2\{(1),(2)\}$ of the coordinates (1) and (2) of the two molecules 1 and 2 such that $(1/V^2)F_2\{(1),(2)\}d(1)d(2)$ is the probability that these two molecules have the configurations indicated by the particular values of the coordinates (1) and (2) within the range symbolized by $d(1)$ and $d(2)$.

The distribution function of two *particular* segments, μ_1 from the first molecule and ν_2 from the second, is obtained by integrating $(1/V^2)F_2\{(1),(2)\}d(1)d(2)$ over the coordinates of all the other segments of the two molecules, holding the relative coordinates of μ_1 and ν_2 fast. The resulting integral will be a function only of $\mathbf{r}_{\mu\nu}$, the vector connecting the segments μ_1 and ν_2, if the internal coordinates of μ_1 and ν_2 may be ignored.

The probability $(nN/V)\rho_2(r)d\tau$, defined above, may now be obtained by summing the integral over all pairs of segments μ_1 and ν_2 and multiplying by a numerical factor.

$$\frac{nN\rho_2(r)}{V}=\frac{N}{nV}\sum_1^n\mu_1\sum_1^n\nu_2 \times\int F_2\{(1),(2)\}d(1)d(2-\mathbf{r}_{\mu\nu}). \quad (6)$$

The symbol $d(2-r_{\mu\nu})$ is intended to indicate that the integration, as mentioned above, is to be carried over all coordinates except the relative coordinates of segments μ_1 and ν_2.

In general, the distribution function $F_2\{(1),(2)\}$ is very complex. It attains a simpler form at infinite dilution, however. In the following para-

[3] See, for example, S. Chandrasekkar, Rev. Mod. Phys. 15, 1 (1943).

** The integration is very readily effected in Cartesian coordinates.

graphs we shall work with this limiting form, which will lead to an expression for the light scattering correct to the second power of the concentration. Consideration of the succeeding approximations will be deferred until the final section.

The limit of $F_2\{(1), (2)\}$ as the concentration is indefinitely decreased will be designated $F_2^*\{(1), (2)\}$. The corresponding limit for $\rho_2(r)$ will be $\rho_2^*(r)$.

In a previous paper[4] it was postulated that two thread-like molecules most commonly interact with each other by touching at only one place, so that only one segment from each molecule is involved at one time. If this is so, it is possible to approximate $F_2^*\{(1), (2)\}$ as a product of the internal distribution functions of the molecules, $F_1(1)$ and $F_1(2)$, and a sum of segment interaction functions, $\chi(\kappa_1, \lambda_2)$:

$$F_2^*\{(1), (2)\} = F_1(1)F_1(2) \times[1+\sum_1^n \kappa_1 \sum_1^n \lambda_2\chi(\kappa_1, \lambda_2)]. \quad (7)$$

The functions $F_1(i)$ are defined as follows:

> $\frac{1}{V}F_1(i)d(i)$ is the probability that the molecule i has the configuration symbolized by (i) in the hypervolume element $d(i)$.

The functions $\chi(\kappa_1, \lambda_2)$ were discussed in the previous work (4). It is only important here that they are the same for all pairs of segments and that they vanish whenever the distance between the pair of segments involved is much greater than the size of the segments themselves.

We must note that in using this formula configurations in which more than one segment from each molecule are interacting are explicitly ignored. In order for this approximation to be reasonable it is at least necessary that the segments themselves be long and threadlike. Since the segments are arbitrarily chosen, subject only to the restriction that they be much smaller than the whole molecule (and also, as will be seen, much smaller than the wave-length λ), it is not unduly restrictive that they be long and threadlike.

Eq. (7) may now be introduced into Eq. (6) for $\rho_2(r)$. Further, remembering that the functions $\chi(\kappa_1, \lambda_2)$ are short-range functions while $F_1(1)$ and $F_1(2)$ vary relatively slowly with (1) and (2), the integral may be factored to yield the following approximate expression:

$$n^2\rho_2^*(r) = n^2+\sum_1^n \mu_1 \sum_1^n \kappa_1 \sum_1^n \lambda_2 \sum_1^n \nu_2 \times\int\Big[\int F_1(1)d(1-\mathbf{r}_{\kappa\lambda})\Big] \times\Big[\int F_1(2)d(1-\mathbf{r}_{\lambda\nu})\Big] \times\Big[\int \chi(\mathbf{r}_{\kappa\lambda})d\mathbf{r}_{\kappa\lambda}\Big]d\tau_\kappa. \quad (8)$$

The symbols $\int\cdots d(1-r_{\mu\nu})$ etc., indicate that the integration is to extend over all the coordinates of molecule 1 except the relative coordinates of segments κ and μ_1, etc. A more complete discussion of this type of integral has been given on page 177 of reference 4.

It can be seen that $\int F_1(1)d(1-\mathbf{r}_{\lambda\mu})$ is the distribution function of the segments κ_1 and μ_1 relative to one another and hence is given by Eq. (3) with κ and μ in place of i and j, respectively, and $r_{\kappa\mu}$ in place of r. A similar formula holds for $\int F_1(2)d(2-r_{\lambda\nu})$. The integral $\int \chi(r_{\kappa\lambda})dr_{\kappa\lambda}$ has the same value for all pairs of segments κ and λ; it will be designated by the symbol X for brevity.

When these results are introduced in (8), $\rho_2^*(r)$ becomes:

$$\rho_2^*(r) = 1+\frac{X}{n^2}\left(\frac{3}{2\pi b^2}\right)^{\frac{3}{2}} \times\sum_\mu \sum_\kappa \sum_\lambda \sum_\nu [1/(|\mu-\kappa|)(|\nu-\lambda|)]^{\frac{3}{2}} \times\int \exp\left(\frac{-3r_{\kappa\mu}^2}{2b^2(|\mu-\kappa|)}\right) \times\exp\left(\frac{-3r_{\kappa\nu}^2}{2b^2(|\nu-\lambda|)}\right)d\tau_\kappa. \quad (9)$$

In this formula it has been recognized that the coordinates of segment κ_1 must be nearly the same as those of segment λ_2, since $\chi(\kappa_1, \lambda_2)$ vanishes if this is not so. Therefore, the coordinates of κ_1 and λ_2 have explicitly been made identical.

[4] B. Zimm, J. Chem. Phys. **14**, 164 (1946).

It is now convenient to consider the light-scattering problem, which requires the evaluation of the integral:

$$\int \rho_2^*(r) \exp\left(\frac{2\pi i \mathbf{s}\cdot\mathbf{r}}{\lambda}\right) d\tau. \qquad (10)$$

Fortunately, this may be expressed in terms of the function $P(\vartheta)$ already calculated in Eq. (5).

In any term of the sum in (9), $\mathbf{r}=\mathbf{r}_{\kappa\mu}+\mathbf{r}_{\kappa\nu}$, since $\mathbf{r}$ is the vector between the two segments from the different molecules, which in the given term are the segments μ_1 and ν_2. Considering this fact, Eq. (10) may be rewritten:

$$\int \rho_2^*(r) \exp\left(\frac{2\pi i \mathbf{s}\cdot\mathbf{r}}{\lambda}\right) d\tau$$

$$= \int \exp\left(\frac{2\pi i \mathbf{s}\cdot\mathbf{r}}{\lambda}\right) d\tau + \frac{27X}{(2\pi b^2)^3 n^2}$$

$$\times \sum_{\mu}\sum_{\kappa}\sum_{\lambda}\sum_{\nu}\left(\frac{1}{(|\mu-\kappa|)(|\nu-\lambda|)}\right)^{\frac{1}{2}}$$

$$\times\left[\int \exp\left(\frac{-3r_{\kappa\mu}^2}{2b^2(|\mu-\kappa|)}+\frac{2\pi i \mathbf{s}\cdot\mathbf{r}}{\lambda}\right) d\tau_\mu\right]$$

$$\times\left[\int \exp\left(\frac{-3r_{\kappa\nu}^2}{2b^2(|\nu-\lambda|)}+\frac{2\pi i \mathbf{s}\cdot\mathbf{r}_{\kappa\nu}}{\lambda}\right) d\tau_\nu\right]. \qquad (11)$$

The first term of (11) may be neglected except for very small angles of scattering when s is also very small. The second part of the expression may be factored into two factors, each of which is similar to Eq. (5).

$$\int \rho_2^*(r) \exp\left(\frac{2\pi i \mathbf{s}\cdot\mathbf{r}}{\lambda}\right) d\tau$$

$$= X\left\{\frac{1}{n}\left(\frac{3}{2\pi b^2}\right)^{\frac{3}{2}} \sum_{\kappa}\sum_{\mu}\frac{1}{(|\mu-\kappa|)^{\frac{3}{2}}}\right.$$

$$\left.\times \int \exp\left(\frac{-3r^2}{2b^2(|\mu-\kappa|)}+\frac{2\pi i \mathbf{s}\cdot\mathbf{r}}{\lambda}\right) d\tau\right\}$$

$$\times\left\{\frac{1}{n}\left(\frac{3}{2\pi b^2}\right)^{\frac{3}{2}} \sum_{\lambda}\sum_{\nu}\frac{1}{(|\nu-\lambda|)^{\frac{3}{2}}}\right.$$

$$\left.\times \int \exp\left(\frac{-3r^2}{2b^2(|\nu-\lambda|)}+\frac{2\pi i \mathbf{s}\cdot\mathbf{r}}{\lambda}\right) d\tau\right\}$$

$$= n^2 X P^2(\vartheta). \qquad (12)$$

Finally, the use of (12) and (5) in (1) gives the expression for the intensity of the light scattered by a unit volume of solution as

$$I(\vartheta) = \frac{kn^2N}{V}\left[P(\vartheta)+\frac{Nn^2X}{V}P^2(\vartheta)\right]. \qquad (13a)$$

If conversion is made to the usual concentration units, weight per unit volume, so that $c=NM/VN_0$, where M is the molecular weight of the chain molecule, (13b) is obtained,

$$I(\vartheta) = Kc[MP(\vartheta) - 2A_2M^2P^2(\vartheta)c], \qquad (13b)$$

where $A_2=-N_0n^2X/2M^2$, with N_0 Avogadro's number, and $K=n^2k/M^2$.

Comparison with Eq. (7) shows that

$$A_2 = -\frac{N_0}{2M^2V}\int [F_2\{(1),(2)\} - F_1(1)F_1(2)]d(1)d(2). \qquad (14)$$

It is already known,[4,5] however, that if the osmotic pressure Π of the solution is represented as a power series in the concentration, A_2 is the coefficient of the second power.

$$\Pi = RT[(c/M)+A_2c^2+A_3c^3+\cdots]. \qquad (15)$$

Analogously, the first terms of the expression for the reciprocal of the intensity of the scattered light, multiplied by c, are:

$$[Kc/I(\vartheta)] = [1/MP(\vartheta)]+2A_2c. \qquad (16)$$

It will be shown later that expression (16) is a good approximation to the true state of affairs at much higher concentrations than its reciprocal, expression (13b). When ϑ is zero, $P(\vartheta)$ is unity, and (16) is seen to be the derivative of the osmotic pressure over RT with respect to c, in agreement with the well-known results from fluctuation theory.[6]

The simplicity of this result is noteworthy. The intercept of the plot of $[Kc/I(\vartheta)]$ *vs.* c depends on ϑ, but the initial slope does not.

The approximation which is most likely to have a serious effect on this result is that the

[5] W. G. McMillan and J. E. Mayer, J. Chem. Phys. **13**, 276 (1945).

[6] S. Bhagavantam, *The Scattering of Light and Raman Effect* (Chemical Publishing Company, Brooklyn, New York, 1942).

thread-like molecules exert forces on each other through only one segment of each molecule at a time. This may fail especially for very long and highly coiled threads. It remains for experiment or more involved calculations to assess the magnitude of the deviations.

As a corollary to the linear relation (16), it may be remarked that the reciprocal of the quantity which has been called the dissymmetry coefficient, q, should be likewise linear. If ϑ_1 and ϑ_2 are two angles equidistant from the normal to the direction of the incident beam, $q=[I(\vartheta_1)/I(\vartheta_2)]-1$, ϑ_2 being the greater angle. Use of (16) results in the relation

$$\frac{1}{q}=\frac{1}{[q]}+\frac{2A_2MP(\vartheta_1)}{[q]}c, \tag{17}$$

where $[q]$ is the limit q approaches as c approaches zero. Such a linearity has already been observed empirically.[7]

It may be noted that there is nothing in the derivation which restricts the procedure to a coiling chain. If, for instance, the chain were rigid, in the shape of a straight line, the same formulae would hold, provided only that $P(\vartheta)$ is given by:

$$P(\vartheta)=\frac{1}{x}\int_0^{2x}\frac{\sin u}{u}du-\left(\frac{\sin x}{x}\right)^2, \tag{18a}$$

$$x=\frac{2\pi L\sin(\vartheta/2)}{\lambda}. \tag{18b}$$

L is the end-to-end length of the chain and u is a variable of integration. The function

$$\int_0^y(\sin u/u)du$$

is the so-called "integral sine," which may be found in tables of functions.

IV. CONCERNING HIGHER POWERS OF THE CONCENTRATION

In the preceding section the limiting distribution function, $F_2^*\{(1),(2)\}$, was used to obtain an expression for the light scattering valid to the term in the second power of the concentration. In this section a short examination will be made of the nature of some of the higher terms.

The deviations of $F_2\{(1),(2)\}$ from its limiting form at infinite dilution, $F_2^*\{(1),(2)\}$, may be expressed in terms of interactions of the molecules 1 and 2 with other molecules in their neighborhood. Adapting the results of Mayer and Montroll[8] we assume that $F_2\{(1),(2)\}$ is given by the equation,

$$F_2\{(1),(2)\}=F_2^*\{(1),(2)\}\times\{1+\sum_{m\geq 1}H_{2m}\{(1),(2)\}v^{-m}\}, \tag{19}$$

when v is V/N, the volume per molecule, and the $H_{2m}\{(1),(2)\}$ are complicated functions of the coordinates of molecules 1 and 2, as discussed below.

The interaction of two molecules, i and j, at infinite dilution may be conveniently described by a function $g_2^*\{(i),(j)\}$,

$$g_2^*\{(i),(j)\}=F_2^*\{(i),(j)\}-F_1(i)F_1(j). \tag{20}$$

The first coefficient in the sum in (19), $H_{21}\{(1),(2)\}$, will now be given by:

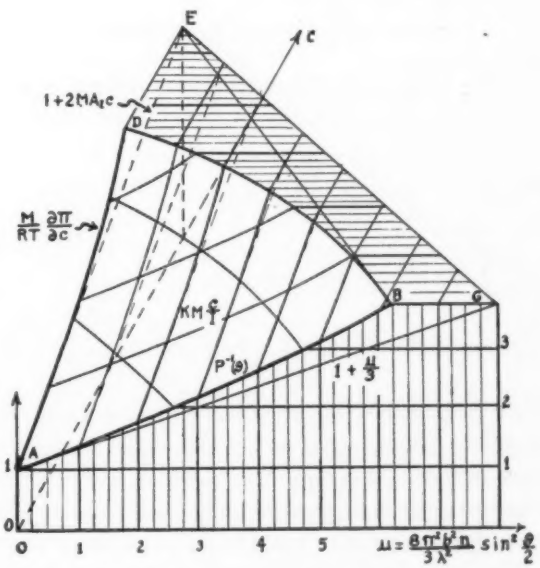

FIG. 1. The reciprocal intensity surface, KMc/I.

[7] P. Doty, W. Affens, and B. Zimm, Trans. Faraday Soc. **42B**, 66 (1946).

[8] J. E. Mayer and E. Montroll, J. Chem. Phys. **9**, 2 (1941), Eqs. (40), (44), and (52).

$$H_{21}\{(1),(2)\}=\int g^*\{(1),(3)\}g^*\{(2),(3)\}d(3)$$
$$+\int g^*\{(1),(2)\}g^*\{(1),(3)\}$$
$$\times g^*\{(2)(3)\}d(3). \quad (21)$$

Considering for the moment the first integral in (21), comparison with the preceding section shows that we must evaluate the expression:

$$\sum_1^n \mu_1 \sum_1^n \nu_2 \int \exp(2\pi i\mathbf{s}\cdot\mathbf{r}/\lambda)$$
$$\times g^*\{(1),(3)\}g^*\{(2),(3)\}d(1)d(2)d(3). \quad (22)$$

If the position of one of the segments, ξ_3, of 3 is chosen as origin of coordinates, and $\mathbf{s}\cdot\mathbf{r}_{\mu\nu}=\mathbf{s}\cdot\mathbf{r}_{\mu\xi}+\mathbf{s}\cdot\mathbf{r}_{\xi\nu}$, then (22) divides into two factors, one containing the integration over $d(1)$ and the other over $d(2)$, in a form somewhat similar to Eq. (12). The final result is to introduce a term $4A_2^2P^4(\vartheta)c^2$ into Eq. (13b).

The second integral in (21) resists this method of attack, at least if applied rigorously. In recognition of this irreducibility, it has been used to define[4,5] a quantity, A_3, which has already appeared in Eq. (15),

$$A_3=-\frac{N_0^2}{3M^3V}\int g^*\{(1),(2)\}g^*\{(2),(3)\}$$
$$\times g^*\{(1),(3)\}d(1)d(2)d(3). \quad (23)$$

For the light scattering problem, we must now define a new function, $Q(\vartheta)$, by the equation:

$$Q(\vartheta)A_3=-\frac{N_0^2}{3n^2M^3V}\Big\{\sum\mu_1\sum\nu_2$$
$$\times\int g^*\{(1),(2)\}g^*\{(2),(3)\}g^*\{(1),(3)\}$$
$$\times\exp(2\pi i\mathbf{s}\cdot\mathbf{r}_{\mu\nu}/\lambda)d(1)d(2)d(3)\Big\}. \quad (24)$$

Since $s=2\sin(\vartheta/2)$ approaches zero as ϑ approaches zero, $Q(0)=1$. The real part of $(\exp(2\pi i\mathbf{s}\cdot\mathbf{r}_{\mu\nu}/\lambda)$ is equal or less than unity for all other values of ϑ, so that $Q(\vartheta)$ must also be less than unity for finite values of ϑ.

The next higher term in the power series for the light scattering results from $H_{22}\{(1),(2)\}$. An analysis similar to the preceding shows that it can be expressed in terms of A_2 and A_3 with $P(\vartheta)$ and $Q(\vartheta)$, plus A_4 in association with a new function of ϑ. It seems profitless, in the present development, to follow the investigation further along this line.

We will now use the preceding results to write an expression for $I(\vartheta)$, correct to the third power of the concentration,

$$I(\vartheta,c)=K\{MP(\vartheta)c-2A_2M^2P^2(\vartheta)c^2$$
$$+[4A_2^2M_2^3P^4(\vartheta)$$
$$+3A_3M_2^2P^2(\vartheta)Q(\vartheta)]c^3+\cdots\}. \quad (25)$$

Taking the reciprocal of (25) leads to the form which converges more rapidly:

$$K\frac{c}{I(\vartheta,c)}=\frac{1}{MP(\vartheta)}+2A_2c$$
$$+[3A_3Q(\vartheta)-4A_2^2P(\vartheta)(1-P(\vartheta))]c^2+\cdots. \quad (26)$$

The right-hand side of Eq. (26) is correct to the second power of c. The coefficients A_2 and A_3 are the same as those appearing in Eq. (15) for the osmotic pressure. The function $Q(\vartheta)$ has not yet been calculated in detail. Since $P(\vartheta)$ and $Q(\vartheta)$ both approach unity as ϑ approaches zero, the right-hand side of Eq. (26) approaches the derivative of Eq. (15) with respect to c as I approaches zero.

V. GRAPHICAL REPRESENTATION OF THE RECIPROCAL INTENSITY FUNCTION

The reciprocal intensity function, Kc/I, depends on the two independent variables of concentration, c, and angle, ϑ. It may be represented by a surface in three-dimensional space, putting MKc/I along the vertical axis and c and ϑ along the horizontal axes. Such a surface is shown in Fig. 1 for the scattering from a coiling chain solute.

The surface, which is somewhat concave, is represented by ABD in the figure. In general, it is tangent at A to the plane AGE, whose boundary AG at the $c=0$ plane is the limiting tangent of $P^{-1}(\vartheta)$, which is $1+u/3$, and whose boundary AE at the plane $\vartheta=0$ is the limiting tangent $1+2MA_2c$. The result peculiar to this study, that A_2 is independent of ϑ, is represented by the fact that the reciprocal intensity surface is tangent along AB to the *cylindrical* surface

ABE, all of whose elements are parallel to the $\vartheta=0$ plane and have the slope $2MA_2$.

Experimental points will generally lie in the interior parts of the surface, while the quantities of interest, molecular length and extension, are only obtainable from the boundary at $c=0$. A process of extrapolation is therefore necessary. Knowledge of the linearity of the surface at small values of c is important in performing the extrapolation properly.

THE JOURNAL OF CHEMICAL PHYSICS VOLUME 16, NUMBER 12 DECEMBER, 1948

Apparatus and Methods for Measurement and Interpretation of the Angular Variation of Light Scattering; Preliminary Results on Polystyrene Solutions

BRUNO H. ZIMM
Department of Chemistry, University of California, Berkeley 4, California

(Received June 2, 1948)

A photoelectric apparatus for the measurement of the angular dependence of light scattering from solutions is described in detail and its performance is discussed. Methods of calculation for the determination of the average extension of the scattering molecules from the data are described. Data are presented for two fractions of polystyrene in various solvents, showing the effect of changing solvent power and temperature, and also confirming a theoretically derived formula for the concentration dependence of the scattering.

I. INTRODUCTION

WHEN light is scattered from a macromolecule, such as a high polymer chain, an intensity distribution results which may be considered as a simple form of interference pattern. From appropriate measurements on the pattern the spatial extension of the molecule may be deduced.

The present paper describes new apparatus for obtaining the intensity distribution of the scattering. Several previous investigators[1,2,3] have also described apparatus for this purpose. The present equipment incorporates some important refinements over the previous types.

Theoretical developments, such as described by Debye[4] and by the author in the preceding paper,[5] are indispensable to the proper interpretation of the raw data. A method of application of the theory is therefore presented in some detail.

Finally, data on polystyrene solutions are given. They seem to confirm the formulae derived in the preceding paper,[5] in addition to having physico-chemical interest of their own.

Although the average spatial extension of the molecules of a polymeric material affects most of its properties, light scattering from dilute solution seems to be the only way this dimension can be unambiguously determined. Approximate relative values can be found in some cases from viscosity measurements. For example, it has long been recognized that the "intrinsic viscosity" of a given polymer is smaller in thermodynamically poor solvents than in good ones, and this effect has been interpreted as indicating a curling up and contraction of the polymer chain in the unfavorable solvent.

An attempt has already been made to compare viscosity and light-scattering measurements of the solvent effect in polystyrene solutions.[6] The results were confusing in that a large change occurred in the viscosity but very little in the light scattering. The measurements have been repeated in part with the new apparatus and the earlier data have been found to be in error by a small but significant amount. In the new meas-

[1] R. S. Stein and P. M. Doty, J. Am. Chem. Soc. **68**, 159 (1946).
[2] P. P. Debye, J. App. Phys. **17**, 392 (1946).
[3] R. Speiser and B. A. Brice, J. Opt. Soc. Am. **36**, 364 (1946).
[4] P. Debye, J. Phys. Coll. Chem. **51**, 18 (1947).
[5] B. Zimm, J. Chem. Phys. **16**, 1093.
[6] P. Doty, W. Affens, and B. Zimm, Trans. Faraday Soc. **42B**, 66 (1946).

urements there is substantial agreement between the viscosity and light-scattering results.

Another effect of interest is the change of the spatial extension of the chains with temperature, since this is related to the relative energies of the different configurations the chain may assume. Some preliminary results on polystyrene are given.

II. APPARATUS

The apparatus described here was built primarily to measure the intensity distribution of light scattered from dilute polymer solutions, the ultimate aim being to determine the extension of the molecules. In considering the design of such apparatus, the following general points may be kept in mind.

When a high polymer solution is illuminated by a beam of parallel and polarized light, the intensity of the scattered light varies smoothly with the angle of scattering. (A typical curve is shown in Fig. 6, curve *D*.) Except in the case of unusually large molecules, most of the variation occurs between the angles of 30° and 150°. The intensity of scattering is always small, of the same order of magnitude as the scattering from the solvent alone, since the solutions must be dilute to minimize intermolecular interferences. Dust specks in the solution are therefore a source of much trouble, especially at small angles where the large dust particles scatter most strongly. In consideration of the foregoing, it is not usually desirable to make measurements at angles close to the incident beam.

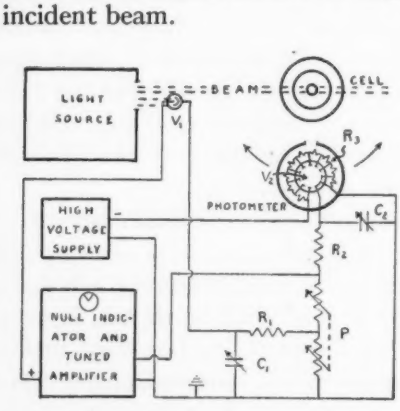

FIG. 1. Block diagram of apparatus.

R_1, R_2, 0.1 megohm
R_3, ten 50,000 ohm resistors in series
C_1, C_2, 500 $\mu\mu$f
V_1, RCA 926
V_2, RCA 931A

Experience has shown that freedom of the solution from foreign particles is the quality that limits the precision of measurement, provided the measuring apparatus itself can attain a precision of one percent or better.

The general specifications on an apparatus are therefore the following: (1) The apparatus should be capable of measurements of the relative intensity of scattering at angles from 30° to 150°, with a resolving power of about 5°; (2) it should make these measurements on liquids whose turbidities are of the order of magnitude of those of the common organic solvents (10^{-4} cm^{-1}), with a precision of at least one percent.

As a primary detector of the scattered light, the recently developed multiplier phototube has important advantages. The output current of this tube is large enough to be measured with ordinary low-impedance equipment (less than 1 megohm), even when the light intensity is of the low order encountered in this investigation. In addition the response characteristic is stable and linear as long as the tube is not exposed to strong light.

To eliminate the effect of fluctuations in the light source, the intensity of the scattered light, as measured by the photomultiplier, may be compared to the intensity of a portion of the incident beam, measured by an ordinary vacuum photocell. The ratio of the currents is readily measured by passing them in opposite directions through a potentiometer.

A complication arises since the photomultiplier has a large dark current from the amplified thermionic emission of the photocathode. The difficulty was avoided by modulating the light at a definite frequency and phase and using only the components of that frequency and phase in the photocurrents. Further amplification is then easy using standard a.c. amplification techniques. Since a mercury arc lamp is naturally modulated at 120 c.p.s. when operated on an a.c. power line, this offers a very convenient way of eliminating the dark current.

1. General Plan

A block diagram of the apparatus is shown in Fig. 1.

The projector emits a beam of monochromatic light, modulated at 120 c.p.s., which passes

through the solution cell. A portion of the beam falls on the vacuum phototube V_1. Light scattered from the sample in the cell illuminates the sensitive photomultiplier tube V_2, which may be moved to receive light scattered at any desired angle.

The a.c. components of the currents from the two photo-cells are 180° out of phase because of the opposite polarity of the two cells. The currents are balanced in the precision potentiometer P by means of the tuned amplifier and electron-ray indicator. When the indicator shows a minimum, the setting of the potentiometer gives the ratio of the currents. The potentiometer readings are therefore proportional to the ratio of the scattered and incident intensities, which is the quantity desired.

The phase-shift networks R_1-C_1 and R_2-C_2 are used to sharpen the balance by compensating for the different capacities of the connecting wires.

The high negative voltage for the photomultiplier is supplied by a high voltage rectifier, while the positive voltage for the other phototube comes from a tap on the power supply of the electron-ray indicator.

2. The Light Source and Projector

A diagrammatic cross section of this part of the apparatus is shown in Fig. 2. The lamp, A, is a 100-watt medium-pressure mercury arc, General Electric Type AH-4. A pair of condensing lenses B forms an image of the lamp on the diaphragm D, thus providing an accessible secondary source whose size and shape may be easily adjusted. The filter C is included to isolate the desired wave-length. An image of the diaphram D is produced in the middle of the solution cell J by the lens G.

Part of the beam is focused on the phototube V_1 by the concave mirror F.[7] The remainder passes through a clear hole in the center of the mirror.

The plastic[8] prism H deviates the beam upward at an angle of eight degrees to compensate for the downward refraction suffered at the solution cell

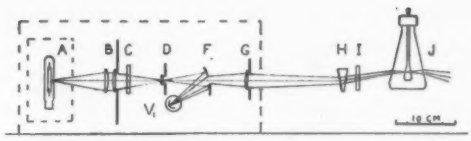

FIG. 2. Projector optical system.

J. By removing the prism a horizontal beam for use with other types of cells is easily obtained.

I is a "Polaroid" disk.

All elements are mounted on a sturdy optical bench and covered by a hood to contain stray light.

Over-all dimensions are indicated in the figure. The sizes of the important apertures are as follows: the lenses B, which serve as aperture stop for V_1, are 30 mm diameter; the opening in diaphram D, serving as field stop of the system, is 6 mm (vertically) by 2 mm (horizontally); the aperture in F, which limits the aperture of the beam to the solution cell, is 15 mm (vertically) by 10 mm (horizontally). The maximum divergence of rays in this beam is about three degrees.

Some explanation of the design considerations may be useful at this point. It is desired to produce a beam of maximum intensity within the limits of the solution cell. The angular divergence of this beam is restricted also within specified limits (three degrees horizontally and five vertically in this case). Given the fixed dimensions of the lamp and solution cell, these conditions are to be achieved by the arrangement of the other elements of the system.

The positions of maximum illumination are images of the source. Therefore, an image of the lamp is focused in the solution cell J. The image is made larger than the cell and stopped down to the proper size by the diaphram D, which also lies at an image of the lamp. In this way the cell is filled with a uniform illumination. The angular divergence is controlled by the aperture of lens G, which is actually determined by F.

The exact dimensions were determined by the materials and space available, within the limits specified by the above conditions.

3. The Solution Cell

The design and preparation of a suitable cell to hold the solution under investigation required more care than any other phase of this work.

[7] The mirror F, which does not require a good figure, was made simply by silvering an ordinary watch glass.

[8] The prism H was easily made with casting resin in a mold of microscope slides. The resin used was "Castolite" (The Castolite Company, Kenilworth, Illinois).

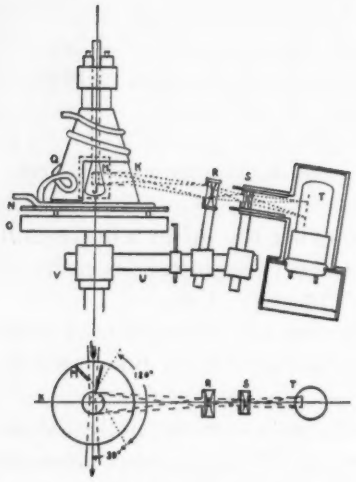

FIG. 3. Detail of solution cell and photometer.

Previous investigations have generally employed long rectangular cells with the beam traversing the long axis. In such a cell it is easy to eliminate stray light, but the volume of solution seen by the photometer changes with the angle of observation and the cell is large and wasteful of solution. Cylindrical cells have also been used, but in such cells multiple reflections of the incident beam occur and are very troublesome at angles other than those close to 90°.

The ideal cell would be small, compact and give by itself negligible scattering so that its whole volume could be observed by the photometer at all angles. It was found possible to approach this ideal by the arrangement shown in Fig. 3. The cell proper J is a thin-walled (0.2 mm) bulb of glass.[9] It is immersed in an outer vessel filled with a liquid of approximately the same refractive index as the solution in the bulb. The conical profiles of the bulb and outer vessel K are chosen to send reflections of the incident beam up or down out of the plane of the photometer, thus avoiding the principal defect of cylindrical cells. The thin walls of the bulb J are necessary to minimize scattering from the glass and foreign particles in it. Immersion in an outer liquid makes possible the small size without significant distortion of the light paths.

The illuminating light is confined to a narrow sharp-edged beam L which crosses the middle of the cell as shown in Fig. 3. The beam is unavoidably surrounded by a halo of diffuse light scattered from the front surface of the outer cell and preceding elements of the optical system. If this halo were allowed to strike the edges of the bulb J, reflections would result which would seriously interfere with measurements of forward scattering. To prevent this, blackened brass shields M are introduced, just outside the main beam, arranged as shown so that they do not interfere with the photometer at angles between 30° and 150°. At angles less than 30° some diffuse light from the edge of the shield M enters the photometer, although the amount is not serious except for the solutions of the lowest scattering power. As will be seen, measurements between 30° and 150° are adequate for most polymer solutions.

The outer vessel K is an ordinary 250 cc. Pyrex Erlenmeyer flask. Here, as in several other places in the optical system, it is unnecessary to have surfaces of high optical quality and very simple pieces of glassware may be used effectively. The outside of all parts of the flask K that do not have to transmit light are covered with black paint. The flask is cemented to a brass plate N. Three brass feet are brazed to the plate position of the assembly automatically by fitting into a set of grooves machined in the table O. The whole cell assembly is thus removable for cleaning and filling but can be replaced accurately and easily.

Partially surrounding K is a heavy copper jacket Q bearing a loop of copper tubing through which heating or cooling water may be passed. A loop of this coil is also soldered to the base plate N. Good thermal contact between the glass and copper was achieved by filling the space with typemetal.

The inner bulb J is held by a brass fitting with three adjustable jaws which rests on the top of the flask K. The top of the flask is squared off by grinding against a flat plate.

The liquid used to fill the flask should not be excessively volatile or corrosive, should have a refractive index close to that of the solution being studied, and should preferably have a low scattering power. Water, which has the lowest scattering power of any of the common liquids, becomes turbid rapidly from microörganisms and is not suitable on this account. 1-propanol,

[9] This bulb is made by heating a portion of a clean and scratch-free piece of 8 mm Pyrex tubing in a blast lamp until soft, then blowing and stretching in one operation an elongated bulb. One end of the bulb is then sealed off.

$n_D = 1.37$, has a relatively low scattering power and makes a substitute for water. Other liquids found suitable are toluene, $n_D = 1.50$, and 1,2-dichloroethane, $n_D = 1.44$. The latter two unfortunately have rather high scattering powers. In any case, it is necessary to clean the liquids carefully to exclude dust.

4. The Photometer

The photometer assembly is also included in Fig. 3.

Scattered light from the cell is received by the objective lens R and an image of the cell is focused on the diaphram at S. The lens S forms an image of the diaphram R on the cathode of the photomultiplier tube T. The diaphram at S serves as the field stop of the photometer, excluding stray light arising in other parts of the optical system, such as especially the places where the beam enters and leaves the flask K and reflections of these spots from the walls. The diaphram at R, which measures 3×10 mm, is the aperture stop of the system. Its image on the photocathode T remains constant in size, shape, and uniformity of illumination as the photometer is moved. Since the photocathode varies in sensitivity over its surface, this constancy is an important consideration.[10]

The phototube is totally enclosed by a brass housing as shown. A cap may be placed over the opening at S to protect the tube from daylight. A compartment also encloses the tube socket and the ten 50,000 ohm resistors which are soldered to it. The tube and its housing may be conveniently removed from the rest of the assembly so that the optical system may be adjusted.

The whole photometer assembly is adjustably mounted on the rod U, which revolves around the central support of the cell assembly on a bearing at V. A graduated scale on the rim of the table O and a pointer on U show the angle of observation.

5. Power Supply

The two milliamperes at 600–900 volts for the photomultiplier tube are supplied by the regulated rectifier shown in Fig. 4. Since this is an adaptation of a well-known circuit, it will not be described completely. Regulation is accomplished by a degenerative pentode circuit, actuated by the variation of the output voltage with respect to a standard potential supplied by the "B" battery.

The resistor R_2 is included to provide negative feedback and diminish the effects of drift in the characteristics of the control tube V_5, which seems to be the main source of instability. Negative feedback would normally reduce the efficiency of regulation, but a compensating over-regulating effect is introduced by connecting the screen grid of V_5 to a tap on the unregulated input voltage. Selection by trial of the proper feedback resistance leads to almost perfect cancellation of these two effects.

It was found desirable to place the "B" battery at some distance from the regulator in an enclosed cupboard to protect it from rapid temperature variations. Another source of instability was eliminated by the use of wire-wound resistors in the voltage control network, as specified in Fig. 4.

The small residual drift occurs mainly in the

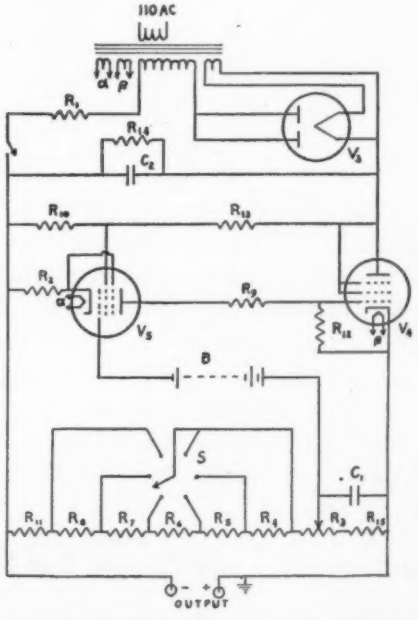

FIG. 4. Regulated high voltage supply.

R_1, 1500 ohms
R_2, 6000 ohms wirewound
R_3–R_8, 10,000 ohms wirewound
R_9, 25,000 ohms
R_{10}, 50,000 ohms
R_{11}, 140,000 ohms wirewound
R_{12}, 250,000 ohms
R_{13}, 500,000 ohms
R_{14}, 1 megohm
R_{15}, 1 megohm wirewound
C_1, 0.01 μf
C_2, 2 μf
V_3, 80
V_4, 6AG7
V_5, 6J7
B, 90 volt "B" battery

[10] It was first attempted to focus the image of the cell directly on the photocathode, but it was soon found that the response of the tube varied by fifty percent when the image changed its shape during the revolution of the photometer about the solution bulb.

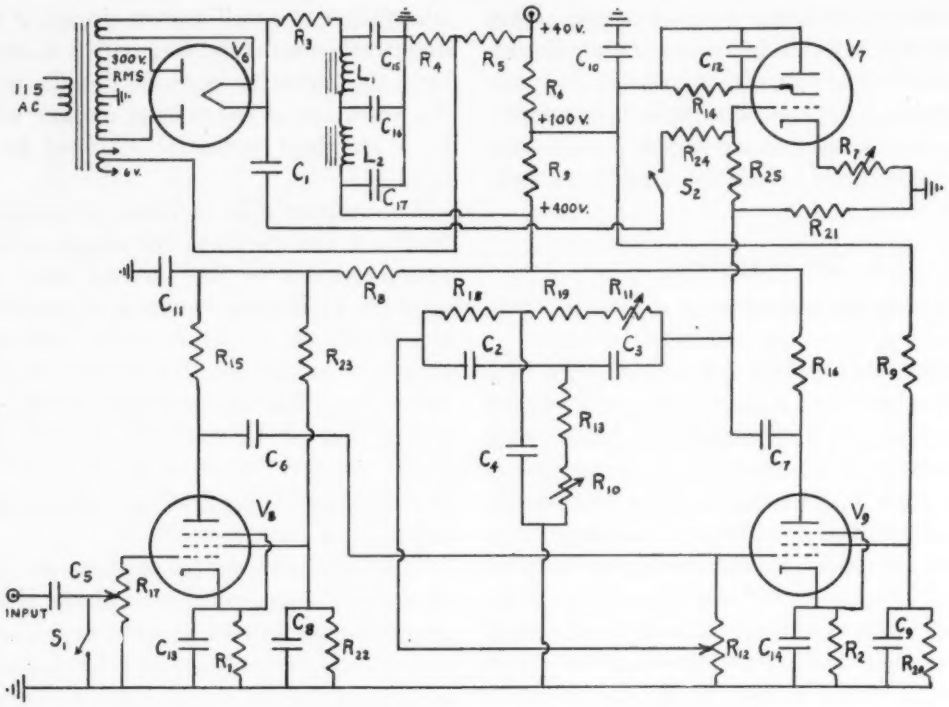

FIG. 5. Narrow-band amplifier and electron-ray indicator.

R_1, R_2, 2250 ohms
R_3, R_4, 5000 ohms
R_5, R_6, 20,000 ohms
R_7, R_8, 50,000 ohms
R_9, R_{10}, R_{11}, 0.1 megohm
R_{12}, R_{13}, 0.25 megohm
R_{14}–R_{18}, 0.5 megohm
R_{19}, 0.75 megohm
R_{20}–R_{22}, 1 megohm
R_{23}, 3 megohm
R_{24}, 5 megohm
R_{25}, 10 megohm

C_1, 250 $\mu\mu$f
C_2, C_3, 2500 $\mu\mu$f
C_4, 5000 $\mu\mu$f
C_5, C_6, C_7, 0.01 μf
C_8, C_9, 0.05 μf
C_{10}, 0.1 μf
C_{11}, 0.25 μf
C_{12}, 2 μf
C_{13}–C_{17}, 8 μf
L_1, L_2, 15 h
V_6, 80
V_7, 6E5
V_8, V_9, 6J7

first two hours after the current is turned on. During this time the voltage variations cause a change in the sensitivity of the photomultiplier of about five percent. Thereafter, the drift is slow and not a serious hindrance to measurements. It is usually less than one percent per day.

The inclusion of manual control (R_3 and S) of the output voltage so the phototube may be set at any desired sensitivity has proven to be most useful.

6. Tuned Amplifier and Electron-Ray Indicator

As explained previously, measurement consists of adjusting the potentiometer P of Fig. 1 until the 120 cycle component of the voltage across it reaches a minimum. To observe this voltage the tuned amplifier diagrammed in Fig. 5 was constructed.

Essentially the amplifier is a two-stage resistance-capacity-coupled high gain voltage amplifier with a frequency dependent feedback network added to the second stage. Except for the latter, the construction is entirely conventional, the circuit constants those recommended by the tube manufacturer.[11] Careful shielding of the input stage is necessary.

The feedback network is the "twin-T" type. It was adjusted, with the temporary aid of an oscilloscope, essentially in the manner described by Sturtevant,[12] to supply regeneration at 120 c.p.s. and degeneration at other frequencies. The amount of feedback, which is controlled by the potentiometer R_{12}, is usually adjusted so that the amplifier is just short of oscillation and so that

[11] *Receiving Tube Manual* (RCA Manufacturing Company, Inc.).
[12] J. M. Sturtevant, Rev. Sci. Inst. **18**, 124 (1947).

the response time of the amplifier is about 0.5 second ($Q \sim 300$). The use of a remote cut-off tube in this stage with a small (0.25 megohm) resistance in the grid circuit was found to give smoother control of the regeneration than more conventional arrangements.

It is necessary to use a narrow-band amplifier such as described here since the noise level in the highly amplified photocurrent is unusually high.

The output of the amplifier is detected by the electron-ray ("magic eye") tube V_7. In operation the bias control R_7 is set so that the tube is near cut-off and the eye is just closed when the input of the amplifier is short-circuited by switch S_1. A signal then causes the eye to open. A signal of about 10^{-5} volt causes a perceptible response at full gain. The capacitor C_{12} on the ray control electrode raises the response time of the tube to one second, enabling it to integrate over more rapid fluctuations in the photocurrent.

To aid in trimming the frequency of the feedback network, which drifts slightly, a standard 120 c.p.s. signal from the power supply may be imposed on the grid of the electron-ray tube by closing the switch S_2. The beats between this signal and the self-oscillations of the amplifier may then be observed. The frequency of oscillation is adjusted by trimming R_{19}. R_{25} isolates the oscillations from the test signal voltage.

When the utmost precision is desired, it is advantageous to study the output of the amplifier on an oscilloscope, observing the phase as well as the amplitude of the voltage as the measuring potentiometer (P in Fig. 1) is balanced.

7. General Construction

The potentiometer P of Fig. 1 was constructed by ganging together the corresponding dials of two 99,990 ohm decade boxes in such a way that the sum of the resistances of the two remains constant at 99,990 ohms while the ratios vary from 0 to ∞.

The whole apparatus was mounted on a table which was covered by a grounded aluminum sheet. Shielded cable was used in all exposed wiring, and all metal parts not otherwise connected were grounded. These precautions reduced interfering voltages from the power lines, etc., to a satisfactory level.

No attempt was made to enclose the apparatus in a light-excluding case. Instead the room was darkened while measurements were made. A red light was used for illuminating the scale, recording data, and general manipulation (the photomultiplier being relatively insensitive to red). The principal consideration in this procedure was the desire always to have the cell open to visual inspection, to detect misalignment or dust, or suspended matter in the solutions under observation.

8. Performance

The performance of the photomultiplier tube, which is the heart of the apparatus, was in accord with that described by other authors.[13] Relevant to this work are the fatigue, dark current, and linearity characteristics of the device. There is great variation among individual tubes. The following remarks apply only to the better ones tested.

Fatigue was found to be negligible as long as the output was limited to five μa. At higher currents fatigue was noticeable. The potentiometer arrangement used limits the photomultiplier current to less than the balance tube current, which is approximately two μa. Fatigue is therefore not important.

Linearity was tested by measuring the transmission of a screen of 35.6 percent transmission over the usable range of light intensities. No deviation within the precision of measurement could be found.

The dark current of the tube used was found to vary from 0.005 to 0.05 μa, depending on the voltage. With a total voltage of 800 volts the current was 0.01 μa and the fluctuations were of the order of 10^{-4} μa per second. This would correspond to the amplified statistical fluctuation of a thermionic emission of about 10^5 electrons per second plus the spontaneous fluctuations of the multiplying stages. For comparison, the photocurrent from a cell full of butanone, the measurement of lowest intensity encountered, was approximately 0.01 μa at this voltage. Statistical fluctuations in the photocurrent are also of the order of 10^{-4} μa per second, so that the over-all

[13] R. W. Engstrom, J. Opt. Soc. Am. **37**, 420 (1947); Fitz-Hugh Marshall, J. W. Coltman, and L. P. Hunter, Rev. Sci. Inst. **18**, 504 (1947).

TABLE I. Relative intensity of scattering from cell containing butanone.

Angle	Intensity
25.8°	6.78
36.9°	2.22
53.0°	1.29
66.4°	0.81
78.4°	0.58
90.0°	0.47
101.6°	0.41
113.6°	0.47
126.9°	0.54
143.1°	0.66

precision of the measurement is limited to about 1.5 percent.

At higher light intensities the fluctuation of the dark current becomes negligible, but the fluctuations of the photocurrent persist, varying as the square root of the intensity. In fact, the limit of precision is set by these fluctuations. The size of the fluctuations may be diminished by increasing the rise time of the amplifier. Since they decrease only as the square root of the time, while the tedium of measurement increases at least directly with the time, it is not usually desirable to increase the latter beyond one second, however. Probably the best procedure is to increase the power of the light source.

The stability of the photo-multiplier itself, as long as it was not exposed to strong light, apparently was limited only by the stability of its power supply. After having been run for several hours, the slow drift of the latter produced a variation of sensitivity of about one percent per day. It was necessary in accurate work to adjust the voltage occasionally by measuring the scattering of a standard of known scattering power.

The reading of the whole device was nearly independent of the fluctuations in the intensity of the light source, changing about one percent when the latter changed by a factor or two. The cause of this remaining change may have been that the light falling on the two phototubes did not come from exactly the same part of the source in each case.

It was generally found possible to make reproducible readings with a precision of 0.2 percent, when the statistical fluctuations of the electron current allowed, if a standard were measured within fifteen minutes of the reading.

The performance of the photometer in measuring the true angular variation of intensity of the scattered light was checked by measuring the fluorescence of a dilute solution of fluorescein (in water) or diacetylfluorescein (in toluene or dichloroethane). The solutions were illuminated with the blue lines of the mercury lamp while a yellow filter, opaque to the exciting light but transparent to the green fluorescence, was placed in front of the photometer. The solutions were dilute enough so that loss of light by absorption was negligible. Under these conditions the only causes of angular dissymmetry must lie in the geometry of the apparatus. It was found that there was a diminution of intensity at 90° of about three percent compared to 30° or 150°. Such a variation is to be expected, since the cell is not an ideal point source. The observed variation was used to correct subsequent measurements of scattering for this factor.

As an example of the intensity of the background and stray illumination when scattering (not fluorescence) was being measured, Table I is given. In this case the cell contained clean butanone and the outer vessel clean 1-propanol. The light observed at 90° is mainly the scattering of the butanone in the cell. The principal increase at larger and smaller angles occurs as larger volumes of the illuminated portion of the outer liquid contribute their scattering, while at the small angles scattering from imperfections in the cell walls and from the edges of the shields becomes important. The practical limit is reached at 10°, where the scattering from the spot at which the beam enters the outer vessel first comes into the photometer.

As pointed out above, an object of constant scattering power is needed as a reference in accurate work. After some experimentation, a rectangular block was made of polystyrene to which five percent of methyl acrylate had been added when the polymerization was half completed. The addition of the acrylate produced a copolymer of somewhat different internal pressure in the latter half of the polymerization. The mixture shows the opalescence expected from a one-phase liquid mixture near the consolute point. (Too much acrylate causes the separation of a second phase.) This block has served its purpose well, but its turbidity varies with temperature so that

it is desirable to keep it thermostated. A less sensitive material would be desirable.

As concrete examples of the results obtained, the curves of Fig. 6 are shown. The solid lines are the polar plot of the experimental intensity of scattering from a monodisperse sulfur sol, prepared according to the method of Johnson and LaMer.[14] Such a sol consists of spherical drops of liquid sulfur suspended in water. The maxima and minima, which may be considered as resulting from interference effects, are clearly shown. Comparison with Johnson and LaMer's results places the radius of these particles at 0.45 micron. The incident light here, as in all the other angular variation measurements, was polarized perpendicularly to the plane of measurement.

The dotted line in Fig. 6 is the scattering from a sample of polystyrene, to which reference will be made later in Section IV 1, dissolved in toluene to the concentration of 0.0002 g per ml. The "blank" obtained from the cell full of pure toluene has been subtracted from these measurements so that the curve represents the excess of scattering of the solution beyond that of the solvent. The curve itself is the plot of the theoretical equation, Eq. (1), while the circles are the experimental points. While the region between 25° and 150° only is readily accessible experimentally at low scattering intensities, it may be noted that most of the variation occurs within this range. This fortunate fact holds true even more strongly for polymers of smaller size.

It should finally be pointed out that the graph of the scattering from a suspension of ideally small particles would be a circle centered on the origin, such as the coordinate circles in Fig. 6.

III. METHOD OF HANDLING DATA

It was shown by the theoretical treatment of the preceding paper[5] that at low concentrations the intensity of scattering, I, is related most simply to the concentration, c, and angle, ϑ, by the equation

$$K(c/I)=1/MP(\vartheta)+2A_2c, \qquad (1)$$

where $P(\vartheta)$ is a known function of ϑ, M is the solute molecular weight, and A_2 and K are constants. It may be anticipated that there will be deviations from this equation if either the molecular weight or the concentration becomes too high. Nevertheless, it should be useful as a rough guide even in the latter case.

It is usually desired to obtain M, the molecular weight of the polymer, and $P(\vartheta)$, from which the average spatial extension of the chain may be calculated. Obviously these quantities can only be found by extrapolation of the experimental values of c/I to infinite dilution.

1. Some Properties of $P(\vartheta)$

Assuming for the moment that the extrapolation to infinite dilution may be accomplished, let us consider the function $P(\vartheta)$.

For a suspension of linear coiling chain molecules of uniform degree of polymerization, n, with light of wave-length λ, $P(\vartheta)$ is given by

$$P(\vartheta)=(2/u^2)(e^{-u}-1+u), \qquad (2)$$

where

$$u=(8\pi^2b^2n/3\lambda^2)\sin^2(\vartheta/2)=Cb^2n\sin^2(\vartheta/2). \qquad (3)$$

The constant b has the dimensions of length. It is determined by the average size and geometric arrangement of the bonds of the chain skeleton (see Eq. (20) below). The root-mean-square end-to-end chain distance, L, which is often employed, is equal to b^2n.

To find the characteristic length, b (or L), from the observed $P(\vartheta)$, it is convenient to enlarge on some observations by Debye.[4] If $P(\vartheta)$ is expanded in terms of $\sin^2(\vartheta/2)$, the following series results:

$$P(\vartheta)=1-(C/3)nb^2\sin^2(\vartheta/2)+(C^2/12)n^2b^4\sin^4(\vartheta/2)-\cdots. \qquad (4)$$

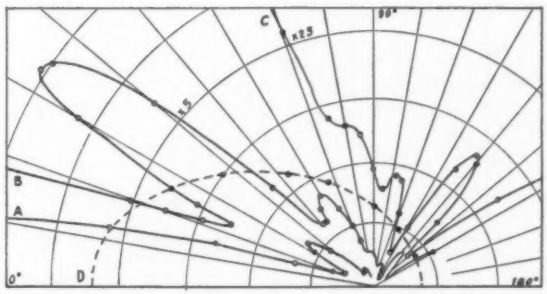

FIG. 6. Typical scattering curves, polar plots of intensity of scattering against angle of scattering. A, Sulfur sol of 0.45 microns radius in water; B, curve A times five; C, curve A times 25; D, excess scattering from polystyrene RT−H in toluene, concentration 0.0002 g/ml. (Radius vectors in arbitrary units.)

[14] I. Johnson and V. K. LaMer, J. Am. Chem. Soc. 69, 1184 (1947).

It is apparent that b may be found from the initial slope of the curve. Diminished curvature results if the reciprocal of $P(\vartheta)$ is taken,

$$P^{-1}(\vartheta)=1+(C/3)nb^2\sin^2(\vartheta/2)+(C^2/36)n^2b^4\sin^4(\vartheta/2)-\cdots. \quad (5)$$

The characteristic length, b, is then easily found if the initial slope of the plot of $1/P(\vartheta)$ against $\sin^2(\vartheta/2)$ can be determined.[15] Fortunately such a plot already results if Eq. (1) is used to extrapolate the observations to infinite dilution.

When $u=Cb^2n\sin^2(\vartheta/2)$ is less than unity $P^{-1}(\vartheta)$ is practically linear in $\sin^2(\vartheta/2)$ and there is no difficulty in obtaining the initial slope. But when u is larger than unity, the plot shows a gentle upward curvature and it is not always easy to find the initial slope directly.

A plot of $P^{-1}(\vartheta)$ against u is shown in Fig. 7 (curve of $z=\infty$) together with its initial slope and its asymptote for large values of u. The asymptote may be seen from (2) to be

$$\lim_{u\to\infty} P^{-1}(\vartheta)=(u+1)/2. \quad (6)$$

Equation (6) is a line of intercept $\frac{1}{2}$ and slope $\frac{1}{2}$, while the initial slope of $P^{-1}(\vartheta)$ is $\frac{1}{3}$ and the intercept is 1. It is obvious that data falling on any limited portion of the curve could be mistakenly thought to determine a straight line whose intercept and slope would not agree with the true intercept and initial slope. A correction table, to be described, is useful in such a case.

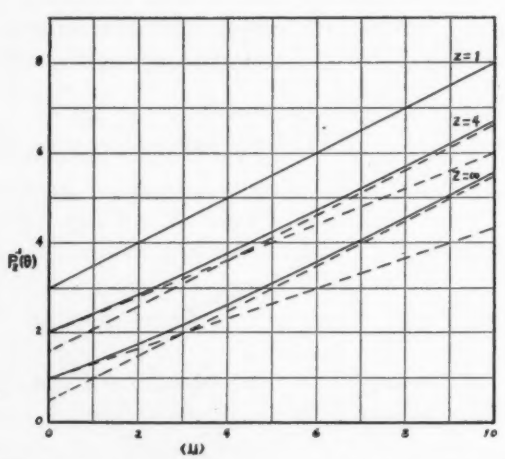

FIG. 7. $P_z^{-1}(\vartheta)$ plotted against $\langle u\rangle=(8\pi^2\langle n\rangle b^2/3\lambda^2)\sin^2(\vartheta/2)$ for three values of z. The curve for $z=4$ is displaced upward one unit and that for $z=1$ two units.

[15] As Debye points out, the initial slope gives in general the moment of inertia of the particle about its center of mass, regardless of the shape of the particle.

When the particles under observation have other shapes than random coils, similar methods may still be used, although the forms of the equations are different. For example, if the particles are rigid linear rods of length L, $P(\vartheta)$ is given by

$$P(\vartheta)=\frac{1}{x}\int_0^{2x}\frac{\sin v}{v}dv-\left(\frac{\sin x}{x}\right)^2, \quad (7)$$

where x is given by

$$x=(2\pi L/\lambda)\sin(\vartheta/2). \quad (8)$$

In this case $P^{-1}(\vartheta)$ may be expanded in x^2 to give the form analogous to Eq. (5);

$$P^{-1}(\vartheta)=1+x^2/9+7x^4/2025+\cdots. \quad (9)$$

The asymptote of $P^{-1}(\vartheta)$, analogous to Eq. (6), is

$$\lim_{x\to\infty} P^{-1}(\vartheta)=2/\pi^2+2x/\pi. \quad (10)$$

2. Polydispersity

Further complications arise if the solute exhibits a distribution of degrees of polymerization, as is usually the case in practice. Let us assume that instead of only one degree of polymerization, n, there is a distribution, $f(n)$, such that $f(n)dn$ is the weight fraction of material of degree n in the range dn. At infinite dilution, the total light scattering will be the sum of the scattering from each of the individual components. From Eq. (13b) of the previous paper,[5] the total scattering may then be found to be:

$$I(\vartheta)/c=K'\int nf(n)P(\vartheta)dn, \quad (11)$$

where $K'=nk/M$ is a constant independent of n.

Considering now only the situation in the case of coiling solute particles, let us first examine it for small values of $u=Cb^2n\sin(\vartheta/2)$. If $P(\vartheta)$ is expanded as in Eq. (4), and then integrated according to (7), the following series eventually results:

$$\frac{c}{I(\vartheta)}=\frac{1}{K'\langle n\rangle}\left[1+\langle n\rangle\left(1+\frac{\langle\Delta n^2\rangle}{\langle n\rangle^2}\right)\times\frac{Cb^2}{3}\sin^2\frac{\vartheta}{2}+\cdots\right], \quad (12)$$

where

$$\langle n\rangle = \int nf(n)dn,$$

and

$$\langle \Delta n^2\rangle = \int (n-\langle n\rangle)^2 f(n)dn.$$

The quantity $\langle n\rangle$ is the weight-average degree of polymerization and $\langle \Delta n^2\rangle$ is the dispersion of the distribution. It is interesting that the quantity $\langle n\rangle(1+\langle \Delta n^2\rangle/\langle n\rangle^2)=\langle n^2\rangle/\langle n\rangle$ is the kind of average degree of polymerization which has been called the "Z-average" by writers on the theory of the ultracentrifuge.[16]

Comparing (12) with (1) and (5) leads to interesting conclusions. The molecular weight obtained from the extrapolation to zero angle is the weight-average molecular weight, but the average entering the slope from which the characteristic length is determined is the "Z-average," which is always larger than the weight average. If the dispersion, $\langle \Delta n^2\rangle$, of the distribution can be found, one can be calculated from the other.

For large values of average u,

$$\langle u\rangle = Cb^2\langle n\rangle \sin^2(\vartheta/2),$$

Eq. (12) converges slowly and it is difficult to determine the initial slope. We will therefore develop a special method which will sometimes be useful in such cases.

For many materials, it will be possible to approximate the distribution $f(n)$ by a function of the form

$$f(n) = (y^{z+1}/z!)n^z e^{-yn}, \tag{13}$$

where y and z are adjustable parameters. This is a function with a single peak whose width is determined by the parameter z. By integrating the function, we find

$$\int f(n)dn = 1, \tag{14a}$$

$$z = (\langle n\rangle^2/\langle \Delta n^2\rangle) - 1, \tag{14b}$$

and

$$y = \langle n\rangle/\langle \Delta n^2\rangle = (z+1)/\langle n\rangle. \tag{14c}$$

The distribution is therefore characterized by the average degree of polymerization and its dispersion.

The advantage of this function for the present problem lies in the fact that the integration in Eq. (11) may be performed easily. When it is applied to the calculation of $c/I(\vartheta)$, the result is

$$\frac{c}{I(\vartheta)} = \frac{C^2b^4\langle n\rangle \sin^4\vartheta/2}{2K'}\left\{\frac{z(1+z+Cb^2\langle n\rangle \sin^2\vartheta/2)^z}{(1+z)^{1+z}-(1+z-zCb^2\langle n\rangle \sin^2\vartheta/2)(1+z+Cb^2\langle n\rangle \sin^2\vartheta/2)^z}\right\},$$
$$= (1/K'\langle n\rangle)P_z^{-1}(\vartheta). \tag{15}$$

The new function, $P_z^{-1}(\vartheta)$, is plotted in Fig. 7 for $z=4$ (dispersion, $\langle \Delta n^2\rangle$, equal to $0.20\langle n\rangle^2$) and $z=1$ ($\langle \Delta n^2\rangle = 0.50\langle n\rangle^2$), in addition to the plot of the reciprocal of Eq. (2), to which $P_z(\vartheta)$ reduces when z approaches infinity (dispersion approaches zero).

The case where $z=1$ is of special interest,[17] since here the distribution of sizes, $f(n)$, is just that expected in certain types of polymerization.[18] Examination of Eq. (15) shows that here also $P_z^{-1}(\vartheta)$ assumes an especially simple form:

$$P_1^{-1}(\vartheta) = 1 + Cb^2\langle n\rangle \sin^2(\vartheta/2)/2. \tag{16}$$

In this case obviously the characteristic length b may be found easily from a linear plot of $c/I(\vartheta)$ against $\sin^2(\vartheta/2)$.

In general, Eq. (15), with the use of Eq. (14b), approaches the linear form (12) as $\langle u\rangle$ approaches

TABLE II.

$z=\infty$				$z=4$				$z=19$			
u	$P^{-1}(\vartheta)$	Limiting tangent	Ratio	u	$P_4^{-1}(\vartheta)$	Limiting tangent	Ratio	u	$P_{19}^{-1}(\vartheta)$	Limiting tangent	Ratio
0	1.00	1.00	1.00	0	1.00	1.00	1.00	0	1.00	1.00	1.00
1	1.36	1.33	0.98	1	1.42	1.40	0.99	1	1.37	1.35	0.98
2	1.76	1.67	0.95	2	1.86	1.80	0.97	2	1.70	1.70	0.95
3	2.19	2.00	0.91	3	2.32	2.20	0.95	3	2.22	2.05	0.92
4	2.65	2.33	0.88	4	2.78	2.60	0.93	4	2.68	2.40	0.89
5	3.12	2.67	0.85	5	3.27	3.00	0.92	5	3.15	2.75	0.87
6	3.60	3.00	0.83	6	3.75	3.40	0.91	6	3.63	3.10	0.85
7	4.08	3.33	0.82	7	4.23	3.80	0.90	8	4.61	3.80	0.82
8	4.57	3.67	0.80	8	4.72	4.20	0.89	10	5.59	4.50	0.81
9	5.07	4.00	0.79	9	5.20	4.60	0.88	∞	—	—	0.70
10	5.56	4.33	0.78	10	5.71	5.00	0.88				
∞	—	—	0.667	∞	—	—	0.80				

[16] Svedberg and Petersen, *The Ultracentrifuge* (Oxford University Press, Oxford, 1940).

[17] I am greatly indebted to Professor Debye for pointing this out to me.

[18] P. J. Flory, Chem. Rev. **39**, 137 (1946).

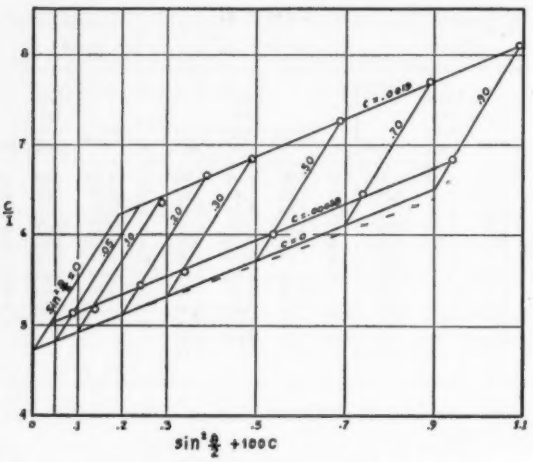

FIG. 8. Projection of the reciprocal intensity surface of polystyrene EP-2 in butanone at 67°C. The dotted line is the limiting tangent.

zero, and as $\langle u \rangle$ becomes infinite Eq. (15) moves toward the line,

$$\frac{c}{I(\vartheta)} = \frac{1}{K'\langle n \rangle}\left[\frac{z+1}{2z} + \frac{Cb^2\langle n \rangle \sin^2(\vartheta/2)}{2}\right], \quad (17)$$

as an asymptote. These limiting lines are also shown in Fig. 7. It can be seen that they come closer as z decreases until they fuse at $z=1$ into one line.

Except when $z=1$, the curvature of $c/I(\vartheta)$ may add difficulties to the determination of the characteristic length, b, from experimental data, as mentioned before. Table II has been prepared to facilitate the process. In the second column of each section is given $P_z^{-1}(\vartheta)$, in the third column the value of the corresponding limiting form (12). The ratio of the two quantities is given in the fourth column. By the use of the ratio, data falling on the curve may be reduced to the limiting line, from which b is easily found. Examples are given in Section IV, 4.

It remains to find $\langle \Delta n^2 \rangle$, the dispersion of the distribution. In principle, the shape of the plot of $c/I(\vartheta)$ against $\sin^2\vartheta/2$ should furnish the dispersion, but in practice it seems hopeless to obtain data of sufficient precision to yield information on this point in any but extreme cases. Fortunately, the converse is also true; it is not necessary to have an accurate value of the dispersion in order to obtain b reasonably well from the data.

In this paper $\langle \Delta n^2 \rangle$ will be estimated from the mode of preparation of the material. It will be assumed that the distribution of the original polymer is given by (13) with $z=1$. Using the solubility theory of Scott[19] distributions corresponding to the fractions prepared from the original material will be calculated. From these $\langle \Delta n^2 \rangle$ will be found numerically.

To anticipate some of the results, it seems that $z=19(\langle \Delta n^2 \rangle/\langle n \rangle^2 = 0.05)$ corresponds fairly well to fractions prepared by several precipitations from dilute solution, if only a small part (e.g. ten percent) of the original material appears in the fraction in question. On the other hand, $z=4(\langle \Delta n^2 \rangle/\langle n \rangle^2 = 0.20)$ would seem to correspond to a crude fraction containing approximately one-fourth of the original material and prepared by a single precipitation.

To summarize, the dispersion, $\langle \Delta n^2 \rangle$, of the distribution should be estimated. From a plot of the limit of $c/I(\vartheta)$ at infinite dilution against $\sin^2(\vartheta/2)$, by taking the ratio of the initial slope to the intercept, the quantity $8\pi^2\langle n \rangle b^2(1+\langle \Delta n^2 \rangle/\langle n \rangle^2)/3\lambda^2$ may be found. A more accurate slope may be obtained by using the provisional slope and the dispersion in conjunction with Table II to rectify the plot. The quantity $\langle n \rangle b^2 = L^2$ is the weight average of the mean square distance between the ends of the chains, while $\langle n \rangle b^2(1+\langle \Delta n^2 \rangle/\langle n \rangle^2)$ is the "Z-average" of the same quantity.

3. The Extrapolation to Infinite Dilution

Equation (1) shows that c/I is a linear function of c at low concentrations. We have just seen that it is also approximately a linear function of $\sin^2(\vartheta/2)$. Consequently, a bilinear method of plotting the data is indicated.

The procedure used in this work has been to plot c/I against $\sin^2(\vartheta/2)+k'c$, where k' is an arbitrary constant (e.g., $k'=100$, 2, $\frac{1}{2}$, etc.) chosen for convenience. The data then fall on patterns such as are illustrated in Figs. 8 and 9. Lines may be drawn through points of the same value of $\sin^2(\vartheta/2)$ to extrapolate to infinite dilution.

The characteristic patterns seen in Figs. 8 and 9 may be thought of as projections of the reciprocal intensity surface,[5] on a plane containing the

[19] R. L. Scott, J. Chem. Phys. **13**, 178 (1945).

c/I axis and forming an acute angle with both the $c=0$ and $\vartheta=0$ coordinate planes.

For some materials, especially those of very high molecular weight, a difficulty arises when terms in higher powers of the concentration become important, giving appreciable curvature to the lines. Theory indicates that the curvature should increase with both A_2 and with M. Consequently, as the molecular weight goes up, it becomes necessary to measure points at lower concentrations to obtain a linear extrapolation. Examples are to be found in the data which follow.

It should also be noted that the derivation of Eq. (1) is not rigorous when A_2 or M are too high. An apparent dependence of A_2 on ϑ might result in such a case.

IV. EXPERIMENTAL DETAILS AND RESULTS

1. Materials

Two samples of polystyrene were used in this work. The first, designated by the code letters RT-H, was the same material measured previously and reported in an earlier paper.[6] It was prepared in the following manner: The monomer was washed with alkali to remove inhibitors, distilled at 15 mm, then allowed to stand six months at room temperature. The polymer was precipitated by pouring the one-third-polymerized mixture into alcohol. A broad fraction was obtained by precipitating about one-fourth of the sample from a one percent solution in butanone with methanol.

An attempt was made to calculate the dispersion of the molecular weight distribution of fraction RT-H, using the theory as developed by Scott.[19] The distribution function of the original polymer was assumed to be given by Eq. (9) with $z=1$. The various parameters of Scott's equations were adjusted so that the concentration and weight of the precipitate agreed with the actual values, and the distribution curve of the precipitate calculated. The ratio of the dispersion to the square of the mean degree of polymerization $\langle\Delta n^2\rangle/\langle n\rangle^2$, was then calculated numerically from the distribution curve. The result was $\langle\Delta n^2\rangle/\langle n\rangle^2=0.2$.

The other sample of polystyrene, for which the code EP-2 is used, was prepared by fractionation from an emulsion polymer, kindly supplied the author by Dr. A. Goldberg of the Polytechnic Institute of Brooklyn. The polymer had been prepared using ammonium stearate as suspending agent and persulfate ion as catalyst, in the same manner as described by Goldberg, Badgely and Mark.[20] The fractionation of this polymer was carried only far enough to yield a small fraction from the higher end of the distribution curve. The fraction was reprecipitated from dilute solution, yielding EP-2. Calculation by Scott's method, as described above, gave $\langle\Delta n^2\rangle/\langle n\rangle^2=0.05$.

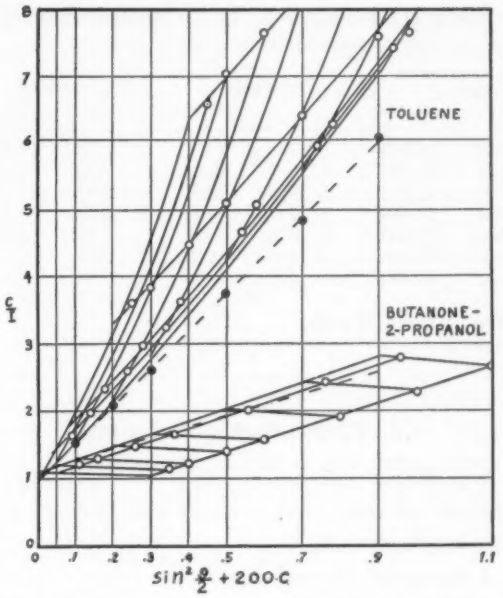

FIG. 9. Projection of the reciprocal intensity surfaces of polystyrene RT—H in toluene and in a butanone (89 percent), 2-propanol (11 percent) mixture at 20°C. The dotted lines are the limiting tangents. The toluene values have been divided by 3.54 (the theoretical ratio of the intercepts).

No extensive attempt was made to obtain chemically pure solvents, since only the relative solvent power was of interest. The benzene and toluene used were Baker and Adamson's "reagent," meeting A.C.S. specifications. The 1,2-dichloroethane was a commercial compound but the boiling point was 83.6° (corr.) (literature, 83.5°–.7°). The butanone was first dried with $CaCl_2$ to remove a considerable amount of water and alcohol and was then distilled, b.p. 79.5° (corr.) (lit. 79.6°). The isopropanol was not investigated.

[20] A. I. Goldberg, W. P. Hohenstein, and H. Mark, J. Polymer Sci. 2, 503 (1947).

TABLE III. Polystyrene EP-2 in butanone at 67°C.

Concentration (g/ml):		0.0019		0.00038	
ϑ	$\sin^2(\vartheta/2)$	I	$(c/I)\times10^5$	I	$(c/I)\times10^5$
25.8°	0.050	—	—	7.38	5.13
36.9	0.100	29.8	6.36	7.34	5.18
53.0	0.200	28.5	6.66	6.96	5.45
66.4	0.300	27.9	6.84	6.78	5.61
90.0	0.500	26.2	7.27	6.29	6.02
113.6	0.700	24.7	7.70	5.88	6.47
143.1	0.900	23.5	8.10	5.54	6.84

$\lim_{c\to0,\ \vartheta\to0} c/I = 4.72\times10^{-5}$.

TABLE IV. Polystyrene RT−H in butanone (89 percent)-2-propanol (11 percent) at 20°C.

Concentration (g/ml):		0.00148		0.000296	
ϑ	$\sin^2(\vartheta/2)$	I	$(c/I)\times10^5$	I	$(c/I)\times10^5$
25.8°	0.050	129.0	1.14	24.5	1.21
36.9	0.100	120.0	1.23	23.1	1.28
53.0	0.200	106.0	1.40	20.2	1.47
66.4	0.300	93.5	1.58	18.0	1.65
90.0	0.500	77.2	1.92	14.7	2.02
113.6	0.700	65.2	2.27	12.2	2.43
143.1	0.900	55.1	2.69	10.5	2.81

$\lim_{c\to0,\ \vartheta\to0} c/I = 1.11\times10^{-5}$.

2. Preparation of Solutions

A problem unique to light scattering is the removal of dust and foreign suspended matter from the solutions.

A bacterial filter of the Seitz type was found useful for some solutions if the asbestos pad was impregnated with Bakelite varnish and cured by baking. Without the treatment asbestos fibers were introduced in the solutions. Such filters seemed to remove particles larger than a few microns in diameter.

In some cases, however, suspended matter persisted even after this treatment, as shown by an excessive scattering at low angles from the solution. The solutions were then centrifuged at 15,000 times gravity for thirty minutes in a high-speed angle-head centrifuge, with marked improvement in the results.

The solvents were distilled in a small all-glass still with a sealed condenser just before use.

It was found that dilutions of the centrifuged solution could be made with distilled solvent and introduced into the measuring cell without the introduction of noticeable dust if all bottles, pipettes, etc. were carefully cleaned and rinsed with distilled solvent immediately before use.

It may be remarked that considerably more care in cleaning the solutions is required if angular dependence measurements are to be made than if only the transverse scattering alone is measured, as a result of the great dissymmetry of the radiation envelope of the dust particles. The scattering from the sulfur sol shown in Fig. 6 is typical, except for details, of that from other compact particles in the micron size range.

3. Procedure

Solutions, cleaned as described above, were introduced into the conical scattering cell and the intensities scattered at several angles in the, horizontal plane were measured. The incident light was vertically polarized and consisted of the 5461A line of the mercury spectrum plus some continuum for several hundred Angstrom units on either side of the line. Its mean wave-length was taken as 5460A.

Drifts of the voltage supply were checked by measuring the turbid polymer block (Section II, 8)

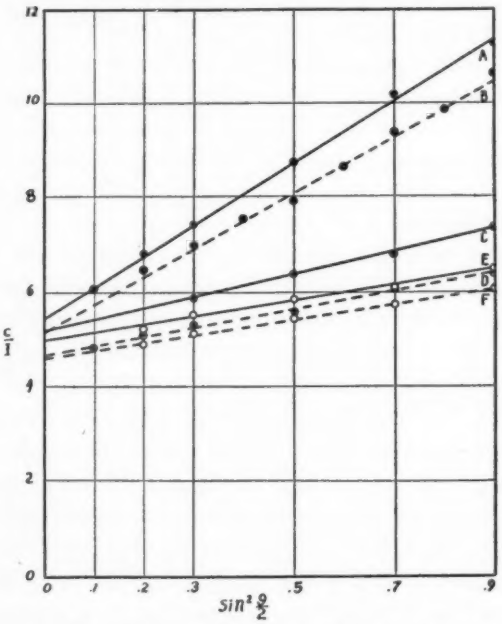

FIG. 10. Limiting tangents for polystyrene EP-2.

A, toluene, 20°C, divided by 3.54
B, toluene, 67°C, divided by 3.23
C, butanone, 20°C
D, butanone, 67°C
E, butanone (87 percent), 2-propanol (13 percent), 20°C
F, butanone (87 percent), 2-propanol (13 percent), 67°C

immediately before and after a series of measurements.

The determination of relative, not absolute, intensities was the primary aim of these experiments. However, the relative intensity scattered transversely from some of the solutions was compared to that from benzene. If previous measurements of the absolute scattering power of benzene are valid,[21] the absolute scattering of these solutions may be found. The comparison was made in rectangular cells giving negligible background scattering. Unpolarized light was used in this case. Since the depolarization of the excess light scattered from such solutions is very small,[22] there should be negligible change in the intensity of the excess transverse scattering in going to unpolarized illumination.

In order to get the temperature dependence of the scattering most accurately, the same samples of solution were measured at 20°C and 67°C in succession without refilling the cell.

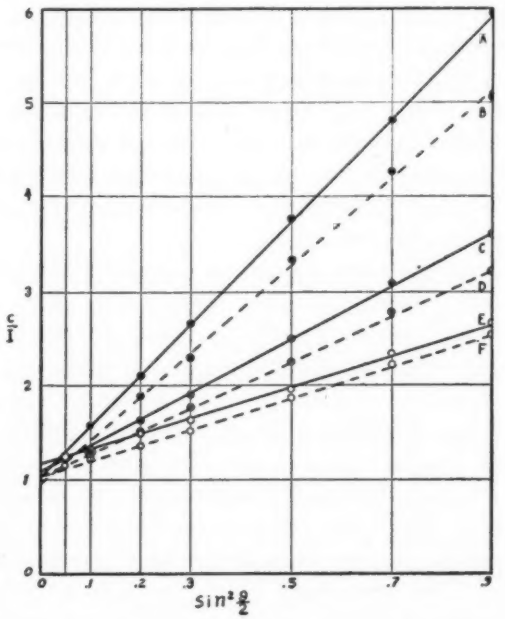

FIG. 11. Limiting tangents for polystyrene RT−H.

A, toluene, 20°C, divided by 3.54
B, toluene, 67°C, divided by 3.23
C, butanone, 20°C
D, butanone, 67°C
E, butanone (89 percent), 2-propanol (11 percent), 20°C
F, butanone (89 percent), 2-propanol (11 percent), 67°C

[21] S. Bhagavantam, *Scattering of Light and the Raman Effect* (Chemical Publishing Company, Brooklyn, New York 1942).

[22] P. Doty and H. S. Kaufman, J. Phys. Chem. **49**, 583 (1945).

TABLE V. Polystyrene RT−H in toluene at 20°C.

Concentration (g/ml):		0.00200		0.00100		0.00040		0.00020	
ϑ	$\sin^2(\vartheta/2)$	I	$(c/I)\times10^5$	I	$(c/I)\times10^5$	I	$(c/I)\times10^5$	I	$(c/I)\times10^5$
25.8°	0.050	8.65	23.2	7.86	12.8	5.82	6.89	3.49	5.74
36.9	0.100	8.02	24.9	7.38	13.6	4.88	8.17	2.89	6.94
53.0	0.200	7.41	27.0	6.37	15.8	3.82	10.5	2.18	9.18
66.4	0.300	6.88	29.0	5.58	18.0	3.12	12.8	1.74	12.4
90.0	0.500	5.95	33.7	4.42	22.6	2.25	17.9	1.22	16.4
113.6	0.700	5.35	37.5	3.73	26.9	1.80	22.1	0.952	21.0
143.1	0.900	4.79	41.7	3.15	31.8	1.48	27.0	0.763	26.2

$\lim_{c\to0,\ \vartheta\to0} c/I = 3.47\times10^{-5}$.

Viscosities were measured in specially constructed Ostwald pipettes having a low rate of shear. Comparison of results in different pipettes showed no dependence on shear rate in the range used.

4. Results

In Tables III–V are given the intensities of scattering of the polymers in some typical cases, relative to the transverse (90°) scattering from benzene illuminated with unpolarized light at 20°C. The polymer solutions were illuminated with polarized light, and only the excess scattering over that of the solvent is given in each case. Concentration is given in terms of grams of polymer per milliliter of solution at the temperature of measurement. A small correction for the geometry of the cell has been applied, as described in Section II, 8.

A. Form of Reciprocal Intensity Surface

Plots of the results are shown in Figs. 8–11. In Figs. 8 and 9 are shown the complete projections of the reciprocal intensity surface[5] for three systems, EP-2 in butanone at 67°C, and RT-H in toluene and a butanone-propanol mixture at 20°C. From the theoretical development of the preceding paper,[5] it is expected that the portion of the c/I surface near the origin should be nearly planar. When plotted as in Fig. 8, the curves of constant c and constant ϑ should then form two sets of parallel lines in this region. The figure shows that the expectation is well borne out; the maximum deviation of the slopes is less than five percent.

The data on RT-H in toluene, shown in Fig. 9, cover a larger region of the c/I surface, since the molecules are relatively much larger than those

TABLE VI. Mean length, L, and related quantities of polystyrene EP-2.

Solvent	Temperature	A_2M	L(A)
Toluene	20°C	180±15	1285±5%
	67	180±25	1220±5%
Butanone	20	80±10	887±5%
	67	80±10	828±5%
Butanone (87%), 2-Propanol (13%)	20	−10±10	745±5%
	67	+10±10	764±5%

TABLE VII. Mean length, L, and related quantities of polystyrene RT−H.

Solvent	Temperature	A_2M	L(A)	$[\eta]$ (ml/g)	$L^3/[\eta]$
Toluene	20°C	930±70	2680±5%	767±15	2.5±15%×10²³
	67	690±70	2520±5%	742±15	2.3±15%×10²³
Butanone	20	300±30	1935±5%	315±10	2.2±15%×10²³
	67	300±30	1900±5%	261±10	2.6±15%×10²³
Butanone (89%), 2-Propanol (11%)	20	−100±30	1490±5%	—	—
	67	+ 90±30	1585±5%	—	—

giving rise to Fig. 8. The curvature of the surface is clear in Fig. 9.

To obtain the limiting tangents to the surfaces in the ϑ-plane, use is made of Table II (section III. 2). Equation (12) shows that the expression $\langle n\rangle(1+\langle\Delta n^2\rangle/\langle n\rangle^2)Cb^2/3$ is the ratio of the initial slope to the intercept of the curve of c/I against $\sin^2(\vartheta/2)$ at $c=0$. From values of the slope and intercept estimated from the curve, the above expression may be approximated. Values of $\langle u\rangle=\langle n\rangle Cb^2\sin^2(\vartheta/2)/3$ may then be calculated for each value of $\sin^2(\vartheta/2)$. The fourth column of Table II then gives the factor that yields the point on the limiting tangent line when multiplied into the corresponding value of c/I. When the limiting tangent has been drawn through the points located in this way, the slope and intercept are determinable with greater precision than before. The process of approximation may be repeated with the new values, if necessary.

The dotted lines in Figs. 8 and 9 are the limiting tangents calculated as above. It is evident, especially in Fig. 9, that their use aids materially in determining the initial slopes.

In Fig. 9 some deviations from parallelism in the families of curves are noticeable at the larger values of $\sin^2(\vartheta/2)$. The effect may represent the beginning of a failure of the "single-contact" approximation of the preceding paper.

B. The R.M.S. Chain Length

The data are apparently represented by Eq. (1) rather well. To save space, the complete reciprocal intensity surfaces are not shown for all the systems, but the tangent lines are reproduced in Figs. 10 and 11. From these $(b^2\langle n\rangle)^{\frac{1}{2}}=L$, the weight-average root-mean-square end-to-end chain distance, may be calculated according to Eqs. (12) and (3). The results are shown in Tables VI and VII.

Also shown in Tables VI and VII are some intrinsic viscosities and the values of the product A_2M which may be evaluated with the aid of Eq. (1) from the data. The quantity A_2 is a measure of the deviation of the solution from Van't Hoff's law for the osmotic pressure and is therefore a measure of solvent power.[23] Large values of A_2 occur with "good" solvents and small or negative values with "poor" solvents (in the thermodynamic sense). Since M is constant for the same material in different solvents, A_2M also serves as a relative measure of solvent power.

It is at once evident that there is a large change in the molecular extension, as measured by the mean length, L, when the solvent power is changed at constant temperature. Toluene is one of the best solvents for polystyrene known while the butanone-propanol mixture is near the precipitation point.

Parallel to the change in L goes a change in intrinsic viscosity. The data show that the intrinsic viscosity varies as the cube of L, as might be expected for large coiled molecules of this type.

These conclusions are qualitatively similar to those reached from earlier experiments on fraction RT-H,[6] but quantitatively the changes with solvent are much more pronounced. The discrepancy in the butanone value is especially large. The inaccuracy is felt to lie in the older experiments, which were done with comparatively crude apparatus and evaluated without theoretical refinements. The new viscosity determinations agree well with the old ones, indicating that the sample had not changed during the two years that elapsed between measurements. However, the extrapolation of the old data has had to be revised in the light of the new measurements,

[23] B. Zimm, J. Chem. Phys. 14, 164 (1946).

TABLE VIII. Molecular weight, M, characteristic length, b, and related quantities of polystyrene EP-2.

Solvent	Temperature	$[I_v]$	$\partial\mu/\partial c$	M	b(A)	$\cos\varphi$
Toluene	20°C	0.067	0.108	696,000	11.3	0.930
	67				10.8	0.922
Butanone	20	0.251	0.221	732,000	7.85	0.855
	67				7.30	0.835
Butanone (87%), 2-Propanol (13%)	20	0.264	0.221	771,000	6.58	0.800
	67				6.76	0.810
			Average	733,000		

TABLE IX. Molecular weight, M, characteristic length, b, and related quantities of polystyrene RT−H.

Solvent	Temperature	$[I_v]$	$\partial\mu/\partial c$	M	b(A)	$\cos\varphi$
Toluene	20°C	0.375	0.108	3,890,000	10.7	0.919
	67				10.1	0.908
Butanone	20	1.17	0.221	3,420,000	7.68	0.848
	67				7.58	0.837
Butanone (89%), 2-Propanol (11%)	20	1.17	0.221	3,420,000	5.95	0.760
	67				6.32	0.785
			Average	3,580,000		

giving more weight to the points at low concentrations.

C. *The Effect of Temperature*

The effect of temperature on the mean extension, L, is noteworthy. In considering the phenomena, it must be borne in mind that the molecules are considerably more extended than would be the case if there were free rotation about the bonds of the chain skeleton, as is shown in section D, below. In toluene, a good solvent, there is apparently only a very slight tendency for the molecule to curl up and become smaller as the temperature rises. This would seem to indicate that the chain is extended by energies considerably larger than the average thermal agitation energy, as measured by kT, which most probably result from some kind of steric hindrance between the segments. If the large extension were the result of a normal (~4000 cal.) barrier to rotation about the single bonds of the chain skeleton, as calculated by Taylor[24] for paraffins, the temperature coefficient of L would be much larger than actually found.

In the butanone-propanol mixtures, which are very poor solvents, an *increase* of the mean extension with increase of temperature is noted. It would seem that the presence of a poor solvent gives rise to attractive forces between the chain segments, the energies associated with these forces being of the same order as kT so that a large temperature coefficient results. The energies also cause the chain to favor the more highly curled configurations giving rise to the observed small extensions in the poor solvent.

Another interesting effect appears in the change of the product A_2M with temperature, which reflects the variation of A_2 alone, since presumably M does not change. (The change of intercept with temperature in Figs. 10 and 11 can be explained as the result in changes of the refractive indices.) It has been shown previously[23] that the heat of dilution of the system, $\Delta\bar{H}_1$, is related to A_2 in dilute solutions by the equation,

$$\Delta\bar{H}_1 = -R(\partial(A_2/V_1)/\partial(1/T))\,V_1^2c^2, \quad (18)$$

where R is the molar gas constant and V_1 is the volume of the solvent per mole. Since V_1 increases by nearly five percent when the temperature changes from 20°C to 67°C, while A_2 either does not change or decreases slightly in toluene, $\Delta\bar{H}_1$ must be negative in this system (i.e., heat is evolved on dilution).[25]

Negative heats of dilution are not commonly observed in hydrocarbon mixtures. While it is not appropriate here to discuss exhaustively possible explanations, the two following seem likely: (a) It has been shown that A_2 decreases as the extension of the molecule decreases,[23] and a small decrease with increasing temperature seems possible in view of the data in Tables XVII and XVIII. (b) It is well known that the thermal expansion coefficient of the polymer is less than that of the common solvents. Since A_2 is of the nature of an excluded volume of a polymer molecule, it would not be expected to increase as fast with temperature as the molar volume, V_1, of an indifferent solvent. Cooperation of the two effects could explain the observations. It may be noted that both are peculiar to macromolecular solutions.

In the poor solvent, the butanone-propanol mixture, A_2 increases with temperature, corresponding to a positive heat of mixing, as expected.

Pure butanone seems to be an intermediate case.

[24] W. J. Taylor, J. Chem. Phys. 16, 257 (1948).

[25] Professor P. M. Doty has informed me that he has observed the same effect in osmotic measurements on this system.

D. Determination of Molecular Weight

The molecular weight of the samples may be found if the ratio of the intensity of scattering to the incident intensity can be evaluated. The absolute scattering power of benzene has been reported by two authors.[26,27] Their results give the quantity $i_{90}r^2/I_u^0$, where i_{90} is the intensity scattered at 90° at a distance r from a cubic centimeter of liquid, and I_u^0 is the intensity of the unpolarized incident beam. For the discussion, we shall define the following terms:

$I(\vartheta)$, the *relative intensity*, expressed in terms of some convenient quantity (in this paper the transverse scattering from the same volume of benzene at the same distance, the benzene being under unpolarized illumination),

$\mathbf{I}_{\vartheta u}=i_\vartheta r^2/I_u^0$, the *reduced intensity* with unpolarized illumination,

$\mathbf{I}_{\vartheta v}=i_\vartheta r^2/I_v^0$, the *reduced intensity* with vertically polarized illumination, and

$\tau=2\pi\int_0^\pi \mathbf{I}_{\vartheta u}\sin\vartheta d\vartheta$, the *turbidity*, equal to the total scattering per centimeter of path (polarization of incident light immaterial).

In addition, the term *reciprocal scattering function* has already been used for the quantity $c/I(\vartheta)$.

A well-known formula relates the reciprocal of the limit of $c/\mathbf{I}_{\vartheta v}$ as c and ϑ approach zero to the weight-average molecular weight $\langle M\rangle$. The relation follows, with μ the refractive index of the solution and λ_0 the wave-length *in vacuo*:

$$\lim_{c\to 0,\ \vartheta\to 0}\frac{\mathbf{I}_{\vartheta v}}{c}\equiv[\mathbf{I}_v]=\frac{4\pi^2\mu^2(\partial\mu/\partial c)^2}{\lambda_0^4 N_0}\langle M\rangle,$$
$$=K\langle M\rangle. \qquad (19)$$

The term *intrinsic scattering* (either relative or reduced), with the symbol $[I]$, might be proposed for the important quantity $\lim I/c$.

Cabannes and Daure[26] report a value of 10.7×10^{-6} for the reduced intensity $\mathbf{I}_{90u}$, with an average wave-length in vacuum, λ_0, of 5440A and at a temperature of 15°C. Peyrot[27] reports 34.8×10^{-6} for the same quantity with 4358A light at 25°C. From these we estimate a value of 13×10^{-6} for $\mathbf{I}_{90u}$ for benzene at 20°C with light of 5460A. Multiplication of the relative intensities by 13×10^{-6} then leads to the reduced intensities, from which the molecular weight is obtained by Eq. (19).

The results are given in Tables VIII and IX, together with the values of $\partial\mu/\partial c$ which were used in the calculation. The latter quantities were estimated from several previous determinations.[28] It may be noted that the determinations in different solvents agree tolerably well.

Also in Tables VIII and IX are the results for $\cos\varphi$, the average of the cosine of the angle of rotation of the carbon atoms about the bonds joining them in the chain, calculated from Taylor's[24] formula,

$$L^2=\sigma^2\left(\frac{1+\cos\alpha}{1-\cos\alpha}\right)\left(\frac{1+\cos\varphi}{1-\cos\varphi}\right)(2\langle n\rangle), \qquad (20)$$
$$=b^2\langle n\rangle,$$

where σ is the length of a single bond (1.55A) and α the bond angle (70.5°). It can be seen that $\cos\varphi$ is the same for the two materials in any given solvent, which seems to show that the microstructure of the different polymers is the same. It is also important that $\cos\varphi$ is much greater than zero in all cases, showing that rotation about the chain bonds is not free.[29]

V. CONCLUSION

The data that have been quoted in the preceding section seem to show that the combined theoretical and experimental techniques of light scattering are sufficiently developed to yield important results concerning the extension of macromolecular chains. As more data, especially on temperature dependence, become available, it may be possible to theorize with some confidence concerning the intramolecular energies that determine the shape and size of such complicated structures as the polystyrene molecule. The results of this investigation at least encourage such a hope.

ACKNOWLEDGMENT

It is a pleasure to acknowledge the help of Mr. C. I. Carr in construction of the apparatus.

[26] J. Cabannes and Daure, Comptes rendus **184**, 520 (1927).

[27] P. Peyrot, Comptes rendus **203**, 1512 (1936).

[28] P. M. Doty, B. H. Zimm and H. Mark, J. Chem. Phys. **12**, 144 (1944); also unpublished data of the author's.

[29] Comparison of these molecular weights with previous osmotic determinations on similar materials makes the values in Table XIX seem surprisingly low. A critical study of the reduced intensity determination has therefore been started. Pending further results, these molecular weights should be considered as provisional values.

THE JOURNAL OF CHEMICAL PHYSICS VOLUME 16, NUMBER 12 DECEMBER, 1948

Entropy, Enthalpy, and Free Energy of the Electrical Double Layer at an Ideal Polarized Electrode. Part I. Thermodynamic Theory

DAVID C. GRAHAME
Moore Laboratory of Chemistry, Amherst College, Amherst, Massachusetts
(Received June 7, 1948)

There are several kinds of entropy, enthalpy, and free energy changes associated with the electrical double layer. Definitions of the thermodynamically significant quantities are given, together with equations for their evaluation. It is shown that the ideal polarized electrode may be regarded as one electrode in a galvanic cell and that the usual thermodynamic treatment of cells may be applied. The electrochemical process occurring in such a cell is identified, and a method of evaluating a new property, the transference number of the ions of the double layer, is given. The relationship between electrocapillary properties of metals and the thermodynamic properties of colloids is indicated. The thermodynamics of gas adsorption on solids is presented as an aid to the interpretation of the above.

THE thermodynamic properties of the electrical double layer most often considered are those of interfacial tension and its related properties, surface charge density, differential capacity, and electrical potential. There are, in addition, a number of properties ascribable to the ionic species separately and derivable by methods previously described.[1] Beyond these, it is possible to define and to outline methods of measurement for thermodynamic quantities such as the entropy, enthalpy, free energy, heat capacity, and the like of the double layer. Except in the work of Gibbs, who defines the entropy of an interface, the very existence of these quantities as properties of the double layer has gone almost unremarked and presumably unrecognized. It is the purpose of this paper to define the more important of these properties and to outline the steps by which they may be evaluated. In a later paper some of them will be evaluated in an actual case.

I. THE ELECTROCHEMICAL PROCESS AT AN IDEAL POLARIZED ELECTRODE

From an experimental point of view the easiest thermodynamic quantities to evaluate, apart from the familiar electrocapillary properties, are those related to the electrochemical process which accompanies the transfer of charge into or out of the electrical double layer in a reversible manner. Consider the cell

$$\mathrm{Hg}\,\vdots\,\mathrm{KCl}\,|\,\mathrm{KCl},\ \mathrm{HgCl},\ \mathrm{Hg},$$

where the dotted vertical line represents the interface of an ideal polarized electrode, an interface which charges may approach in the manner of charges on a condenser, but which they do not cross. Such a cell has a definite electromotive force, dependent upon the total electronic charge q on the plates of the "condenser," i.e., on the charge per square centimeter of interface. It is in every sense a galvanic cell except that the electrochemical process is not what is ordinarily called a chemical reaction but resembles more closely a process of adsorption or desorption. The ordinary thermodynamic treatment of galvanic cells is not thereby invalidated, however, so that one may use the familiar equations of the galvanic cell:

$$\Delta G' = -n\mathfrak{F}E, \tag{1}$$

$$n\mathfrak{F}(dE/dT)_q = \Delta S', \tag{2}$$

$$\Delta H' = \Delta G' + T\Delta S', \tag{3}$$

where the symbols have their usual meanings and the primes designate that the process involved is the special electrochemical process to which we have been referring and which we shall presently identify. In practice one actually imposes the desired value of the electromotive force, E, from an external source and then measures q, the electronic surface charge density, but this is of no consequence to the thermodynamic treatment.

We now proceed to identify the electrochemical process to which these equations refer. Following the usual convention, we write all cell reactions in the direction corresponding to the flow of positive

[1] D. C. Grahame, Chem. Rev. 41, 441 (1947).

charge from left to right within the cell. Then at the left-hand electrode, designated by the subscript a (which may also be thought of as designating "adsorbed" since ions at that electrode are adsorbed on the surface of the mercury),

$$Hg_a = Hg_a^+ + e^-, \quad \text{(a)}$$

$$\tau_+ K_a^+ = \tau_+ K_{aq}^+, \quad \text{(b)}$$

$$\tau_- Cl_{aq}^- = \tau_- Cl_a^-, \quad \text{(c)}$$

where the subscript aq designates the solution phase (unadsorbed ions), and Hg_a^+ is not an ion in the ordinary sense but an atom of mercury in the metallic phase which has lost an electron. τ_+ is the number of equivalents of cation transferred from the interface to the solution per faraday of charge transferred from the left to the right-hand electrode. τ_+ will be called the transference number of the cation within the double layer. As usual, $\tau_+ + \tau_- = 1$, but values of τ are not restricted to positive values, and negative values of τ_+ prove to be very common.

At the right-hand electrode (subscript b) the half-cell reaction is the familiar calomel cell reaction

$$HgCl + e^- = Hg_b + Cl_{aq}^-. \quad \text{(d)}$$

The sum of these four reactions is

$$HgCl + \tau_+(K_a^+ + Cl_a^-) = Hg_a^+ + Cl_a^- + \tau_+(K_{aq}^+ + Cl_{aq}^-), \quad \text{(e)}$$

or

$$HgCl + \tau_+(KCl)_a = Hg_a^+ + Cl_a^- + \tau_+(KCl)_{aq}. \quad \text{(f)}$$

In arriving at Eq. (e) we have made use of the fact that the transfer of a mercury atom from one electrode to the other involves no change of entropy, enthalpy, or free energy, so that it is proper to cancel Hg_a against Hg_b. Although the transfer of potassium and chloride ions from the interface to the interior of the solution involves no change of free energy (since they are in equilibrium), the same cannot be said of their entropy and enthalpy.[2] Hence it is not permissible to cancel K_a^+ against K_{aq}^+ or Cl_a^- against Cl_{aq}^-. Equation (f) is written as a shorthand notation for Eq. (e).

In the preceding equations it would have been possible to write for Hg^+ and Cl^- any other metallic cation and anion whose salt is relatively insoluble. For combinations of ions whose salts are soluble, the counterpart of Eq. (e) does not lead to results of any apparent interest.

It is sometimes convenient to break Eq. (f) into two equations whose sum represents the over-all cell reaction, thus:

$$HgCl = Hg_a^+ + Cl_a^-, \quad \text{(g)}$$

$$\tau_+ KCl_a = \tau_+ KCl_{aq}. \quad \text{(h)}$$

It is seen that the first of these reactions involves the transfer of one mole of mercurous chloride to the polarized interface, the mercurous ion being within the metallic phase and the chloride ion being within the solution phase of the electrical double layer. The second reaction, (h), involves the transfer of τ_+ equivalents of potassium and chloride ions from the solution phase of the double layer to the interior of the solution itself.

One important result may be deduced immediately. Since there is no free energy change associated with reaction (h), the whole free energy change associated with the potential E is ascribable to reaction (g). Therefore

$$\Delta G_g = -\mathfrak{F}E. \quad (4)$$

This result has immediate application in correlating the properties of the electrical double layer with the properties of colloids, as will be shown in Section II.

In order to interpret experimental values of $\Delta H'$ and $\Delta S'$ it is necessary to understand the significance of Eqs. (g) and (h). This understanding is facilitated by considering various particular values of τ_+. There is a potential (called the Γ_{min}^+-potential in reference 1) where $\tau_+ = 0$. At that potential Eq. (h) drops out and a transfer of charge through the external circuit has the effect of converting solid mercurous chloride into mercurous ions within the mercury surface and chloride ions in the immediate vicinity of the surface. Values of $\Delta H'$ and $\Delta S'$ measured at this potential thus correspond to a single definite chemical reaction. Since these values of $\Delta H'$ and $\Delta S'$ correspond to the particular value of q prevailing at the Γ_{min}^+-potential, a series of values corresponding to different values of q may be obtained by working at various concentrations of electrolyte.

[2] In ordinary galvanic cells this point does not arise because the substances involved are always transferred or transformed with a change of free energy.

When an ideal polarized electrode is made negative by imposing a negative electronic charge on the metallic surface, τ_+ is found to approach unity rapidly and asymptotically. Then Eqs. (g) and (h) reduce to

$$HgCl = Hg_a^+ + Cl_{aq}^-, \quad \text{(i)}$$

$$K_a^+ = K_{aq}^+. \quad \text{(j)}$$

These correspond to the transformation of one mole of mercurous chloride to a gram atom of mercurous ion within the metallic phase (where it reduces the negative charge by one faraday) and one equivalent of chloride ion within the solution. At the same time one gram atom of potassium ion leaves the interface (because of the disappearance of negative charge on the metal) and enters the solution. It is equally easy to visualize Eqs. (g) and (h) in this case by imagining chloride ions to be adsorbed in reaction (g) and desorbed in reaction (h). The process then consists in the transfer of one mole of mercurous chloride to the double layer and the removal of one mole of potassium chloride.

At sufficiently large positive polarization τ_+ becomes negative. Under these circumstances no simplification of Eqs. (g) and (h) is possible, but the process is conceptually easy to grasp. It involves the conversion of one mole of HgCl to the adsorbed state, with the mercurous ions in the metallic phase, and the transfer of $-\tau_+$ equivalents of potassium chloride from the interior of the solution to the interface. From kinetic considerations it is quite certain that the anions are held to the interface by forces analogous to those prevailing in solid mercurous chloride, that is to say, by a combination of Coulombic and covalent bond forces. The positive ions are undoubtedly held by Coulombic forces, which means that they are kinetically a part (the major part) of the diffuse double layer. The whole electrochemical process is conveniently viewed as a chemisorption of mercurous chloride and potassium chloride.

It will be noted that when τ_+ is positive, Eq. (h) represents a desorption. Equation (g) always represents an adsorption. It is therefore misleading to call $\Delta G'$ for the process (f) (which is the sum of Eqs. (g) and (h)) either the free energy of adsorption or of desorption. Since it is both conventional and convenient to identify a process by a name which suggests its direction as well as its nature, we shall call $\Delta G'$ of reaction (f) the differential free energy of adsorption-desorption.[3] Thus the first-named process refers to the calomel adsorption, which never changes sign (reaction (g)), while the last-named process refers to the salt adsorption and is named for the process which occurs when τ_+ is positive.

From reaction (b) it will be seen that τ_+ is equal to $-d\Gamma_+/dq$,[3a] since this gives the rate at which positive ions accumulate in the electrical double layer per faraday of charge transferred. Methods of evaluating Γ_+ and q as a function of E have already been presented,[1] so that the evaluation of τ_+ offers no new difficulty. $\Delta G'$ is readily evaluated from Eq. (1) and is rendered significant by the evaluation of τ_+, since this is the only unknown in the electrochemical reaction. $\Delta S'$ is given by Eq. (2), where the coefficient $(dE/dT)_q$ is to be evaluated not only at constant surface charge density but also under conditions such that the reference electrode changes temperature at the same time. Thus there are no liquid junction potentials involved in this or any other measurement here discussed. $\Delta H'$ is given by Eq. (3).

II. APPLICATION TO COLLOIDAL ELECTROLYTES

The foregoing treatment includes as a special case such systems as $AgCl \vdots Cl^-$ or $BaSO_4 \vdots SO_4^=$, and suggests an interesting and possibly important new approach to the study of colloids. Consider again the system

$$Hg \vdots KCl | KCl, HgCl, Hg.$$

When $E=0$ the mercury in the left-hand electrode is covered with chloride ions to such an extent that the transfer of mercurous chloride from the adsorbed state to the solid state can occur without change of free energy Eq. (4). Thus the surface is thermodynamically equivalent to the surface of solid mercurous chloride. By extending measurements of ideal polarized electrodes into the non-polarized range of potentials (which is easily done), information can be obtained about the composition of the electrical double layer in systems of colloidal electrolytes. For example, it may be observed from data

[3] The reverse process would be called desorption-adsorption.

[3a] Γ_+ is defined in Section V or more fully in reference 1.

already in the literature that mercurous chloride in contact with unimolar alkali metal chloride solutions has a diffuse double layer containing about 14 μcoulomb/cm^2 of the alkali metal ion. About 4 μcoulomb/cm^2 of chloride ions are repelled from the interface by the Coulombic repulsion of the adsorbed chloride ions, which must therefore be present at a concentration of about 18 μcoulomb/cm^2.[4] In the same way one could calculate the approximate potentials of the inner and outer Helmholtz planes.[5] The latter is presumably identical with the zeta-potential.

In addition to the thermodynamic properties discussed above there are a considerable number of properties which it is theoretically possible to evaluate but for which there are at present no adequate experimental methods of investigation. For the sake of completeness, we shall indicate what these are and how they are to be evaluated in principle. Since the problem is closely related to the corresponding problem in the thermodynamics of gas adsorption on solids, we shall clarify the ideas involved by first summarizing the thermodynamic treatment of that type of system. Parts of what we shall have to say on this latter subject have been said before, but not in a form to which we can conveniently refer in the discussion which follows.

III. GAS ADSORPTION AT AN INTERFACE

Consider a system composed of a solid in equilibrium with a gas at fugacity f. The free energy change dG involved in transferring dn moles of gas from a standard state of fugacity f^0 to the surface is equal to the free energy change accompanying its decompression to the equilibrium pressure.

$$dG/dn = RT \ln f/f^0. \tag{5}$$

The quantity dG/dn is the differential free energy of adsorption, and its numerical value depends upon one's choice of the standard state. We take for this the liquid state at the temperature T and at a constant pressure of one atmosphere. Then f/f^0 is the activity a of the adsorbed vapor, and Eq. (5) becomes

$$dG/dn = RT \ln a. \tag{6}$$

The integral free energy of adsorption, ΔG, is given by

$$\Delta G = RT \int_0^n \ln a \, dn, \tag{7}$$

which gives the free energy change associated with the process of taking n moles of liquid and putting them on a surface initially bare.

From the definition of free energy we are entitled to write for an isothermal process

$$dG/dn = dH/dn - TdS/dn. \tag{8}$$

The quantity dH/dn is the differential heat of adsorption, and the quantity dS/dn the differential entropy of adsorption.

Consider the adsorption process

Liquid (st'd state)→Gas (adsorbed)

and apply to this the familiar equation $(d\Delta G/dT)_p = -\Delta S$. In accord with our previous nomenclature we shall, however, write dG/dn for ΔG, and so on, giving

$$[d(dG/dn)/dT]_{p,N} = -(dS/dn). \tag{9}$$

The condition of constancy of pressure, it will be recalled, applies to each phase separately and does not mean that the phases need be at the same pressure. The standard state is maintained at constant pressure by definition. The adsorbed gas plus adsorbent (the solid phase) is not ordinarily maintained at constant pressure during a change of temperature, although this could be done by the introduction of an inert, non-adsorbable gas whose pressure is maintained constant, or by other means. The neglect of this thermodynamic requirement introduces an exceedingly small error for which a correction could in principle be made through the relationship $d \ln a/dP = (\bar{V}_1 - V_l)/RT$ where $\bar{V}_1$ is the partial molal volume of the adsorbed gas and V_l the molal volume of the pure liquid. Although $\bar{V}_1$ is not ordinarily known, it is doubtless substantially equal to V_l. In any case the correction is very small because V_l/RT is of the order of 0.3 percent per atmosphere for typical adsorbates.

It will be recalled that in the derivation of the equation $(d\Delta G/dT)_p = -\Delta S$ no change in the

[4] These figures are obtained by a slight extrapolation of data in Fig. 10, reference 1. The point of view here adopted is different from that suggested there on p. 497.

[5] The calculation will be identical with that described in reference 1, p. 487. See also Fig. 16.

amounts of the reactants is envisaged, i.e., the reaction to which ΔG and ΔS refer is not allowed to take place as a result of the change of temperature to which the equation refers. Applied to our system this means that the amount of adsorbed gas must not change, or what are called isosteric conditions must prevail. This result, indicated by the subscript N, has long been familiar, although its logical basis has sometimes been thought obscure.

Combination of Eqs. (6), (8), and (9) gives

$$(d \ln a/dT)_{p,N} = -(dH/dn)/RT^2, \quad (10)$$

which is the counterpart of the Clausius-Clapeyron equation applied to the system here considered.

It is probably helpful to show how these equations are related to the Gibbs adsorption theorem. Recalling the identity

$$uv = \int u dv + \int v du,$$

one has from Eq. (7)

$$\Delta G = nRT \ln a - RT \int_0^n n d \ln a. \quad (11)$$

It will be recalled that this is the free energy change accompanying the transfer of n moles of gas from the standard state to a surface initially bare, but not remaining so, since the surface is not assumed infinite. We wish to find the free energy change ΔG_1 accompanying the *formation* of one square centimeter of covered surface, starting not with a bare surface, but with no surface at all. Calling σ^0 the surface tension of the bare surface, the total free energy change will be

$$\Delta G_1 = \sigma^0 + \Delta G = \sigma^0 + nRT \ln a - RT \int_0^n n d \ln a. \quad (12)$$

This is the free energy change when the gas is initially in its standard state. The free energy change ΔG_2 involved in reducing the gas from the initial (standard) state to the final equilibrium pressure is the same as that given in Eq. (6), except that we now deal with n moles of gas. Therefore

$$\Delta G_2 = nRT \ln a. \quad (13)$$

The free energy change ΔG_3 accompanying the formation of one square centimeter of new surface and the covering of it with n moles of gas which is initially (and continuously) at the equilibrium pressure is therefore given by

$$\Delta G_3 = \Delta G_1 - \Delta G_2 = \sigma^0 - RT \int_0^n n d \ln a. \quad (14)$$

We note that ΔG_3 is the surface tension σ of the covered surface, since it represents the free energy change accompanying the formation of one square centimeter of new surface from a system in equilibrium with the surface. Also, n is now the number of moles adsorbed per square centimeter, which is usually called Γ in discussions of the Gibbs adsorption theorem. Making these substitutions and differentiating Eq. (14) gives

$$d\sigma = -\Gamma d\mu, \quad (15)$$

where μ is the chemical potential defined by the relation

$$d\mu = RT d \ln a.$$

This is the Gibbs adsorption theorem applied to a single component and held at constant temperature. Its extension to any number of components involves nothing more than a repetition of the above steps for each component. Although this is probably not the simplest possible derivation of the theorem, it has the advantage of displaying the relationship of the theorem to the thermodynamic theory of surfaces presented above.

IV. SALT ADSORPTION AT THE ELECTROCAPILLARY MAXIMUM OF AN IDEAL POLARIZED ELECTRODE

At the potential of the electrocapillary maximum of an ideal polarized electrode the results obtained above can be applied with no more than a change of terminology. The differential free energy of adsorption is related to the activity of the dissolved salt in equilibrium with the electrical double layer through Eq. (6). Equation (9) gives the differential entropy of adsorption which may be written, with the aid of Eq. (6),

$$R \ln a + RT d \ln a/dT = -dS/dn, \quad (16)$$

it being understood that here, as in Eq. (9), the amount of adsorbed material per gram of ad-

sorbate is to be held constant. The interpretation of this equation is as follows: If one measures the amount of salt adsorbed at an interface at the potential of the electrocapillary maximum, then it is possible in principle to find another temperature and concentration of electrolyte such that the amount of salt adsorbed per gram of adsorbent (whose geometric shape must not be allowed to change if the adsorbent is a liquid, such as mercury) is unchanged. This information permits one to evaluate $\ln a$ and $d\ln a/dT$ in Eq. (16), giving all that is needed to evaluate the differential entropy of adsorption. The differential heat of adsorption is found most easily from Eq. (10).

V. SALT ADSORPTION AT POTENTIALS OTHER THAN THAT OF THE ELECTROCAPILLARY MAXIMUM

At potentials other than that of the electrocapillary maximum the amounts of positive and negative ions adsorbed are unequal and one can no longer treat the problem in exactly the manner described above. The necessary modifications are very slight, however. Consider a polarized electrode having an electrical double layer of electronic charge q, a surface concentration of cations Γ_+, and a surface concentration of anions Γ_-.[6] Then from considerations of electrical neutrality

$$q/\mathfrak{F}+\Gamma_+z_++\Gamma_-z_-=0, \qquad (17)$$

where z_+ and z_- are the valences of cations and anions, respectively, including sign. It is possible now to hold q constant while varying temperature and composition independently. This is so because one can always vary the imposed electrical potential in such a way as to maintain a constant value of q. At one particular value of $d\ln a/dT$, Γ_+ and Γ_- will also be constant. Therefore one can evaluate $d\ln a/dT$ at constant q, Γ_+, and Γ_-, that is to say, under isosteric conditions. Pressure is constant in the standard and in the adsorbed states. These are the conditions upon which the validity of the equations derived in Sections III and IV depend, and one can therefore apply them to the present case also.

Equation (16) gives dS/dn, the differential entropy of adsorption of equivalent amounts of cations and anions in the double layer. Equation (6) gives the obvious result that the differential free energy of adsorption of the salt is equal to RT times the logarithm of its activity in the solution with which it is in equilibrium. It may be necessary to recall in this connection that the adsorbed material is always regarded as having started in its standard state. The heat of adsorption, dH/dn, is given either by Eq. (8) or Eq. (10).

It will be noted that reaction (h), Section I, is identical with the reaction discussed here except for the factor τ_+ and except for the fact that it is written as a desorptive rather than as an adsorptive process. Therefore the thermodynamic property changes of Eq. (h) can be computed by the methods of this section. Since the sum of the changes in Eqs. (g) and (h) can also be evaluated by the methods of Section I, the property changes of Eq. (g) can also be found. There are as yet no data sufficiently extensive for the full realization of all the calculations here envisaged.

VI. ADSORPTION OF CATION-ELECTRON PAIRS

The electrical double layer at an electrode may be thought of as consisting of adsorbed salt molecules plus adsorbed cation-electron pairs, the cation being in the solution phase and the electron in the metallic phase. Positively charged surfaces would then be thought of as surfaces from which a certain number of cation-electron pairs had been desorbed, the cations having come initially from adsorbed salt molecules.

From this point of view it will be seen that the application of Eqs. (6), (8), (10), and (16) made in the preceding section need not be confined to the adsorption of salt molecules but may be applied with equal validity to the adsorption of cation-electron pairs. It remains only to identify a in the equations. To avoid cumbersome circumlocution let us suppose that the salt in question is potassium chloride and that the metallic phase is mercury. Then a is the activity of *metallic* potassium in equilibrium with the potassium ion-electron pairs in the double layer. There is a concentration of metallic potassium dissolved in the mercury with which the potassium ion-electron pairs are in equilibrium. This concentration is very low and it is immaterial whether or

[6] Strictly speaking, the excess per sq. cm over that which would be present if the concentration were uniform up to a plane defined by the condition that $\Gamma_{solvent}=0$.

not equilibrium is actually attained.[7] The concentration of metallic potassium in the mercury has no real bearing upon the problem, in fact, except as an aid to the imagination. Regarding the mercury as a very dilute potassium amalgam in equilibrium with the solution and with the double layer, it is a simple matter to calculate the activity of the potassium in the amalgam, and this is also the activity of the potassium ion-electron pairs with which it is in equilibrium if the same standard state (the pure metal) is adopted. The activity a_K of the potassium ion-electron pairs is then given through the equation

$$E = E^0 - (RT/\mathfrak{F}) \ln a_+ a_- / a_K, \qquad (18)$$

where E is the potential imposed upon the system measured relative to (say) a calomel electrode and E^0 is the standard electrode potential of the cell

K, KCl|KCl, HgCl, Hg.

Note that E is not the e.m.f. of this cell. a_+ and a_- are the activities of the cation and anion, respectively, in the solution.

To show this, consider the cell

K(Hg), KCl|KCl, HgCl, Hg,

whose e.m.f. is given by Eq. (18). If the potassium amalgam were made sufficiently dilute, the e.m.f. would fall in the range of potentials where the mercury is regarded as an ideal polarized electrode. Since the system is at equilibrium, the activity of metallic potassium must be the same within the mercury and in the double layer, it being a matter of no consequence that the potassium is "hydrated" in the latter.

Since the entropy, enthalpy, and free energy of adsorption of cation-electron pairs may be expressed in units of energy per faraday, it is appropriate to designate these quantities dS/dq, dH/dq, and dG/dq. This serves to distinguish them from the corresponding quantities for salt adsorption.

[7] This point is discussed in reference 1, p. 445. Results of the calculation in an actual case are there given.

VII. ENTROPY, ENTHALPY, AND FREE ENERGY OF FORMATION OF THE DOUBLE LAYER

At the potential of the electrocapillary maximum the entropy of formation of the double layer from its constituent molecules is easily evaluated by integrating dS/dn over the number of moles of salt adsorbed. One needs to know dS/dn and n at the electrocapillary maximum for a series of concentrations from the value at which one wishes the information down to concentrations so low that n is essentially zero. The *absolute* entropy of the double layer could then be evaluated by adding on the entropy of the adsorbate in its standard state.

At potentials other than that of the electrocapillary maximum the entropy of formation of the double layer can be found by first calculating the entropy at the electrocapillary maximum and then adding on the entropy of adsorption of the additional salt present together with the entropy of the cation-electron pairs. The first of these is found by integrating dS/dn over the range of values of n occurring between the electrocapillary maximum and the potential under consideration. The entropy of the cation-electron pairs is found in an analogous manner by integrating dS/dq over q.

The enthalpy and free energy of formation of the electrical double layer are to be found in exactly the same manner using dH/dn, dH/dq, dG/dn, or dG/dq as the case requires.

Although it is unlikely that enough experimental data will ever be accumulated for the evaluation of all of the thermodynamic quantities described in this paper for even a single case, it is the expectation of the writer that the recognition of the existence of these properties and the evaluation of some of them will prove worth while.

The author is grateful to the Research Corporation[8] for a grant in support of this work.

[8] Frederick Gardner Cottrell grant.

THE JOURNAL OF CHEMICAL PHYSICS VOLUME 16, NUMBER 12 DECEMBER, 1948

Electronic States of Organic Molecules[1,2]

WILLIAM T. SIMPSON[3]
Department of Chemistry, University of California, Berkeley, California
(Received June 11, 1948)

The spectra of three simple dye-like molecules, and of benzene and naphthalene, are treated in a semiquantitative fashion. The methods employed are the bond orbital, the molecular orbital (somewhat modified), the antisymmetrized molecular orbital, and two models, one related to the bond orbital, the other to the molecular orbital. The positions of main and second-order bands, and intensities, are calculated. Extension of the calculations to complex cases is indicated.

I. INTRODUCTION

THE study of the relation between absorption spectra (or, loosely, color) and structure of unsaturated molecules has in the past been hindered by the complicated character of readily available molecules. Even benzene is a rather difficult subject for study, because of the presence of a fourfold transition degeneracy. Accordingly, the writer has completed an extraordinarily simple series by the synthesis of the lower and higher vinylogs[4] of

$$II - Me_2N^{\oplus}{=}CH{-}CH{=}CH{-}CH{=}CH{-}\bar{N}Me_2.[5]$$

The series

$$Me_2N^{\oplus}{=}CH{-}(CH{=}CH){-}\bar{N}Me_2$$
$$I, II, III$$

TABLE I. Colors and intensities of five unsaturated compounds.

Substance			
I	309		
	2700		
II	409	253	
	4610	weak	
III	511	305	266
	6720	weak	weak
Benzene[a]	260	200	180
	weak	strong	strong
Naphthalene[b]	308	275	221
	weak	strong	strong

[a] E. P. Carr and H. Stücklen, J. Chem. Phys. **4**, 760 (1936).
[b] Ultraviolet spectrograms issued by the American Petroleum Institute, Research Project 44, at the National Bureau of Standards (1947). Serial No. 169.

has now been studied. (Actually, compound *III* was obtained with a 4-acetoxy substituent, but it has already been shown[6] that such a substitution has practically no effect on the absorption maximum of similar dyes.)

The spectra of the compounds in the series are shown in Fig. 1.

It will be convenient in referring to these spectra to use λ_{max} in $m\mu$. Moreover, it will prove necessary to consider data for benzene and naphthalene; hence, Table I is presented as a convenient compilation. One can justify the use of λ_{max} by associating it with vertical excitation—excitation in which nuclear motion is slight. The numbers to the right of the colors are

$$\int \epsilon_{10} d \log_{10} \nu.$$

The writer prefers to adopt this integral as a measure of intensity since it is a linear function of the Einstein transition probability and is also simply related to the form taken by spectrophotometric data.

The spectral data will be analyzed in five different ways. Two general quantitative methods for relating color to structure are available. One may be called a natural method, the other, a model. The natural methods used will be the HLSP, or bond orbital, the HMH or molecular orbital, and the Goeppert-Mayer-Sklar (GMS)[7] or antisymmetrized molecular orbital method. In addition, two models will be presented: one, based on the bond orbital, is a modification of the theory of Lewis and Calvin;[8] the other, based on the mo-

[1] Abstracted from a Ph.D. thesis, University of California, Berkeley, California.
[2] This work was supported in part by a fellowship grant from the Shell Development Company, Emeryville, California.
[3] Present address: Department of Chemistry, University of Washington, Seattle, Washington.
[4] To be published elsewhere.
[5] W. König and W. Regner, Ber. **63**, 2823 (1930).
[6] W. König, Ber. **67**, 1274 (1934).
[7] M. Goeppert-Mayer and A. L. Sklar, J. Chem. Phys. **6**, 645 (1938).
[8] G. N. Lewis and M. Calvin, Chem. Rev. **25**, 273 (1939).

lecular orbital point of view, was recently given by Bayliss[9] (and was independently developed by the writer[10]).

II. THE BOND ORBITAL METHOD

The application of the method to the calculation of resonance energies is well known. Sklar[11] used solutions of the secular equation other than just that for the ground state and was able to calculate the positions of some but not all of the absorption bands of benzene. Others[12,13] have applied a more generalized form, a form which appears to destroy the quantitative aspects to a certain degree, to more complex molecules.

The aim in the following will be to use the less "general" method, in which almost all of the canonical wave functions are employed.* Drastic simplifications inherent in the method[14] are augmented by several more.

The Coulomb integral is constant in benzene, but cannot be expected to remain constant in the less symmetrical dyes. Yet constancy of Q is assumed. The ionic mesomers, taken over into the bond orbital method as representing wave functions, would cause one to introduce a variety of integrals. The simplification is therefore made that ionic mesomers are associated with excited covalent functions. For instance, the mesomer:

of benzene would be represented by the Rümer diagram

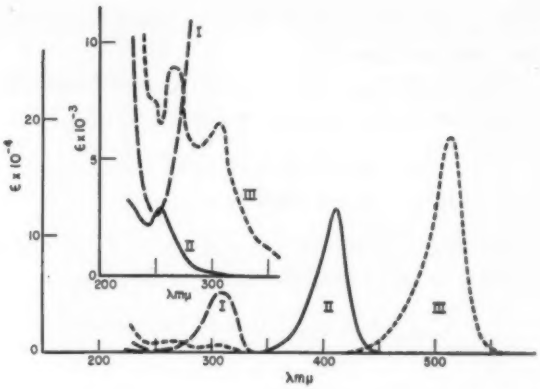

FIG. 1. Spectra of dyes *I*, *II*, and *III*.

which Rümer diagram is usually associated with the mesomer

The general scheme is to treat all long bonds and all bonds to X as having exchange integral zero, but to allow one parameter in addition to the "all-purpose" C—C exchange integral α. This parameter, γ, is the exchange fraction of the C—N bond. For example, the mesomeric form

$$Me_2N^{\oplus}{=}CH{-}\bar{C}^{\ominus}H{-}CH{=}N^{\oplus}Me_2$$

is represented by the Rümer diagram

and the energy of the form, obtained from Pauling's rules[15] and

is

$$H=Q+2\gamma-\alpha.$$

It will be seen that since the coefficient of Q is the same as that of Δ in the secular equation, and Q is assumed to be constant,

$$\Delta W=f(\alpha,\gamma).$$

Hence the colors of dyes *I* and *II* determine α

[9] N. S. Bayliss, J. Chem. Phys. **16**, 287 (1948).
[10] The model presented by Bayliss appeared in publication at the time of the completion of the writer's Ph.D. thesis.
[11] A. L. Sklar, J. Chem. Phys. **5**, 669 (1937).
[12] K. F. Herzfeld and A. L. Sklar, Rev. Mod. Phys. **14**, 294 (1942).
[13] T. Förster, Zeits. f. physik. Chemie **B47**, 245 (1940); **B48**, 12 (1941).
* All the mesomeric forms with one positive charge at some point in the dye chain, as well as all the forms with one negative charge on a carbon, are represented.
[14] A. S. Coolidge and H. M. James, J. Chem. Phys. **2**, 811 (1934).
[15] L. Pauling, J. Chem. Phys. **1**, 280 (1933).

and γ, and the method may be used to calculate the color of dye *III*.

Putting in λ_{max} for *I* and *II* one obtains (after computation for various ratios of γ/α),

$$\alpha = 39.0 \text{ kcal./mole},$$
$$\gamma = 1.55\alpha.$$

Then one computes the color of *III* using the same γ/α ratio and the same α, obtaining

$$\lambda_{max} = 466\ m\mu \text{ (allowed transition)},$$

while

$$\lambda_{max} \text{ (observed)} = 511\ m\mu \text{ (intensity} = 6720).$$

Although a factoring into symmetric and antisymmetric parts of the secular equation was obtained, the computation was still quite laborious. It appears that an expansion of the empirical basis in order to represent ionic mesomers more rigorously (and necessitating the simultaneous fitting of more data) would not be feasible.

III. THE MODIFIED LEWIS AND CALVIN MODEL

Perhaps a method that uses an exact solution of the Schrödinger equation (but which is associated with the dyes in a rather more farfetched manner than the B.O. method) might have value. The use of the equation for the harmonic oscillator in molecular vibration problems is a similar device. The success of the theory is unquestioned, so that now one thinks of the atoms of molecules as oscillators. The Lewis and Calvin method[10] for polyenes (but not for cyanines) is based on a model, the harmonic oscillator. An analogous treatment of the simple dyes considered in the foregoing based on the "particle in a box" will be given. Some of the concepts of the Lewis and Calvin method are changed in order to improve the plausibility of association of molecule with model.

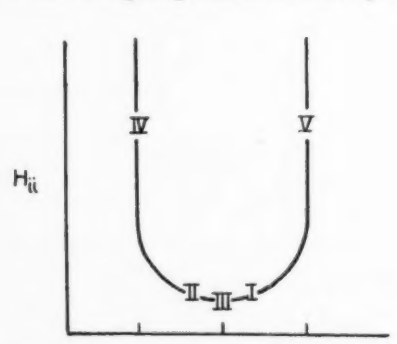

FIG. 2. Units of C—C distance; plot of energy *vs.* position of center of mass of unsaturation electrons for a three carbon dye of type *I*.

Description of the Model

The Lewis and Calvin theory is reviewed. Experimentally, in the diphenylpolyenes the color is a linear function of $n^{\frac{1}{2}}$, where n is the number of double bonds. The quantitative aspect of the theory is just that it predicts the same relation. It is assumed that the unsaturation electrons are coupled so as to move in concert in an approximate force field $-kx$, with an effective mass $m = nM$, where M is the mass of two electrons. The mesomeric forms:

$$—(CH{=}CH)_n— \qquad \text{(a)}$$

$$\oplus\ominus{=}(CH—CH)_n{=}\ominus\oplus \qquad \text{(b)}$$

suggest such a motion in that there is one less bond, and charge separation, in the (b) set of mesomeric forms.

The amidinium dyes *I*, *II*, and *III* (and many other vinylene homologous series) obey approximately the rule $\lambda = 100n + c$, where $n-1$ is the number of double bonds, and, as is verifiable,

$$m = nM$$

gives the mass of unsaturation electrons.

The model, a particle in a box, has a color

$$\lambda = (8Mca^2/3h)n,$$

where m is the mass, a is the box dimension, and $m = nM$ is substituted. The exponent of n, unity, conforms to the behavior of the amidinium dyes. Thus, it remains to be shown that the mesomeric forms suggest the motion of a particle in a box in order that the association of model with experiment be as plausible as Lewis and Calvin's treatment of the polyenes.

Rather than assume that the unsaturation electrons move in concert (in order to be able to make the substitution, $m = nM$), we make the assumption that *the center of mass of the unsaturation electrons is quantized*, and it is the motion of this center of mass that gives rise to the characteristic electronic energy levels. It is felt that motion in concert does not in any sense take place, and that in the diphenylpolyenes as well,

it is the harmonic oscillation of the center of mass that gives rise to the color.

The B.O. method can be used, in principle, as a tool for plotting points representing the potential function in which the center of mass moves. Considering the mesomers:**

$$I \quad A^{\oplus}{=}CH{-}CH{=}CH{-}\bar{A},$$
$$II \quad \bar{A}{-}CH{=}CH{-}CH{=}A^{\oplus},$$
$$III \quad A^{\oplus}{=}CH{-}\bar{C}^{\ominus}H{-}CH{=}A^{\oplus},$$
$$IV \quad \bar{A}{-}\bar{C}^{\ominus}H{-}\bar{C}^{\ominus}H{-}C^{\oplus}H{-}A^{\oplus\oplus},$$
$$V \quad A^{\oplus\oplus}{-}C^{\oplus}H{-}\bar{C}^{\ominus}H{-}\bar{C}^{\ominus}H{-}\bar{A},$$

as bond eigenfunctions, one plots the diagonal elements of the secular equation against the center of mass of the unsaturation electrons (Fig. 2). One can write many more mesomers, and, in fact, can easily conceive of the points being joined to form a smooth curve. The essential feature of the curve is that it goes rapidly to "infinity" as the center of mass moves a distance C—C from the midpoint of the potential box. Several of the mesomers for the next higher homolog, the dye $VI\ A^{\oplus}{=}CH{-}CH{=}CH{-}CH{=}CH{-}\bar{A}$,

$$VII \quad \bar{A}{-}\bar{C}^{\ominus}H{-}\bar{C}^{\ominus}H{-}\bar{C}^{\ominus}H{-}C^{\oplus}H{-}C^{\oplus}H{-}A^{\oplus\oplus}$$
$$VIII \quad \bar{A}{-}\bar{C}^{\ominus}H{-}\bar{C}^{\ominus}H{-}C^{\oplus}H{-}CH{=}CH{-}A^{\oplus\oplus},$$

are plotted on a similar curve (see Fig. 3), and it is seen that the potential rises rapidly as the center of mass moves a distance 1½ C—C from the midpoint, but that even as the center of mass moves C—C the potential has become very high, perhaps as high as the points *IV* and *V* in the graph for the three-carbon dye. The center of mass can move farther than the limiting values *IV*, *V*, and *VII* only by utilization of states corresponding to the next higher value of the principal quantum number. Even though the values H_{ii} are not known, it can hardly be questioned that the walls are steep. It can also be seen that, in contradistinction to the diphenylpolyene case, there is freedom of movement of the center of mass on the bottom of the box.

If we use the fact that c is almost zero in $\lambda = 100n + c$, we can solve for the box dimension in

$$\lambda = (8Mca^2)/3h)n.$$

The latter equation expresses the change in color of a dynamical system as a function of the mass of the particle measured in electron pairs. Correlating the former equation with the latter amounts to the assertion that the effect of adding vinyl groups, of increasing the center of mass of the unsaturation electrons, is only to add to the mass of the moving particle without changing the box dimension. The argument of the preceding paragraph was intended to indicate the plausibility of the assumed constant box dimension. $a = A$ is found to be 2.13A, a value which, from the plots of H_{ii} *vs.* C—C, is seen to be reasonable. (C—C is approximately 1.40A.)

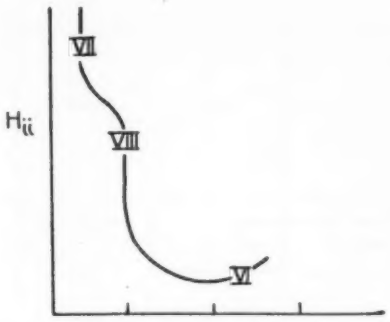

FIG. 3. Units of C—C; plot of energy *vs.* center of mass for dye type *II*.

Extension to Complex Cases

The c in $\lambda = 100n + c$ is not always close to zero. It is occasionally negative as with $(O{=}CH{-}CH{=}CH{-}CH{=}CH{-}\bar{O}^{\ominus})$[16] for which $\lambda = 362$ $m\mu$. This case is explained in a rather forced manner by the assumption of motion of somewhat less than $n+1$ electron pairs. The dyes

$$\phi{-}N^{\oplus}H{=}CH{-}CH{=}CH{-}\bar{N}H{-}\phi$$

and

$$\phi N^{\oplus}H{=}CH{-}CH{=}CH{-}CH{=}CH{-}\bar{N}H\phi$$[17]

for which c is positive (the usual sign of c), are represented approximately by

$$\lambda = 100n + 84.$$

** The use of Roman numerals to denote the mesomers is not to be confused with the abbreviations for the simple amidinium dyes,

[16] G. Schwarzenbach, K. Lutz, and E. Felder, Helv. Chim. Acta. **27**, 579 (1944).

[17] L. G. S. Brooker, F. L. White, G. H. Keyes, C. P. Smyth, and P. F. Oesper, J. Am. Chem. Soc. **63**, 3194 (1941).

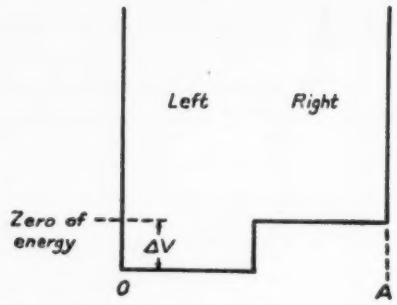

FIG. 4. Potential box representing unsymmetrical dyes.

Here the formal explanation is that the end phenyls contribute a constant amount equal to about 0.84 of the mass of an electron pair, but that each new vinyl group contributes a full electron pair.

It is possible to represent unsymmetrical dyes by a similar model possessing the attribute that the bottom of the box has a step. The step is arbitrarily placed in the middle of the box, and the solution of the problem obtained exactly. For instance, if $n=4$ and there is a flat bottom, the color is $\lambda=400\ m\mu$, while if a potential as shown in Fig. 4, where $\Delta V=-h^2/32MA^2$ is used, a computation reveals that the color is 389 $m\mu$. Furthermore, if $n=5$ had been considered, the ΔV term would have been correspondingly larger so that the color would have been "less" than 489 $m\mu$. The results of Brooker[18] and co-workers can thus be explained in terms of the model. The calculations follow.

The Particle in a Stepped Well

The potential is illustrated in Fig. 4. Then, if $K=8\pi^2m/h^2$, the two Schrödinger equations for the left and right regions are:

$$\psi_L''+K(E-\Delta V)\psi_L=0,$$
$$\psi_R''+K(E)\psi_R=0.$$

For the right region

$$\psi_R=R_1\exp(i\alpha x)+R_2\exp(-i\alpha x);\quad(\alpha=(KE)^{\frac{1}{2}})$$

is a solution, while for the left,

$$\psi_L=L_1\exp(i\beta x)+L_2\exp(-i\beta x);$$
$$(\beta=(K(E-\Delta V)^{\frac{1}{2}}.)$$

When $x=0$, we want ψ_L to be zero, so we particularize ψ_L to

$$\psi_L=L\sin\beta x$$

by setting $L_2=-L_1$.

To accomplish the same thing with respect to the right region we rewrite ψ_R:

$$\psi_R=\bar{R}_1\exp(i\alpha x)\exp(-i\alpha A)+\bar{R}_2\exp(-i\alpha x)\exp(i\alpha A),$$
$$=\bar{R}_1\exp(i\alpha(x-A))+\bar{R}_2\exp(-i\alpha(x-A)).$$

Then as for the left, if $\bar{R}_2=-\bar{R}_1$,

$$\psi_R=R\sin\alpha(x-A).$$

The condition that, at $A/2$, $\psi_L=\psi_R$ and $\psi_L'=\psi_R'$ leads to the quantum conditions:

$$\frac{L}{R}=\frac{\sin(\alpha A/2)}{\sin(\beta A/2)}=-N,$$

$$\frac{L}{R}=\frac{(\alpha A/2)\cos(\alpha A/2)}{(\beta A/2)\cos(\beta A/2)}=N,$$

or, with

$$\theta=\alpha A/2\quad\text{and}\quad\phi=\beta A/2,$$
$$\sin\theta/\sin\phi=-N;\quad\theta\cos\theta/\phi\cos\phi=N.$$

The Numerical Value

If $\Delta V=0$, the ground state energy is

$$E_0{}^0=h^2/8mA^2.$$

This becomes (if there are n electron pairs, each of mass M), $E_0{}^0=(h^2/8MA^2)/n$, and, selecting a typical case, $n=4$; we obtain:

$$E_0{}^0=h^2/32MA^2.$$

If ΔV is taken to be only a small fraction of $E_0{}^0$, the energy levels are shifted but the color E_1-E_0 remains virtually unchanged. If $\Delta V=-h^2/32MA^2$, on the other hand, an appreciable change in the color occurs. (This $\Delta V\cong1$ ev for $A=2.13$A.) It is clear that the ratio of ΔV to $E_0{}^0$ increases for dyes for which n, the number of electron pairs, has increased, so that the difference $(E_1-E_0)-(E_1{}^0-E_0{}^0)$ would be expected to become greater with increasing n.

We compute $\phi=\phi(\theta)$.

$$\phi=A/2(K(E-\Delta V))^{\frac{1}{2}}=((A^2/4)KE-(A^2/4)K\Delta V)^{\frac{1}{2}}.$$

Since $\theta=A/2(KE)^{\frac{1}{2}}$, with $m=4M$,

$$\phi=(\theta^2+\pi^2/4)^{\frac{1}{2}}.$$

[18] L. G. S. Brooker, Rev. Mod. Phys. **14**, 275 (1942).

Next we employ the quantum conditions by plotting $N=N(\theta)$ for each condition. The common points of the two functions lie at

$$\theta=1.038,\ 2.956,\ \cdots.$$

From these values we can compute the energies:

$$E_0=0.436h^2/8mA^2,\quad E_1=3.524h^2/8mA^2,$$

and find $\Delta E=3.088h^2/8mA^2$, corresponding to 389 $m\mu$. We continue the discussion of complex cases.

Steric Hindrance

The findings of Brunings and Corwin[19] with regard to steric hindrance in cyanines can be understood in terms of the model. One must be willing to consider that the effect can be represented by a potential well of the form illustrated in Fig. 5. Then simple perturbation theory shows that the ground state is raised in energy while the excited state, which ψ has a node at the midpoint, is affected only slightly by the perturbing potential hump. The energy difference is decreased and the color shifts towards longer wave-lengths. If the width of the hump were decided by convention, the height could be calculated exactly from the colors of a given pair of dyes in which the only distinguishing feature (with respect to effects on the unsaturation electron system) was steric hindrance.

The Intensity

The Einstein absorption coefficient B_{12} for the particle in a box is found to be[20]

$$B_{12}=(2048/243)e^2A^2/\pi h^2,$$

or, if E is the charge of an electron pair and n the number of electron pairs,

$$B_{12}=(2048/243)E^2A^2/\pi h^2n^2=2.57\times10^{19}n^2.$$

A is assumed to be 2.13A. The relation between ϵ and B, where ϵ is defined by

$$I/I_0=10^{-\epsilon K\Delta x},$$

K is the concentration in moles per liter, and Δx the path length, is:

$$\int \epsilon d\ \log_{10}\nu=BNh/(2.303)^2\cdot1000\cdot c$$
$$=2.50\times10^{-17}B.$$

ν can be measured in cm^{-1}, and N is Avogadro's number.

The intensities of *I*, *II*, and *III* are tabulated along with the calculated intensities (obtained by setting $n=3$, 4, and 5, respectively, in the equation for B_{12}). (See Table II.)

TABLE II. Intensities of dyes I, II, and III.

n	calculated	observed	calc./obs.
3	5,780	2,700	2.14
4	10,300	4,610	2.24
5	16,100	6,720	2.40

Second-Order Bands

The theory predicts one forbidden band at

$$(2^2-1^2)/(3^2-1^2)\lambda=0.375\lambda,$$

if λ is the main band. Dye *III* exhibits two bands (each of which can be identified with the prediction), one at 0.60λ, the other at 0.52λ. The molecular orbital method and the model which is based on the M.O. method give better accounts of the second-order bands.

The modified Lewis and Calvin method makes no provision for a recognition of effects caused by electron spin. The M.O. systems at least formally recognize the possibility of a singlet-triplet split, and so are in better agreement with experiment.

Yet it is felt that the center of mass model is somewhere near the truth, and is likely to be

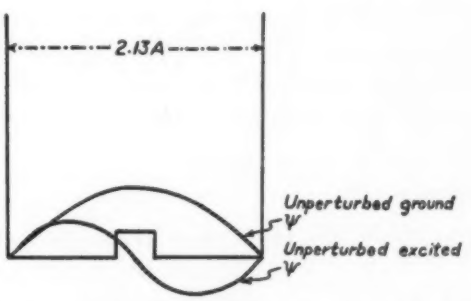

FIG. 5. Potential box representing dyes with steric hindrance.

[19] K. J. Brunings and A. H. Corwin, J. Am. Chem. Soc. 64, 593 (1942).

[20] V. Rojansky, *Introductory Quantum Mechanics* (Prentice Hall, Inc., New York, 1938), p. 167.

TABLE III. Energies and transition energies calculated for dye *I*.

Level	x	W	Transition	ΔW
$3A$	1.831	3.495	$2A, 2B$	1.398
$2B$	1.372	2.133	$1B, 2B$	2.575
$2A$	0.617	0.735		
$1B$	−0.499	−0.442		
$1A$	−1.545	−1.102		

useful in a semiquantitative way, a companion to the mesomeric methods currently being applied.

IV. THE MOLECULAR ORBITAL METHOD

The experimental data available make possible the introduction of a fairly elaborate empirical system, provided that computational difficulties don't interfere. The bond orbital method is tedious to the point that a thorough exploration of the possibilities for constructing a satisfactory theory was not made. The molecular orbital method is more simple.

It was possible to fit the experimental data considered to a rather unexpected degree of precision. Considering the split of the fourfold degenerate transition in benzene to be due to electronic interaction,[21] one would not expect to obtain (from a theory which neglects electronic interaction) results to better than, say, 20 percent. The uncertainty introduced through a neglect of the singlet-triplet split is yet an additional disturbing factor,[22] but by a suitable choice of four parameters one can calculate the positions of ten absorption bands with an accuracy somewhat exceeding the estimated 20 percent.

The method is, of course, not quantum theoretical, but only suggested by quantum mechanics. Its "success" lies in its empiricism. We shall consider the calculation for dye *I* in some detail, and in so doing shall demonstrate a procedure for taking into account the variation of H, the Hamiltonian, with position in the molecule. It is through a recognition of this effect that we can construct a satisfactory theory.

Dye *I*

The dye

$$\underset{1}{Me_2N^{\oplus}}=\underset{2}{CH}-\underset{3}{CH}=\underset{4}{CH}-\underset{5}{\bar{N}}Me_2$$

belongs to C_{2v}. Consequently, the linear combinations of atomic orbitals out of which the one-electron wave functions are to be built must be, according to group theoretic arguments,

$$\begin{aligned} &A && B \\ &\bar{1}=\underline{1}+\underline{5} \quad \text{and} && \bar{1}=\underline{1}-\underline{5}, \\ &\bar{2}=\underline{2}+\underline{4}, && \bar{2}=\underline{2}-\underline{4}, \\ &\bar{3}=\underline{3}, \end{aligned}$$

where $\underline{i}$ is the atomic orbital associated with the ith center. The transition of longest wave-length will be one in which an electron jumps from an A to a B state. The direct product of AB transforms like the vector pointing in the long direction of the molecule; hence the transition is allowed and might be expected to be intense. The general selection rule for the family of dyes *I*, *II*, and *III* is simply that an AB or a BA transition is allowed; BB and AA transitions are forbidden.

We shall make use of the following abbreviations:

$H_{\underline{i}\underline{i}}=Q$ unless $\underline{i}$ is on the end when
$H_{\underline{i}\underline{i}}=Q-q$.
$H_{\underline{i}\underline{j}}=B$ unless $\underline{i}$ or $\underline{j}$ are on the end when
$H_{\underline{i}\underline{j}}=B-b$. (If $|i-j|>1$, $H_{\underline{i}\underline{j}}=0$.)
$\Delta_{\underline{i}\underline{i}}=1$,
$\Delta_{\underline{i}\underline{j}}=s$ (unless $|i-j|>1$ when $\Delta_{\underline{i}\underline{j}}=0$).

Now we can obtain the B levels for dye *I*. We drop the overline so that $\bar{\imath}$ becomes i.

Evaluation of the matrix elements gives

$$\begin{aligned} &H_{11}=2Q-2q, \quad H_{22}=2Q, \quad H_{12}=2B-2b, \\ &\Delta_{11}=2, \quad \Delta_{22}=2, \quad \Delta_{12}=2s, \end{aligned}$$

the secular equation becoming

$$\begin{array}{c|cc} & \bar{1} & \bar{2} \\ \hline \bar{1} & 2Q-2q-2W & 2B-2b-2sW \\ \bar{2} & 2B-2b-2sW & 2Q-2W \end{array} =0.$$

If we substitute $\alpha=B-sQ$[23] and divide by 4 we obtain

$$\begin{vmatrix} (Q-W)-q & \alpha+s(Q-W)-b \\ \alpha+s(Q-W)-b & (Q-W) \end{vmatrix} =0.$$

[21] A. L. Sklar, Rev. Mod. Phys. **14**, 232 (1942).
[22] G. N. Lewis and M. Kasha, J. Am. Chem. Soc. **66**, 2100 (1944).
[23] R. S. Mulliken and C. A. Rieke, J. Am. Chem. Soc. **63**, 1770 (1941).

Then if $Q-W=y$, after several divisions by $(\alpha+sy)$,[24] we have

$$\begin{vmatrix} \dfrac{y}{\alpha+sy}-\dfrac{q}{\alpha+sy} & 1-\dfrac{b}{\alpha+sy} \\ 1-\dfrac{b}{\alpha+sy} & \dfrac{y}{\alpha+sy} \end{vmatrix}=0.$$

Now we let $x=y/(\alpha+sy)$. Then

$$y=\alpha x/(1-sx), \quad W=Q-\alpha x/(1-sx).$$

$b/(\alpha+sy)$ becomes $(b/\alpha)(1-sx)$ and $q/(\alpha+sy)$ becomes $(q/\alpha)(1-sx)$. We obtain

$$\begin{vmatrix} x-(q/\alpha)(1-sx) & 1-(b/\alpha)(1-sx) \\ 1-(b/\alpha)(1-sx) & x \end{vmatrix}=0.$$

It is found that $q/\alpha=1.13$, $b/\alpha=0.08$, and $s=0.26$*** are "selected" by the data. Although it cannot be asserted that the values used are optimal, it is believed that each is determined to within about 10 percent.

The secular equation becomes:

$$\begin{vmatrix} 1.294x-1.13 & 0.021x+0.92 \\ 0.021x+0.92 & x \end{vmatrix}=0,$$

with solutions

$$x=1.372, \quad -0.499.$$

Proceeding in a similar fashion, we find for the A secular equation:

$$\begin{vmatrix} 1.294x-1.13 & 0.021x+0.92 & 0 \\ 0.021x+0.92 & x & 1 \\ 0 & 2 & x \end{vmatrix}=0.$$

The solutions are:

$$x=-1.545,\ 1.831,\ 0.617.$$

The energies are obtained from

$$W=Q-\alpha x/(1-sx).$$

We shall commonly measure energy in units of $-\alpha$ with Q as origin. The energies are tabulated below (Table III). The levels are labeled serially within a symmetry type. A space indicates the boundary between filled and unfilled levels in the ground state.

[24] G. W. Wheland, J. Am. Chem. Soc. 63, 2025 (1941).

*** It turns out that s can be calculated, and is 0.25 or 0.26. The mutual confirmation is somewhat fortuitous.

TABLE IV. Energies and transition energies calculated for dye *II*.

Level	x	W	Transition	ΔW
4*A*	1.892	3.724	2*B*, 3*A*	1.065
3*B*	1.597	2.731	2*A*, 3*A*	1.917
3*A*	1.130	1.600	2*B*, 3*B*	2.196
2*B*	0.470	0.535		
2*A*	−0.345	−0.317		
1*B*	−1.164	−0.894		
1*A*	−1.774	−1.214		

Dye *II*

We proceed just as in the case of dye *I*. The trial functions of proper symmetry are:

A	B
$\bar{1}=\underline{1}+\underline{7}$,	$\bar{1}=\underline{1}-\underline{7}$,
$\bar{2}=\underline{2}+\underline{6}$,	$\bar{2}=\underline{2}-\underline{6}$,
$\bar{3}=\underline{3}+\underline{5}$,	$\bar{3}=\underline{3}-\underline{5}$.
$\bar{4}=\underline{4}$,	

Solving the B problem first, we obtain a secular equation in x:

$$\begin{vmatrix} 1.294x-1.13 & 0.021x+0.92 & 0 \\ 0.021x+0.92 & x & 1 \\ 0 & 1 & x \end{vmatrix}=0,$$

which has solutions:

$$x=0.470,\ 1.597,\ -1.164.$$

The A secular equation is

$$\begin{vmatrix} 1.294x-1.13 & 0.021x+0.92 & 0 & 0 \\ 0.021x+0.92 & x & 1 & 0 \\ 0 & 1 & x & 1 \\ 0 & 0 & 2 & x \end{vmatrix}=0,$$

TABLE V. Energies and transition energies calculated for dye *III*.

Level	x	W	Transition	ΔW
5*A*	1.926	3.858	3*A*, 3*B*	0.832
4*B*	1.717	3.102	2*B*, 3*B*	1.504
4*A*	1.390	2.177	3*A*, 4*A*	1.758
3*B*	0.944	1.251	2*A*, 3*B*	1.997
3*A*	0.378	0.419		
2*B*	−0.271	−0.253		
2*A*	−0.925	−0.746		
1*B*	−1.487	−1.072		
1*A*	−1.866	−1.256		

with solutions

$$x=-0.345,\ 1.130,\ 1.892,\ -1.774.$$

The results are tabulated in Table IV.

Dye *III*

The wave functions are:

$$A \qquad B$$

$$\bar{1}=\underline{1}+\underline{9}, \quad \bar{1}=\underline{1}-\underline{9},$$

$$\bar{2}=\underline{2}+\underline{8}, \quad \bar{2}=\underline{2}-\underline{8},$$

$$\bar{3}=\underline{3}+\underline{7}, \quad \bar{3}=\underline{3}-\underline{7},$$

$$\bar{4}=\underline{4}+\underline{6}, \quad \bar{4}=\underline{4}-\underline{6}.$$

$$\bar{5}=\underline{5},$$

We solve the B problem first. The secular equation is

$$\begin{vmatrix} 1.294x-1.13 & 0.021x+0.92 & 0 & 0 \\ 0.021x+0.92 & x & 1 & 0 \\ 0 & 1 & x & 1 \\ 0 & 0 & 1 & x \end{vmatrix}=0,$$

with solutions:

$$x=0.944,\ -0.271,\ 1.717,\ -1.487.$$

The A secular equation is

$$\begin{vmatrix} 1.294x-1.13 & 0.021x+0.92 & 0 & 0 & 0 \\ 0.021x+0.92 & x & 1 & 0 & 0 \\ 0 & 1 & x & 1 & 0 \\ 0 & 0 & 1 & x & 1 \\ 0 & 0 & 0 & 2 & x \end{vmatrix}=0,$$

with solutions

$$x=0.378,\ 1.390,\ -0.925,\ 1.926,\ -1.866.$$

The results are in the Table V.

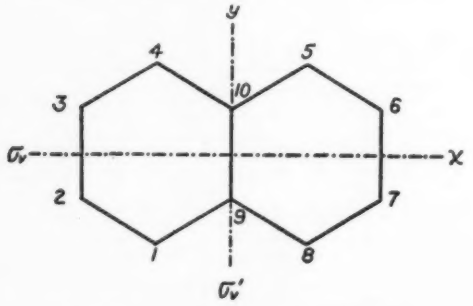

FIG. 6. Coordinates of naphthalene.

Naphthalene

We adopt the conventions, illustrated in Fig. 6, with regard to the numbering and symmetry axes. Then disregarding the horizontal plane we assign the molecule to C_{2v}. The character table is

	E	C_2	σ_v	σ_v'
z, A_1	1	1	1	1
A_2	1	1	−1	−1
x, B_1	1	−1	1	−1
y, B_2	1	−1	−1	1
Γm	10	0	0	2

Applying $\sum_R \chi(R)R$[25] to the atomic orbitals we obtain the following sets of linear combinations:

$$A_1 \qquad A_2$$

$$\bar{1}=\underline{1}+\underline{5}+\underline{4}+\underline{8} \quad \bar{1}=\underline{1}+\underline{5}-\underline{4}-\underline{8}$$

$$\bar{2}=\underline{2}+\underline{6}+\underline{3}+\underline{7} \quad \bar{2}=\underline{2}+\underline{6}-\underline{3}-\underline{7}$$

$$\bar{3}=\underline{9}+\underline{10}$$

$$B_1 \qquad B_2$$

$$\bar{1}=\underline{1}-\underline{5}+\underline{4}-\underline{8} \quad \bar{1}=\underline{1}-\underline{5}-\underline{4}+\underline{8}$$

$$\bar{2}=\underline{2}-\underline{6}+\underline{3}-\underline{7} \quad \bar{2}=\underline{2}-\underline{6}-\underline{3}+\underline{7}$$

$$\bar{3}=\underline{9}-\underline{10}.$$

We now obtain the energy levels for the various symmetry types.

Representations A_2 and B_1

Employing the usual transformations, we obtain for A_2

$$\begin{vmatrix} x & 1 \\ 1 & x-1 \end{vmatrix}=0,$$

with $x=1.618,\ -0.618$.

For B_1 we find

$$\begin{vmatrix} x & 1 \\ 1 & x+1 \end{vmatrix}=0; \quad x=-1.618,\ 0.618.$$

[25] H. Eyring, J. Walter, and G. E. Kimball, *Quantum Chemistry* (John Wiley and Sons, Inc., New York, 1944), p. 189.

TABLE VI. Energies and transition energies calculated for naphthalene.

Level	x	W	Transition	ΔW
$3B_2$	2.181	5.037	$1A_2$, $2B_1$*	1.269
$2A_2$	1.618	2.794	$1A_2$, $2B_2$	1.428
$3A_1$	1.182	1.706	$2A_1$, $2B_1$	1.723
$2B_2$	0.727	0.896	$2A_1$, $2B_2$	1.882
$2B_1$	0.618	0.737		
$1A_2$	−0.618	−0.532		
$2A_1$	−1.326	−0.986		
$1B_1$	−1.618	−1.139		
$1B_2$	−1.989	−1.311		
$1A_1$	−4.442	−2.061		

* Although $1A_2$, $2B_1$ is "allowed" for light plane-polarized in the y direction, there is reason for expecting the intensity to be weak. There are positive and negative terms of the same order of magnitude in the transition moment integral. The issue involved is critical for, according to others [D. P. Craig, unpublished work. I am indebted to Dr. M. Kasha for showing me this paper in manuscript form. L. A. Blumenfeld, J. Phys. Chem. U.S.S.R. 21, 529 (1947).], the first excited electronic level is of symmetry A_1. The satisfactory solution of the contradiction gives promise of allowing one to decide in favor of either the bond orbital or the molecular orbital approximation.

Representations A_1 and B_2

The evaluation of the matrix elements will involve b as well as B, q as well as Q. We find for A_1

$$H_{11}=4Q, \qquad H_{22}=4Q+4B,$$
$$\Delta_{11}=4, \qquad \Delta_{22}=4+4s,$$
$$H_{33}=2Q+2q+2B+4b,$$
$$\Delta_{33}=2+2s,$$
$$H_{12}=4B, \qquad H_{13}=4B+4b,$$
$$\Delta_{12}=4s, \qquad \Delta_{13}=4,$$
$$H_{23}=\Delta_{23}=0.$$

The evaluation is a natural reversal of the procedure used for open chains. For instance, an exchange integral B was considered normal if each of the participating atoms (i,j) had an adjacent atom (h,k):

$$h \quad i\overset{B}{\text{———}}j \quad k.$$

Just as the matrix element was corrected by $-b$ if one of h or k was missing (i or j "end atoms"), so it is corrected if there exist more adjacent atoms. Consider the (9,10) interaction in naphthalene:

$$\begin{array}{ccc} h & & h' \\ & 10 & \\ & | & \\ & B & ; \\ & | & \\ & 9 & \\ k & & k' \end{array}$$

there are two extra adjacent atoms, hence the value of H_{33}.

The secular determinant becomes, under the transformations commonly used,

$$\begin{vmatrix} x & 1 & 1+(b/\alpha)(1-sx) \\ 1 & x+1 & 0 \\ 2+(2b/\alpha)(1-sx) & 0 & x+1+(q/\alpha+2b/\alpha)(1-sx) \end{vmatrix}.$$

Substituting $q/\alpha=1.13$, $b/\alpha=0.08$, and $s=0.26$, we obtain

$$\begin{vmatrix} x & 1 & -0.021x+1.08 \\ 1 & x+1 & 0 \\ -0.042x+2.16 & 0 & 0.665x+2.29 \end{vmatrix}=0;$$

$$x=-1.326,\ 1.182,\ -4.442.$$

Proceeding as with A_1, we find for B_2

$$\begin{vmatrix} x & 1 & -0.021x+1.08 \\ 1 & x-1 & 0 \\ -0.042x+2.16 & 0 & 0.75x-0.03 \end{vmatrix}=0;$$

$$x=0.727,\ 2.181,\ -1.989.$$

As before, we have to obtain the energies from $W=Q-\alpha x/(1-sx)$. They are tabulated, along with the transition energies, below in Table VI.

Benzene

Before proceeding to a comparison with the actual absorption maxima, we shall take benzene into consideration. We make use of the fact that x values can be obtained in simple cases from the previously obtained solutions without overlap.[26] (See Table VII.)

TABLE VII. Energies and transition energies for benzene.

Level	x	W	Transition	ΔW
B_1	2.000	4.167	E_2, E_1	2.145
E_1	1.000	1.351		
E_2	−1.000	−0.794		
A	−2.000	−1.316		

[26] E. Hückel, Zeits. f. Physik 76, 628 (1932).

TABLE VIII. Calculated absorption maxima in $m\mu$.

Substance			
I	299 strong	162 weak	—
II	392 strong	218 weak	190 weak
III	502 strong	278 weak	238 weak
Benzene	195 weak	195 weak	195 strong
Naphthalene	329 weak	292 strong	242 strong

Comparison with Experiment

The transition energies do not depend upon the fact that we arbitrarily set $Q=0$. Thus by selecting α (which we take to be 68.2 kcal./mole), we can construct a table of *calculated* values (Table VIII) to be compared with the previous listing in Table I of *observed* values. It can be seen that a smaller value of α would be more suitable for the dyes; a larger for naphthalene. If we select α so that naphthalene is well represented, we obtain

Naphthalene	306	272	225,

while another α suited to the dyes results in

I	310	168	—
II	406	226	197
III	520	288	246.

V. THE ONE-DIMENSIONAL METAL APPROXIMATION†

The shift of focus to the molecular orbital point of view suggests another model. It is always possible, up to interelectronic interaction, to adopt a molecular orbital point of view. The color is regarded as a quantum jump of one electron. It may happen that the modified Lewis and Calvin theory (the center of mass viewpoint) is also correct. If the M.O. view is always correct†† and if the wave equation separates approximately into the coordinates of the center of mass of the unsaturation electrons in certain cases, then in these certain cases the two outlooks must be regarded as equivalent.

Consider the dye as a long vessel containing free electrons. The color is due to a transition from the highest filled level to the lowest unfilled level. If the dye is imagined to be stretched out, then it becomes possible again to use the one-dimensional particle-in-a-box solution of the Schrödinger equation, though this time in an entirely different way.

If η is the number of carbon and nitrogen atoms in the conjugate chain, the color is obtained from the energy interval

$$\Delta W=[((\eta+1)/2+1)^2-((\eta+1)/2)^2]h^2/8ma^2,$$

where m is the mass of one electron and a is the effective total length of the dye. Thus if the dye considered is

$$Me_2N^{\oplus}{=}CH{-}CH{=}CH{-}\bar{N}Me_2,$$

there are six electrons in the vessel; the color arises from a one-electron transfer from the third to the fourth level.

Within a vinylene homologous series we may expect the length to be $a=(\eta-1)A+C(A)$, where A is the effective carbon-carbon distance and C, not a function of η, is an end effect.

It is found that $C(A)=2.56$A gives a reasonable fit to the colors of the simple dyes considered here, and is not at all unreasonable as a representation of the space available to electrons at the ends of a dye. Then $a=(\eta+1.56)A$, and we obtain

$$\lambda=(8mA^2c/h)(\eta+1.56)^2/(\eta+2).$$

We tabulate values of $(\eta+1.56)^2/(\eta+2)$ against η, and multiplying by 50.2 $m\mu$ obtain a fit to the observed colors:

η	$\frac{(\eta+1.56)^2}{(\eta+2)}$	$\times 50.2\ m\mu$	observed
5	6.15	309	309
7	8.14	409	409
9	10.14	509	511

† It will be noted that the treatment is substantially that given by Bayliss (see reference 11). It is believed that the series of dyes considered here constitutes a fortunate verification of the model, the agreement with regard to intensity being especially noteworthy. Therefore, the sequence of ideas as developed in the writer's thesis is retained even at the risk of having some repetition.

†† It is conceivable that the exaggeration of the B.O. by which electrons are kept apart succeeds in representing interelectronic interaction so well that the M.O. viewpoint would become untenable in comparison.

The effective carbon-carbon distance can be calculated from $50.2\ m\mu = 8mA^2c/h$, and is 1.24A, a fairly reasonable value.†††

The Intensity

It might be possible to distinguish between this method and the modified Lewis and Calvin procedure on the basis of an intensity calculation. It is found that, for $i+j$ odd,

$$B_{ij} = \frac{512e^2a^2}{3\pi h^2} \frac{i^2j^2}{(i^2-j^2)^4}.$$ [20]

The formula used in connection with the center of mass model was obtained by setting $a = 2.13$A; $i=1$, $j=2$; and $e=nE$, where n is the number of electron pairs, and E the charge of an electron pair.

We shall use the expression in a different manner here. We consider three cases, with $\eta = 5$, 7, and 9, so that

$a = 6.56$A, 8.56A, and 10.56A, respectively.

Then, with e the charge of an electron and $A = 1.24$A, found above:

$$B_{34} = 11.5\times10^{19},$$
$$B_{45} = 19.7\times10^{19},$$
$$B_{56} = 30.3\times10^{19}.$$

Comparing calculated and observed intensities we have the results shown in Table IX. The agreement is quite startling. The success of this intensity calculation appears to be very good evidence that unsaturation electrons are essentially autonomous.

Second-Order Bands

We shall construct a table similar to Table I. (See Table X.) For instance, we obtain the next higher transition for dye *III*, $\eta = 9$, from

$$\lambda = 509\cdot(6^2-5^2)/(6^2-4^2) = 280\ m\mu.$$

End Substitution

It is an agreeable attribute of the theory that $C(A)$ determines c in the empirical

$$\lambda = 100n + c,$$

††† If the average of the singlet and singlet-triplet colors were used, the effective carbon-carbon distance would be somewhat closer to the actual value: 1.39A, but discussion of possible refinements of this nature is not in the spirit of the original approximation.

TABLE IX. Intensities of dyes *I*, *II*, and *III* in one-dimensional metal approximation.

η	calculated	observed	calc./obs.
5	2,880	2,700	1.07
7	4,900	4,610	1.06
9	7,580	6,720	1.13

while the length $A = 1.24$A preserves the constant value of 100 $m\mu$ for the vinylene shift. Thus for $C(A) = 2.8A$ we find the sequence of colors:

η	$\frac{(\eta+1.8)^2}{(\eta+2)}$	$\times 50.2\ m\mu$
5	6.61	332
7	8.60	432
9	10.60	532

The method therefore interprets the color of

$$\phi N^{\oplus}H{=}CH{-}CH{=}CH{-}\bar{N}H\phi$$

for which $\lambda = 385\ m\mu$, in a somewhat different fashion than does the center-of-mass model. We see that the phenyls might indeed cause a lengthening of the vessel. For we can write the phenyls as

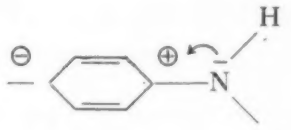

without imagining a very great energy loss.

Benzene

If we use $A = 1.24$A obtained above, and $E = n^2h^2/8\pi mr^2$ [27] $n = 0, \pm1, \pm2, \cdots$, the expression for the energy of a particle constrained to

TABLE X. Colors calculated by the one-dimensional metal method.

Substance			
I	309 strong	—	—
II	409 strong	230 weak	—
III	509 strong	280 weak	233 weak

[27] K. S. Pitzer, Notes: Quantum Theory with Applications to Chemistry (unpublished).

TABLE XI. Comparison of various antisymmetrized M.O. calculations. Energies are in electron volts.

Benzene			Würsters blue			Dye *I*		
Calc.	Obs. $^1E_u^-$	Ratio	Calc.	Obs. $B3_g \rightarrow B1_u$	Ratio	Calc.	Obs. $^1B_1$	Ratio
11.1	6.74	1.65	3.04	2.64	1.15	5.99	4.03	1.49
	$^3B_{1u}$*						$^3B_1$**	
4.50	3.54	1.27				1.93	2.24	0.86

* Roothaan and Mulliken (reference 35) have suggested the reidentification of the observed weak absorption at 350 $m\mu$. It was originally supposed that the upper state in question belonged to E_u^-.

** The author is grateful to Dr. D. S. McClure for obtaining the singlet-triplet energy difference through phosphorescence measurements. The value given is the luminescence maximum and ought not to be compared strictly with the calculation. The calculation applies to vertical excitation in a singlet-triplet absorption process.

move on the circumference of a circle, we obtain $\lambda_{12}=167$ $m\mu$. However, putting in the "observed color," 205 $m\mu$,‡ we obtain the interesting result that the carbon-carbon distance is 1.37A, a value which is close to the experimentally observed 1.39A.

VI. THE ANTISYMMETRIZED MOLECULAR ORBITAL METHOD

The calculation of the color of dye *I* was not actually attempted. Instead, the negative ion of *trans*-1,4 pentadiene, a hypothetical substance with the principal mesomeric forms

$$CH_2{=}CH{-}CH{=}CH{-}\bar{C}^{\ominus}H_2,$$
$$\bar{C}^{\ominus}H_2{-}CH{=}CH{-}CH{=}CH_2$$

was treated. The difference in spectra between the hypothetical and actual cases would probably not be great. The color in 0.1 *N* NaOH of

$$O{=}CH{-}CH{=}CH{-}\bar{O}^{\ominus}$$

is 268 $m\mu$.[28] The well-known bathochromic effect of dimethyl enables us to predict that the color of

$$H_2N^{\oplus}{=}CH{-}CH{=}CH{-}\bar{N}H_2$$

would be $309-26=283$. We then assert that going from oxygen to nitrogen gives a shift of 15 $m\mu$; hence going from nitrogen to carbon might bring about a corresponding shift.

The procedure used by GMS was followed, except that all of the *B*'s and *C*'s were considered (a refinement adopted by Goeppert-Mayer and McCallum).[29] The values of the integrals used were obtained from the table published by Griffing,[30] or were found by a simple electrostatic method as suggested by Goeppert-Mayer and McCallum. An overlap integral of 0.25 was used,[31] although 0.26 would have been a choice consistent with the screening constant chosen for the other integrals.

The wave functions were obtained from the simplest M.O. type of calculation, and may, as a result, be a source of error. The consideration of the change of the Coulomb interaction with position in the chain would lead one to expect a more rapid falling off of the coefficients of atomic orbitals at the ends of the dye.

The results are exhibited along with the GMS results for benzene (as recalculated by London)[32] and those for Würsters Blue of Goeppert-Mayer and McCallum. One can say in defense of the method that the order of calculated colors on the energy scale is that of the observed colors. (See Table XI.)

The principal feature of the method, the avoidance of empiricism, seems to be over optimistic. Even with adjustment of the singlet-singlet transition one obtains the unfortunate result that the singlet-triplet split is too large.

It appears that the molecular orbital method and the metal model are the best treatments, and that the molecular orbital method gives the most promise of successful application to relatively complicated molecules.

ACKNOWLEDGMENT

The writer is greatly indebted to Professor K. S. Pitzer, not only for numerous contributions to the argument, but also for the understanding manner in which he directed the research.

It is a pleasure to thank Professor G. E. K. Branch and Dr. M. Kasha for much valuable discussion.

‡ 205 $m\mu$ is the average, considering degeneracy, of the colors of the three main bands.

[28] Unpublished research.

[29] M. Goeppert-Mayer and K. J. McCallum, Rev. Mod. Phys. **14**, 248 (1942).

[30] V. Griffing, J. Chem. Phys. **15**, 429 (1947).

[31] C. C. J. Roothaan and R. S. Mulliken, J. Chem. Phys. **16**, 118 (1948).

[32] A. London, J. Chem. Phys. **13**, 396 (1945).

THE JOURNAL OF CHEMICAL PHYSICS VOLUME 16, NUMBER 12 DECEMBER, 1948

Does Ultraviolet Absorption Intensity Increase in Solution?*

LOIS E. JACOBS AND JOHN R. PLATT
Department of Physics, University of Chicago, Chicago, Illinois
(Received June 23, 1948)

Absolute absorption intensities and oscillator strengths were determined for isoprene and *cis*- and *trans*-piperylenes in the region 1750–2400A, in vapor and in *n*-heptane solution, using a vacuum fluorite spectrograph. More accurate oscillator strengths are obtained if our measurements at short wave-lengths are combined with the Beckman data of Shell Development Company at longer wave-lengths.

For the three compounds the best values of the experimental Lorentz-Lorenz correction, or ratio of integrated intensities under the molar absorption curves for solution and vapor, were close to unity, a result obtained previously by Pickett and co-workers for cyclopentadiene and cyclohexadiene absorption in this same region. A value of 0.98 ± 0.04 for this correction represents the mean of all five of these determinations. Although the values obtained from our data alone without using the Shell curves showed a much larger spread, every determination was substantially below the correction factor of 1.30 predicted by Chako's classical oscillator theory for this wave-length region and these solvents.

INTRODUCTION

FROM considerations of classical oscillator theory, Chako[1] predicted the effect of a dielectric solvent on electronic absorption intensities of molecules. He concluded that the apparent oscillator strength of a transition, which is proportional to the integrated intensity under the molar absorption curve, should increase by a factor $1/\gamma$ in going from the vapor state to dilute solution. This factor, called the Lorentz-Lorenz correction, is given by

$$1/\gamma=(n_0^2+2)^2/9n_0,$$

where n_0 is the refractive index of the solvent averaged over the absorption band. This result is derived strictly only for allowed transitions[2] and for non-polar solvents. For paraffin solvents in the ultraviolet, the factor is about 1.20 to 1.30. The 2600A bands of benzene and its derivatives have been extensively measured in vapor and in many solvents but are forbidden transitions and hence not suitable for a check of the theory.

The first attempts to test this prediction on appropriate absorption bands were made by Pickett and co-workers.[3,4] Measurements on the 2400A bands of cyclopentadiene and cyclohexadiene, in vapor and in *n*-hexane solutions, gave values of 0.83 and 1.04 respectively for the Lorentz-Lorenz correction.[3] The theoretical value is 1.30 for this wave-length and solvent. On the basis of these studies, Mulliken and Rieke suggested 1.0 to be used for the correction factor in comparing theoretical intensity computations with experimental computations until more data were obtained.[2]

In view of the discrepancy from theory and of the differences between the values obtained on these two compounds, we felt it would be worth while to make new determinations of the correction factor using different compounds and different experimental methods. At the lowest vapor pressures used in this earlier work—a few hundredths of a mm—the vapor flow method which was employed may introduce uncertainties in the pressure measurements.[5] Also it is possible that if the correction factor differs from the classical value, it is not a constant but varies from compound to compound even in non-polar solvents.

In an attempt to clear up these questions, we have determined the absolute absorption intensities for three similar compounds which also have bands near 2250A satisfactory for a test of Chako's theory, isoprene (2-methyl-1,3-buta-

* This work was assisted by the Office of Naval Research under Task Order IX of Contract N6ori-20 with the University of Chicago.

[1] N. Q. Chako, J. Chem. Phys. **2**, 644 (1934).

[2] R. S. Mulliken and C. A. Rieke, Rep. Prog. Phys. **VIII**, 231 (1941).

[3] L. W. Pickett, E. Paddock, and E. Sackter, J. Am. Chem. Soc. **63**, 1073 (1941).

[4] V. Henri and L. W. Pickett, J. Chem. Phys. **7**, 439 (1939).

[5] E. P. Carr and H. Stücklen, J. Chem. Phys. **4**, 760 (1936).

diene) and *cis*- and *trans*-piperylene (1,3-pentadiene). Dienes are especially well suited for this study because quite pure isomers are obtainable; their structure is not too complicated and the character of their electronic transitions is fairly well understood;[2] and still the bands lie at wavelengths long enough that most of their area can be measured on reliable photoelectric instruments and only part of it needs to be determined by the less accurate photographic methods which we use.

Our curves on these compounds were obtained with a small vacuum fluorite spectrograph and cover the range 1750–2400A in vapor and in *n*-heptane solution. These data below 2100A were then used to extend the more precise measurements obtained earlier on the same compounds by the Shell Development Company to this wave-length limit.[6] They used a Beckman spectrophotometer and isooctane solutions. By joining the curves from the two laboratories, oscillator strengths and experimental values of the Lorentz-Lorenz correction can be obtained for each compound. Less accurate values of these quantities are obtainable using our data alone for the complete curves.

APPARATUS AND TECHNIQUES

Since quantitative measurements in the vacuum ultraviolet region considered in this paper are still relatively new, and the possible sources of error have been discussed only briefly before,[7] a rather complete description of the apparatus and techniques employed may prove useful.

The Cario-Schmitt-Ott fluorite spectrograph, kindly loaned by the University of Michigan for our work, has unusually small optics. The spectrum measures 3.8 cm from 4300A to 1700A, and is only 3 mm high. Four spectra can be taken on each plate, two of the unknown and two of a solvent or comparison spectrum, the latter being used for intensity calibration, as described later.

For the solution measurements, a spacer of thickness 0.013 cm placed between the windows of the source and spectrograph formed the cell, through which the solution was allowed to drip slowly.[7] This steady flow reduced errors from photo-decomposition. The solution concentrations ranged from 10^{-2} to 10^{-3} m./l.

The vapor concentrations were measured by filling the spectrograph itself with the vapor from a small gas pipet. This had a known volume ratio with respect to the spectrograph, and the concentrations could be calculated assuming the perfect gas laws to hold at the pressures obtained. This procedure is justified because pressures up to 40 mm, much smaller than the vapor pressure at room temperature, were used in the pipet, corresponding to 6×10^{-2} mm in the spectrograph. The path length through the vapor is the optical distance from the entrance window to the plate, or 35 cm.

There are two advantages of filling the spectrograph itself with vapor rather than placing a cell in front of the spectrograph. First, static pressure measurements can be made, which at such low pressures are probably more reliable than flow measurements. At the same time photo-decomposition effects are decreased, since the vapor is irradiated only during the exposure itself, and the light flux through it is less than if it were in a cell by at least a factor of 10^4. This is an important consideration, since Carr and Stücklen[5] working with similar compounds in a cell in front of the slit found photo-decomposition effects to be appreciable unless special precautions were taken.

Intensity measurements were made by standard photographic methods, using either a Moll microphotometer or a Leeds and Northrop recording densitometer. In order to avoid the effect of random errors at low extinction values and errors from scattered light at high extinction values, the extinctions used were limited to the range 0.2 to 0.8.

Ilford Q plates appeared to be more uniform, and therefore more suited for quantitative work, than Eastman ultraviolet sensitized plates. The Eastman plates have a rather heavy emulsion, which is covered with a waxy, fluorescent material. It is possible to observe visually streaks on many of these plates which appear to be brush marks from the application of the fluorescent sensitizer. The Ilford Q plates, on the other

[6] American Petroleum Institute Research Project 44 at the National Bureau of Standards. Catalog of Ultraviolet Spectrograms. Serial Nos. 46–51, *cis*- and *trans*-piperylenes and isoprene, contributed by the Shell Development Company, Emeryville, California.

[7] J. R. Platt, I. Rusoff and H. B. Klevens, J. Chem. Phys. 11, 535 (1943).

hand, are very similar to Schumann plates in that a very thin emulsion is used with little gelatin so that the silver halide crystals protrude from the surface and make a sensitizer unnecessary, but they are much more uniform and have fewer flaws and dust marks than the usual Schumann plates. Of course, neither the Eastman ultraviolet sensitized plates nor the Ilford Q plates give as reproducible results as Eastman spectrum analysis plates, since the latter are especially designed for accurate quantitative work and have no sensitizing layer, but they are not very useful below 2200A where the gelatin begins to absorb. Therefore Ilford Q plates are used throughout the present study.

The intensity calibration of our plates was carried out by taking exposures on the solvent or blank cell, using one-half and one-fourth the exposure times used on the unknowns. These two spectra determine the slope of the gamma-curve at each wave-length. This procedure would introduce an error because of reciprocity failure unless the latter were determined and allowed for. To measure this failure, fine mesh wire screens were vibrated between the source and slit, the percent transmission of the screens having been determined photometrically. This gave values of the Schwarzschild factor[8] of 0.95 for the Ilford Q plates and 0.83 for the Eastman sensitized plates, essentially independent of wave-length in both cases.

It might be thought that the vapor and solution intensities could be compared directly on the same plate, but a shift of the solution peaks by about 100A to longer wave-lengths from the very sharp vapor peaks makes this method more awkward than the comparison of each spectrum separately with a blank or solvent spectrum. Therefore the absolute absorption intensities of the vapors and solutions were determined independently.

The isoprene sample, from Phillips Petroleum Company, was about 98 percent pure. The piperylenes were obtained from Dr. Robert L. Frank of the University of Illinois, and were better than 99 percent pure *cis* and *trans*. They were distilled in a nitrogen atmosphere immediately before the plates were taken, using a Podbielniak with 50 theoretical plates. The *trans*-piperylene boiled at 42.0°C and had a refractive index of n_D^{20} 1.4293; the *cis*-piperylene boiled at 44.0°C and had a refractive index of n_D^{20} 1.4360. These values checked those received with the samples within the experimental error of the Abbe refractometer.

The concentrations of the solutions were determined by the usual method of diluting a weighed amount of solute to volume. The high volatility of both the solutes and solvent would cause some difficulty in obtaining accurate weights. This was guarded against by rapidly introducing the solute near the surface of a tared amount of the solvent in a narrow necked flask and obtaining the weight by difference. The rate of evaporation was checked and was found to introduce an error of less than 1 percent under these conditions.

TABLE I. Error studies.

	Vapor	Solution
Deviation of independent readings on the same spectra.	—	2%
Average deviation of duplicate exposures on the same sample (same plate).	4%	4%
Average deviation of duplicate exposures on different samples (same plate).	6%	—

Errors in intensity measurements near the peak, by compounds

	Vapor			Solution		
	Mean % deviation	Maximum % deviation	Probable % error of mean area	Mean % deviation	Maximum % deviation	Probable % error* of mean area
Isoprene	7	10	4	5	16	4
Cis-piperylene	11	16	6	16	22	8
Trans-piperylene	6	11	4	13	18	5

* The probable error was computed on the basis of the number of indlvidual plates (from 2 to 6) taken over the peak since measurements on any one plate are not independent.

ERRORS

Reproducibility studies on the Ilford plates showed that the densitometry uncertainty as determined by completely independent re-reading of the same spectra was of the order of 2 percent. For different spectra, values from duplicate exposures of the same solution or vapor sample on the same plate checked within 4

[8] Although the Schwarzchild factor is actually not constant over a large range of intensities and exposure times, it was found to be a useful estimate of reciprocity failure over the small range used. Sheppard and Mees, *Investigations on the Theory of the Photographic Process*, p. 214 (Longmans Green and Company, New York, 1907).

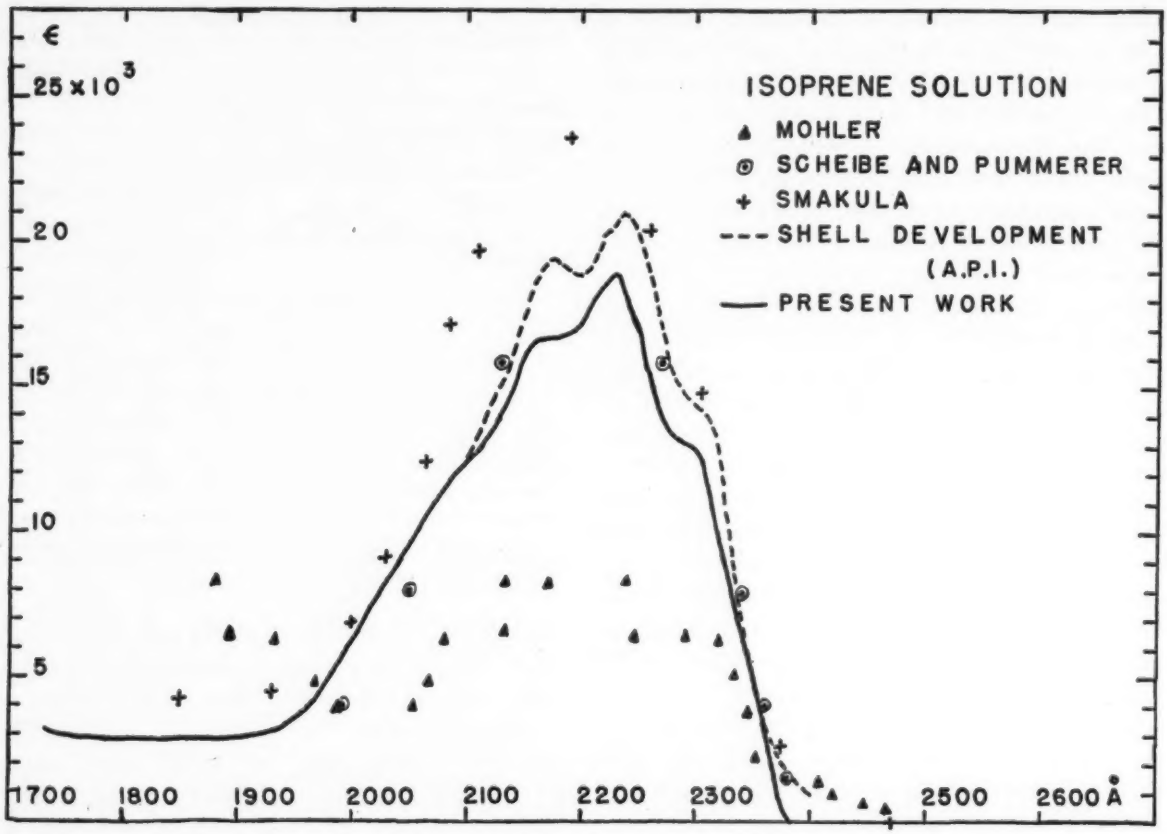

FIG. 1. Comparison of isoprene solution absorption intensities in the ultraviolet.

percent, whereas exposures on different vapor samples, again taken on the same plate, gave an error of about 6 percent.

These were final values. Early vapor studies showed reproducibility errors as large as factors of 4. They were traced, however, to absorption of the vapors by the stopcock grease, vacuum waxes, and possibly pump oil films in the vacuum lines. The errors were reduced to the figures quoted when Silicone stopcock grease was used, the system was cleaned out carefully before each compound was run, and residual vapors were frozen out by a liquid air trap during evacuation of the spectrograph.

As a check on the consistency of separate runs, the ϵ *versus* λ curves were drawn for two sets of data for *trans*-piperylene solutions that were prepared independently and run weeks apart. The two curves as determined from the mean of 2 or 3 plates at every wave-length for each run coincided at most points, the maximum deviation being less than 2 percent.

For each compound, the final curves given here represent the mean of from 2 to 6 independent measurements of the absorption coefficient at a sequence of wave-lengths about 20A apart. The best curve was drawn through these values, taking into consideration the maxima and minima seen in the spectra, which could be located visually on the plates to within 5A. The probable errors were calculated from the mean deviation of the individual points, which range from 5 to 16 percent for the different compounds, and from the number of independent determinations in each case. These gave a value of about 6 percent for the final probable error in the areas under each of the curves. A further breakdown of the errors is shown in Table I.

There may be a systematic error in the *trans*-piperylene vapor results, as our pure sample was exhausted before the vapor curves were finished and most of the plates were taken with a mixture containing some *cis*, correcting the curve for the measured *cis*-absorption. The method of prepara-

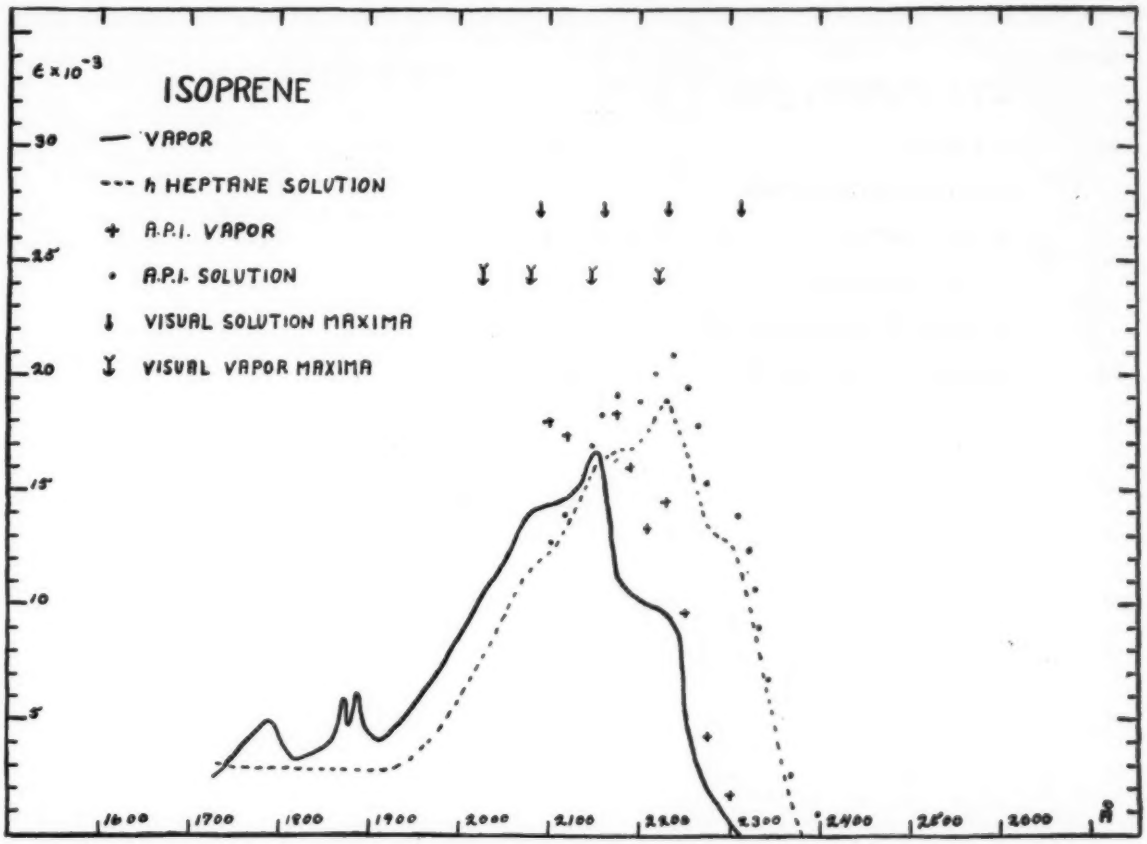

FIG. 2. Isoprene ultraviolet absorption intensities.

tion used for the mixture is known to give a 87:13 ratio of *trans*- to *cis*-piperylenes,[9] and this value of the ratio was used in making the correction. The boiling point of 42.0°C and the refractive index of n_D^{20} 1.4302 determined for the mixture indicated that there was not more than 13 percent *cis*-piperylene present. Since the absorption intensities of the two forms are comparable, the maximum correction introduced by the presence of the *cis*-piperylene was only about 5 percent, which is no more than the probable error of the measurement.

An attempt was made to measure vapor absorption intensities at shorter wave-lengths, using the many-line hydrogen spectrum from 1575 to 1650A, in order to estimate the *f*-values for the $V_{2,3}$ transitions (Mulliken notation; see reference 2) in this region. These are interesting because they are forbidden for a simple diene in its most extended form. Unfortunately we were unable to obtain reproducible results with our present apparatus and pumping system, probably because of the strong oxygen absorption in this wave-length region, which is noticeable at a few microns pressure. This absorption becomes negligible to the red of 1900A and does not affect the measurements of the longer wave-length allowed transitions.

[9] R. L. Frank, R. D. Emmick and R. S. Johnson, J. Am. Chem. Soc. 69, 2313 (1947).

RESULTS

Isoprene was the only substance studied for which there were many previous absorption measurements in inert or non-polar solvents in the literature. Both Smakula[10] and Mohler[11] used hexane as solvent, and Scheibe and Pummerer[12] used methyl cyclohexane. These older data are compared with the more recent work in Fig. 1. Except for Mohler's measurements, the values

[10] A. Smakula, Angewandte Chemie **47**, 657 (1934).
[11] H. Mohler, Helv. Chim. Acta **20**, 811 (1937).
[12] G. Scheibe and R. Pummerer, Ber. d. d. Chem. Ges. **60**, 2163 (1927).

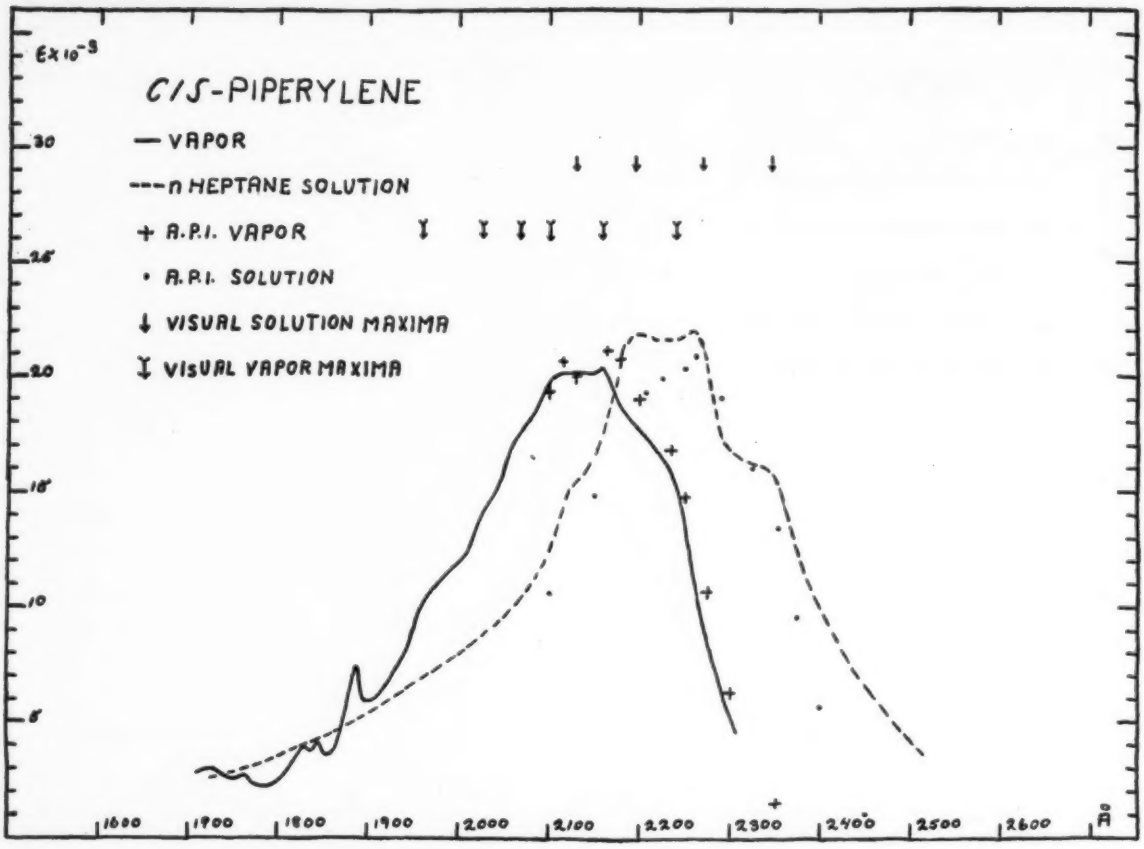

FIG. 3. *Cis*-piperylene ultraviolet absorption intensities.

all lie within about 20 percent of the present measurements. Our complete curves on this and the other compounds are shown in Figs. 2, 3 and 4, with points from the Shell Development Company Beckman curves[6] included for comparison.

The areas under the curves were used to calculate the oscillator strengths from the formula[13]

$$f=4.32\times10^{-9}\int\epsilon_\nu d\nu,$$

where ϵ_ν is the ordinate in the graphs which is given by

$$\epsilon_\nu=(1/ct)\log_{10}I_0/I.$$

The f-values from the Shell curves as extended by our data are listed in column 1 of Table II. Since their data covered over 70 percent of the solution curve areas and over 50 percent of the vapor curve areas, and since their data were sufficient to determine ϵ_{max} in each case (which contributes most of the error in the f-value measurement), the accuracy of the f-values in column 1 is not essentially worse than if they had been obtained from Beckman spectrophotometer data alone, and the values are probably good to about 5 percent. The f-values obtained entirely from our measurements are listed in column 3.

The ratio of f_{soln} to f_{vapor} for each compound gives the experimental Lorentz-Lorenz corrections listed in columns 2 and 4 of Table II. These are to be compared with the value of 1.30 calculated from Chako's theoretical formula. For this calculation the value of 1.461 for the refractive index of n-heptane at 2250A, the maximum of the curves, was taken from Lauer's[14] experimental values of the refractive index in this region.

Strictly, we should use for the comparison

[13] J. R. Platt and H. B. Klevens, Rev. Mod. Phys. **16**, 182 (1944).

[14] J. L. Lauer, J. Chem. Phys. **16**, 571 (1948).

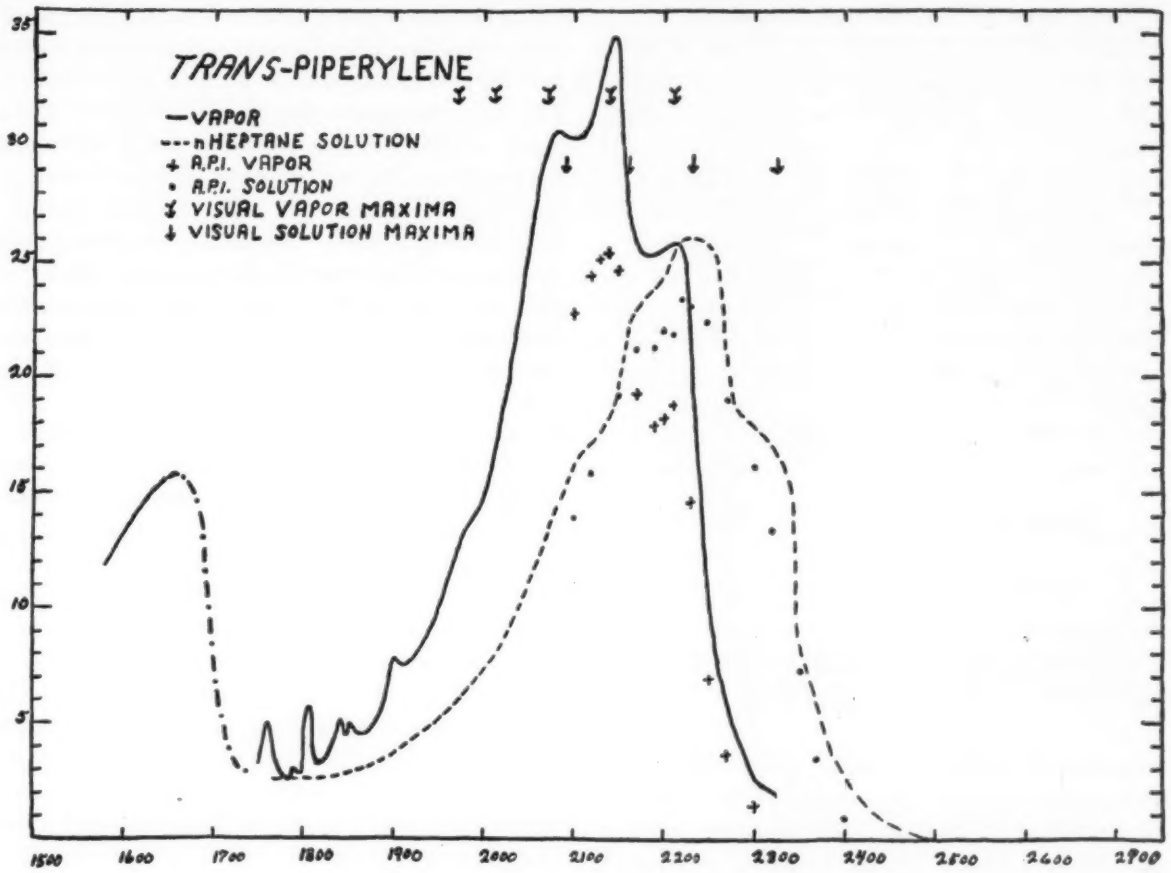

FIG. 4. *Trans*-piperylene ultraviolet absorption intensities.

the average value of $1/\gamma$ over the band instead of the value at the peak. But these practically coincide, as $1/\gamma$ changes only from 1.29 to 1.33 between 2400A and 1950A (by extrapolation of Lauer's data). The value of $1/\gamma$ for iso-octane, Shell's solvent, is also 1.30 at 2250A.

INTERPRETATION

Although for two of the compounds the Lorentz-Lorenz corrections determined from our data alone agree with Chako's prediction of 1.30 within experimental error, they are both low (column 4 of Table II). All of the values obtained by extending the Shell data substantiate the results of Pickett and co-workers that the correction is nearer unity. In fact if we assign the Pickett and Shell-present-data correction factors in Table II uncertainties of ± 0.07, which is optimistic but is not inconsistent with the observed scatter; and if we assume they are all measurements of the same quantity; then the mean value of these five measurements is 0.98 ± 0.04. Our data scatter considerably more, and the slight spread obtained in the extended Shell measurements may be partly the result of the use of our data in making the extensions.

If we give more weight to the fluorite measurements and look just at isoprene where the agreement on individual f-values between Shell's extended data and our data alone is the best, the experimental Lorentz-Lorenz corrections do seem to be distinctly higher than unity and a weighted mean would lie near 1.10 ± 0.06. However, the generally larger spread of our fluorite correction factors suggests that the errors in these measurements must be about 20 percent, and that this high value is not reliable.

These errors in the fluorite measurements are larger than was indicated by our tests on reproducibility. They are also larger than the deviations found in earlier solution studies, as in

TABLE II. The 2250A bands in dienes.

Substance		Shell Development Company plus present data* 1. f number	2. Lorentz-Lorenz correction	Present work 3. f number	4. Lorentz-Lorenz correction	Theoretical Lorentz-Lorenz correction $\frac{1/\gamma}{(n_0^2+2)^2/9n_0}$
Isoprene	vapor	0.45±0.02	1.07±0.08	0.38±0.02	1.23±0.08	
	solution	0.48±0.02		0.47±0.02		
Cis-piperylene	vapor	0.57±0.03	1.00±0.07	0.58±0.03	1.24±0.12	1.30
	solution	0.57±0.03		0.72±0.06		
Trans-piperylene	vapor	0.64±0.03	0.95±0.07	0.80±0.03	0.84±0.08	
	solution	0.61±0.03		0.67±0.04		

		Pickett and Co-workers f number	Lorentz-Lorenz correction
Cyclopentadiene	vapor	—	0.83(±0.07?)
	solution		
Cyclohexadiene	vapor	0.135	1.04(±0.07?)
	solution	0.140	

* For calculation of the Shell error, a standard deviation of 5 percent was used. A private communication from the Spectroscopy Department of Shell Development Company indicates that the errors near the peak values on their vapor curve "could be as great as 20 percent of the value."

substituted anilines[15,16] whose measured intensities lie on a smooth curve with mean deviations of less than 10 percent, and in three mono-*n*-paraffin-benzenes[15,16] whose *f*-values agreed within 7 percent. Larger percentage errors in the Lorentz-Lorenz correction factor, possibly up to 14 percent, would result from taking a ratio of two *f*-values. The additional scatter in the present work is probably due to the new sources of error in the vapor measurements. In order to improve the present determinations, it would be advantageous to devise reliable photoelectric methods of intensity measurement in this region, and to have a vapor cell to be placed in the exit beam of a monochromator and designed to avoid contamination and absorption.

A qualitative estimate can be made of the effect of systematic errors possible with each of the three different methods used so far. In Shell's Beckman technique, the static and covered solution cell would reduce boiling out effects caused by the high volatility of the solutes. Possible photo-decomposition errors from this method are reduced by having the cell behind the exit slit of the spectrophotometer. Comparable photo-decomposition errors would occur in the vapor, and little effect should be noticed in the ratio of the two absorption curves. In Pickett's work, again static solution methods would decrease boiling out effects. However, having both the solution and vapor cells in front of the spectrograph could greatly increase photo-decomposition errors. This would be corrected in the vapor by their flow method. Neglecting uncertainties in pressure measurements from this method, the net effect might be to give low solution absorption, and therefore a low apparent Lorentz-Lorenz correction. Our solution flow method would decrease photo-decomposition effects, but could give low solution absorption from increased boiling out effects. Since, as described earlier, the vapor decomposition effects are minimized in our method, the net result would be low solution absorption and again a low apparent Lorentz-Lorenz correction. Since the results in Table II do not behave systematically in the way to be expected from these considerations more than would be likely from random errors, it can be concluded that systematic errors of these kinds are probably not the reason for the consistently low value of the correction factor.

It is of course possible that the spread in values determined from our data for the different compounds is partly real, and indicates a specific correction depending on the solute, and not accounted for in the classical theory. If this is true, there may also be similar specific effects dependent on the solvent, such that the curves in Fig. 1, for example, may not be strictly comparable. But in view of the many known sources of error in the photographic technique and in our adaptations of conventional gas and solution absorption methods for use with the fluorite spectrograph, it seems unnecessary to postulate a variable correction factor on the basis of the present data.

We conclude that the five best measurements of the Lorentz-Lorenz factor are consistent with the idea that it is a constant and equal to unity within experimental error. It is possible, but seems less probable, that it varies among the dienes; if so, probably not more than 10 percent from this value. None of these five measurements agree at all with Chako's classical theory, and

[15] J. R. Platt and H. B. Klevens, in press.
[16] J. R. Platt and H. B. Klevens, Chem. Rev. 41, 301 (1947).

it seems unlikely that the discrepancy is due to systematic error.

If we take it as real, what is the reason for this discrepancy? The trouble may lie in the failure of the classical theory to describe these molecular interactions; or it is possible that classical and quantum theory would give substantially the same result, but that one or more of Chako's assumptions were not justified. These assumptions are, essentially, that in the vapor state we have a classical electric dipole oscillator in free space; and that, in solution, this oscillator is imbedded in a dielectric which polarizes in response to the oscillator field. Now when we consider the localized character of the molecular π-orbitals on the conjugated carbon atoms in these molecules, we see that it is the first of these assumptions which may not be valid. That is to say, the oscillating part of the molecule, even in the vapor phase, is embedded in a dielectric formed by the saturation electrons and σ-orbitals of the paraffin-like C−H and C−C bonds on the periphery of the molecule. In solution, the interaction with the external molecules of the dielectric solvent will then presumably be an order of magnitude smaller than these interactions with the nearby and closely coupled "dielectric" attached to the very atoms on which the optical electrons are localized. If this view is correct, the oscillator is within a partial cocoon of dielectric in vapor phase, and the differences in absorption intensity in going from vapor to solution will be, as we found, much less marked than the theory would indicate. The true test of the classical theory would then be on some molecule which has no saturated peripheral bonds, such as oxygen, nitrogen, or possibly as intermediate cases, acetylene or diacetylene.*

The red shifts observed in going from vapor to solution do not contradict this notion that the solvent interacts relatively little with the oscillator; for they are probably to be explained by a different mechanism, namely, the reduction in ionization potential when an electron is removed into the dielectric instead of into free space.

If the saturated periphery of a molecule does act as a dielectric, then absorption intensities ought to be higher in vapor phase than would be expected according to the usual theory which neglects this polarization effect. But previous theoretical calculations on electronic spectra have predicted only relative and not absolute absorption intensities, so that this increase cannot be checked.

In current idiom, this amounts to saying that polarizability of attached groups may be as important to absorption intensity as their static induction or hyperconjugation effects. All these effects may of course be correlated to each other, or may be re-expressible in terms of one or two other parameters such as ionization potential or overlap integral of the substituent.

ACKNOWLEDGMENT

We are indebted to Dr. W. C. Price for showing us the gas pipet method of handling vapors, and to Dr. Walter Nudenberg of the Chemistry Department for helpful discussions on purification of the piperylenes. We also wish to thank the Phillips Petroleum Company and Dr. Robert L. Frank of the University of Illinois for the very pure samples which they supplied for these studies.

* *Note added in proof:* Professor R. S. Mulliken suggests another possible factor contributing to the discrepancy. The s-*cis*—s-*trans* equilibrium ratios may differ in vapor and in solution. S-*cis* and s-*trans* refer to the orientation of the double bonds about the single bond connecting them. S-*cis* molecules are supposed to have a much lower absorption intensity than s-*trans* in this region (see reference 2). However, the cyclic dienes studied by Pickett and coworkers are necessarily s-*cis*; and they show the same discrepancy. The effect suggested by Mulliken is, therefore, not the major cause of the discrepancy.

THE JOURNAL OF CHEMICAL PHYSICS VOLUME 16, NUMBER 12 DECEMBER, 1948

The Mercury Photosensitized Reactions of Isobutene*,†

G. A. Allen and H. E. Gunning‡
Department of Chemistry, University of Rochester, Rochester, New York
(Received July 1, 1948)

An investigation has been made of the reaction of isobutene with mercury ($^3P_1$) atoms at 30°C. Acetylene and propylene have been shown not to be among the main products of the reaction. The over-all rate of consumption of isobutene and the rate of pressure decrease both decrease with increasing initial pressure in the complete quenching region. These rates approach constant values for initial pressures of 180 mm and higher The results of this investigation show that isobutene behaves similarly to the other olefins in reacting with mercury ($^3P_1$) atoms at 30°C, in that the reactions can be explained by the following initial steps for the mechanism:

$$i\text{-}C_4H_8+Hg(^3P_1)\rightarrow i\text{-}C_4H_8^*+Hg(^1S_0)$$
$$i\text{-}C_4H_8^*+i\text{-}C_4H_8\rightarrow 2i\text{-}C_4H_8,$$

accompanied by the decomposition of the activated isobutene molecule into reaction-initiating fragments.

The discrepancies between the results of this investigation and those of the earlier work of Gunning and Steacie may be due to the effect of impurities in the original isobutene, since it is shown that small amounts of added propylene or acetylene change the rate of reaction markedly.

INTRODUCTION

It has been shown that ethylene,[1] butadiene,[2] propylene,[3] isoprene,[3] 1-butene,[4] and 2-butene[4] all react with mercury ($^3P_1$) atoms, at room temperature, by an activated molecule mechanism. Isobutene,[5] however, seemed to be inconsistent with the other olefins in this respect, since no rate-decreasing deactivation was detected at initial isobutene pressures up to 84 mm, thus permitting a mechanism postulating an initial split into C_4H_7 radicals and H atoms. However, this point was not firmly established, since pressures of the order of 80 mm, measured on the McLeod gauge used, would have a low degree of accuracy, and the rates determined in the isobutene investigation would be no more accurate than the pressure measurements.

In order to find out more about this apparent difference between the reaction mechanism of isobutene and that of the other olefins, the investigation of the isobutene reaction was repeated and extended to higher pressures, using a more accurate method of determining pressure changes.

EXPERIMENTAL

Static Runs

Static runs were made using a cylindrical quartz cell, 10 cm in length, with windows 5 cm in diameter. Its volume was about 190 ml. The cell was immersed in a metal water bath provided with a fused quartz window. The distilled water in the bath was kept at 30.00±0.01°C by means of a thermoregulating system consisting of a mercury thermoregulator, an immersion heater, and a thermionic relay as described by Serfass.[6] The cell was connected to the rest of the reaction system by means of a standard taper ground-glass joint. The reaction system, comprising the cell, a small finger trap for freezing out condensable materials, and an automatic Pearson type differential manometer,[7] had a zero pressure volume of 280 ml. (The volume, being dependent on the mercury level in the differential manometer, varied with the pressure in the system; since the manometer tube was calibrated, the volume for any given setting of the mercury level could easily be determined.)

* This work was supported by Contract N6onr-241, Task I, with the Office of Naval Research, United States Navy.
† Part of a dissertation submitted by one of the authors (G. A. A.) in partial fulfillment of the requirements for the degree of Doctor of Philosophy at the University of Rochester.
‡ Present address: Department of Chemistry, Illinois Institute of Technology, Chicago, Illinois.
[1] D. J. LeRoy and E. W. R. Steacie, J. Chem. Phys. **9**, 829 (1941).
[2] H. E. Gunning and E. W. R. Steacie, J. Chem. Phys. **12**, 484 (1944).
[3] H. E. Gunning and E. W. R. Steacie, J. Chem. Phys. **14**, 57 (1946).
[4] H. E. Gunning and E. W. R. Steacie, J. Chem. Phys. **14**, 581 (1946).
[5] H. E. Gunning and E. W. R. Steacie, J. Chem. Phys. **14**, 544 (1946).
[6] E. J. Serfass, Ind. Eng. Chem., Anal. Ed. **13**, 262 (1941).
[7] D. J. LeRoy, Ind. Eng. Chem., Anal. Ed. **17**, 652 (1945).

All rates reported refer to the base volume of 280 ml.

The presence of mercury vapor in the reaction cell was ensured by having a pool of mercury in a 1 ml well in the bottom of the cell. After each run, the cell was removed at the standard taper joint, cleaned with chromic acid cleaning solution, and flamed to ensure the removal of any residual polymer. Fresh mercury was placed in the well before reconnecting the cell to the system; fresh Apiezon stopcock grease "*N*" was used on the standard taper joint each time that the cell was reconnected.

Water was circulated through a water jacket surrounding the differential manometer and through a copper coil immersed in the water bath in order to maintain both the reactant in the manometer part of the cell system and the mercury of the manometer at a constant temperature of approximately 30.0°C.

The reaction system was connected by a mercury-operated glass float-valve cut-off to another separable system which included a McLeod gauge. This system in turn was connected by a similar mercury cut-off having glass check-valves to the main manifold, to which were attached gas reservoirs, a double-trap distillation purification apparatus, sampling devices, and the pumping system.

A Hanovia Sc2537 mercury resonance lamp, in the form of a spiral 5 cm in diameter and 10 cm long was clamped firmly broadside on to the quartz window of the water bath, the coils nearest the window being 20 mm from the window. The lamp was enclosed on all sides except that facing the window by a wooden box shield, the interior of which was painted dull black; the shield prevented external draughts from affecting the operation of the lamp, and from changing the concentration of ozone produced by λ1849 line between the lamp and the bath.

The lamp was operated for at least one hour prior to each run, in order to attain equilibrium operating conditions. A thin sheet of metal, placed between the bath and the lamp, served as a removable shutter. The lamp was operated from the secondary of a Jefferson 6000 volt 120 milliampere sign transformer. A.c. line voltage variations of 10 volts were found to affect the rate of pressure change by about 15 percent; therefore the transformer primary was fed 110 volts from a Variac, this input voltage being checked at 5- or 10-minute intervals throughout the course of each run. Normal operating characteristics of the lamp were: lamp current, 100±5 ma, lamp voltage 570±15 volts.

TABLE I. Analyses of original isobutene.

Component	Sample 1, mole percent	Sample 2, mole percent	Average, mole percent
Propylene	1.5	1.5	1.5
Isobutane	1.0	1.0	1.0
n-Butane	0.6	0.5	0.55
Isobutene	96.8	96.9	96.85
Butadiene	0.1	0.0	0.05

The isobutene used in the experiments was obtained from the Matheson Company, East Rutherford, New Jersey, and was stated to be at least 95 percent isobutene. It was further purified by several trap-to-trap distillations, only the middle fraction of each distillation being retained, and was finally stored in a storage flask. The storage flask was connected to the manifold of the system, through a mercury cut-off having glass check valves and also through a modified stock valve as designed by Warrick and Fugassi.[8] Table I gives the mass spectrometric analyses of duplicate samples of purified isobutene.

The propylene used was obtained from the same source, purified in the same manner, and stored in a storage flask which was connected to the manifold by means of a modified stock valve identical to the one used for the isobutene. The acetylene used was commercial grade, and was obtained from the Air Reduction Company. It was purified by several trap-to-trap distillations immediately prior to using.

The nitric oxide used in this work was prepared by the action of mercury on a 2 percent solution of sodium nitrite in concentrated sulfuric acid.[9] It was then purified by several trap-to-trap distillations, from dry ice-acetone bath temperature (−78.5°C) to liquid nitrogen temperature.

To determine whether the surface of the cell

[8] E. Warrick and P. Fugassi, Ind. Eng. Chem., Anal. Ed. **15**, 13 (1943).

[9] A. Klemenc, *Die Behandlung und Reindarstellung von Gasen*, p. 166, (Akademische Verlagsgesellschaft b. Leipzig, 1938).

had any great effect on the rate of pressure decrease, one run was made in which the interior surface of the cell was coated with potassium chloride. The coating was obtained by rinsing the cell with a saturated solution of potassium chloride in alcohol and water, then drying the cell before adding mercury to the cell well and reconnecting the cell to the reaction system.

Single Pass Runs

Two single pass runs were made to make qualitative observations on products. In each of these runs, a few ml of liquid isobutene were distilled from a trap reservoir immersed in dry ice-acetone, passing through a quartz reaction tube 10 mm in diameter to a receiver immersed in liquid nitrogen. The vapor pressure of isobutene at dry ice-acetone temperature is about 10 mm; hence the pressure of the isobutene should be that corresponding approximately to maximum rate of pressure decrease. The isobutene, on leaving the reservoir, was bubbled through or passed over the surface of a pool of mercury at room temperature, to ensure the presence of mercury vapor in the reaction tube. A helical mercury resonance lamp identical with the one used for static runs, was placed coaxially about the quartz section of the reaction tube.

Analytical Methods

After each run, a Dewar flask of liquid nitrogen was placed around the finger trap of the reaction system. When the condensable products and unreacted isobutene were completely frozen out, the cut-off between the reaction system and the McLeod gauge was opened, and the pressure of the non-condensable gas was measured. (Experience showed that it could be assumed that all the condensable substances were completely frozen out within 10 to 20 minutes after the liquid nitrogen was placed around the finger trap.) Gunning and Steacie[5] reported the rates of formation of hydrogen and methane in the reaction; since these were minor products, with very low rates of formation, and since the rate of formation of total non-condensables found in the present investigation agreed reasonably well with the rates of formation of hydrogen plus methane reported by Gunning and Steacie, the non-condensable gas was not analyzed further.

In a number of runs, acetylene was then sought in the mixture of reaction products by the method of Ross and Trumbull,[10] as modified by LeRoy and Steacie.[1]

An attempt was made to determine propylene in the reaction products by means of infra-red spectrometry, but it was found impossible to detect low percentages of propylene in the presence of high percentages (about 80–95 percent) of isobutene.

In order to determine the amount of propylene formed, and to investigate what other products were being formed, arrangements were made with Dr. W. H. Barcus, Manager of the Development Laboratory, Sun Oil Company, to have analyses of the products of several runs covering a wide pressure range performed on the mass spectrometer. In each of these runs, after the gas non-condensable in liquid nitrogen had been determined, the entire condensable portion of the reaction mixture was frozen out into an evacuated sample bulb attached to the main manifold. When the McLeod gauge showed that the pressure in the system had fallen to a constant value approximately equal to the pressure of the non-condensable gases dispersed throughout the combination of the reaction cell, McLeod gauge, and manifold, the sample bulb was sealed off and removed from the system.

TABLE II.

Run No.	P_0 mm	$-\Delta P/\Delta t$ mm/min. $\times 10^2$	Run No.	P_0 mm	$-\Delta P/\Delta t$ mm/min. $\times 10^2$
62	1.08	1.88	50	50	1.57
61	3.65	2.21	47	52.5	1.59
59	7.5	2.28	49	55	1.53
66	10.2	2.09	48	58	1.65
69	12.1	2.0	54	84	1.26
75	12.5	2.01	52	110	0.90
55	13.8	2.14	56	158	0.84
53	23	1.84	57	183	0.76
74	24	1.88	73	240	0.73
58	38	1.43			

Actinometry

The intensity of the light entering the cell was determined by the uranyl oxalate-oxalic acid

[10] W. H. Ross and H. L. Trumbull, J. Am. Chem. Soc. **41**, 1180 (1919).

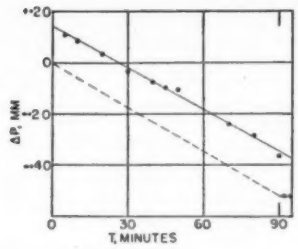

FIG. 1. Pressure decrease *vs.* time for a static run (initial pressure 240 mm), showing the initial pressure rise and the corresponding "dark" pressure decrease when the lamp was turned off at $t = 90$ minutes.

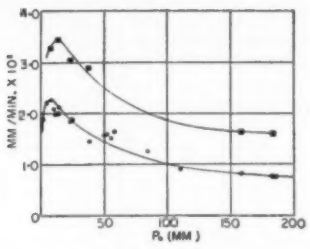

FIG. 2. ■ Rate of consumption of isobutene *vs.* initial pressure. ● Rate of pressure decrease *vs.* initial pressure. (Both rates in mm/minute$\times 10^2$ for a volume of 280 ml.)

method.[11,12,13] The uranyl oxalate was precipitated from a saturated aqueous solution of C.P. uranyl nitrate by the addition of an alcoholic solution of C.P. oxalic acid, washed with alcohol, filtered, dried overnight in a desiccator, and finally dried at 110°C for 3 hours. The actinometry solution was made up approximately 0.001 N in uranyl oxalate and 0.005 N in oxalic acid, and was stored in a light-tight glass bottle. Potassium permanganate solution was made up and its normality determined as 0.0164 N by standardization against C.P. grade sodium oxalate.

For the actinometric runs, 200 ml of uranyl oxalate-oxalic acid solution was pipetted into the reaction cell. The cell was then reconnected to the reaction system, and illuminated for a measured time, the lamp first having been operated for at least an hour in order to ensure equilibrium operating conditions of the lamp. Ten ml concentrated sulfuric acid were added to duplicate 50 ml aliquot portions of the photolyzed solution, which were then titrated at 80–85°C with standard potassium permanganate solution. The oxalate concentration of the original actinometry solution was similarly determined, using duplicate 50 ml portions.

RESULTS

For initial isobutene pressures less than about 10 mm, the plot of pressure decrease against time was a straight line passing through the origin. In the case of initial pressures greater than about 10 mm, an apparent induction period was observed; this apparent induction period was greater the greater the initial pressure, and ranged from 1 to 25 minutes. At higher pressures, a slight initial pressure rise was observable during this period, thus indicating that the apparent induction period was actually due to a pressure rise occurring during the first two minutes of the reaction. Extrapolation of the linear pressure decrease-time curve to zero time produced a positive ΔP intercept ranging from 0.01 to 0.15 mm, being greatest for greatest initial pressures. Moreover, when the lamp was shuttered at the end of a run, the pressure dropped by an amount approximately equal to the pressure rise intercept. These observations are clearly seen in Fig. 1.

The rates of pressure decrease are given in Table II; Fig. 2 shows these data in graphical form.

Products

The rate of disappearance of isobutene and the rates of formation of products, calculated from the pressure rates and the mass spectrometric analyses, are reported for a number of runs in Table III. The rate data reported for the two lowest pressures are not very reliable, since the reactions were carried out to a high percentage decomposition (71 percent and 50 percent for initial pressures of 1.08 and 3.65, respectively). It should be pointed out that the presence of neopentane in the reaction products is uncertain, since no pattern for pure neopentane had been run on the mass spectrometer; it may be that heptanes, octanes, heptenes, and octenes were present, giving rise to lower mass peaks similar to neopentane. Analytical results were calculated on the basis of neopentane, which

[11] W. G. Leighton and G. S. Forbes, J. Am. Chem. Soc. **52**, 3139 (1930).
[12] F. P. Brackett, Jr. and G. S. Forbes, J. Am. Chem. Soc. **55**, 4459 (1933).
[13] G. S. Forbes and L. J. Heidt, J. Am. Chem. Soc. **56**, 2363 (1934).

TABLE III. Rates of formation.

Initial pressure (mm)	1.08	3.65	7.5	13.8	23	38	110	158	183
Component:	(All rates in moles per minute $\times 10^8$)								
isobutene	−51.9	−51.7	−48.6	−51.1	−45.2	−42.7	(−51.3)	−24.3	−23.7
n-butane	8.5	4.3	2.6	7.5	10.8	8.1	(31.6)	2.3	8.4
isobutane	1.9	5.9	8.3	4.1	0.85	0.73	0.16	0.13	0.1
pentenes	3.6	1.9	1.4	2.2	1.7	1.9			
neopentane	5.5	2.9	1.8	5.0	5.6	5.8			
propylene	−1.1	−0.8	−1.1	−0.8	−1.0	1.6	−0.2	9.3	5.5
butadiene	0.33	0.15	0.06	0.46	0.81	1.43	1.56	2.4	2.8
ethane	2.8	0.07							
propane	0.45								
isopentane	0.9	0.28							

would cause the maximum errors in analysis to be in the percentage of propylene and isobutene. An error of 0.1 to 0.2 percent in the propylene analyses at higher pressures would reverse the sign of the reported rates of formation.

Analysis of the products of each of several preliminary one-hour static runs for acetylene by the method of Ross and Trumbull[10,1] indicated less than 4 micromoles of acetylene present. (The reagent blank was of the order of 1.5 micromoles.) No acetylene could be detected by mass spectrometric analysis; assuming that this method could detect 0.1 mole percent, an upper limit of 0.01 micromoles per minute may be given for the rate of production of acetylene.

Products of Single Pass Runs

A viscous polymer which seemed to yellow with continued irradiation was observed on the walls of the reaction tube. The polymer was soluble in benzene and in petroleum ether. Non-condensable gas was formed at a rate of about 0.2 micromoles per minute. After pumping off the gas non-condensable in liquid nitrogen, the bulk of the residual isobutene was distilled off at dry ice-acetone temperature. About 1–2 ml of a liquid product remained in the still at dry ice-acetone temperatures. This liquid had a vapor pressure of 0.03 mm at −78°C, 22 mm at 0.0°C, and 62 mm at 25°C.

TABLE IV.

Run No.	Partial pressure of isobutene	Compound added	$-dP/dt$ mm/min. $\times 10^2$	% change in rate
67	10.3	Nitric oxide, 11%	9	350
68	11.3	Nitric oxide, 1.2%	10	400
71	11	Nitric oxide, 0.91%	3.6	70
77	9.8	Nitric oxide, 0.14%	2.2	0
76	8.7	Propylene, 7.3%	2.82	26
85	21	Acetylene, 5.5%	4.24	120
86	20	Acetylene, 1.5%	2.25	16

Effect of Added Impurities

Several runs were made with small amounts of added nitric oxide, propylene, or acetylene. In all cases, except one, the initial rates of pressure decrease were greater than the rates for the same partial pressure of isobutene without added impurities, as shown in Table IV. With added propylene or acetylene, the pressure decrease was entirely linear with time. However, in the runs with added nitric oxide, the rate of pressure decrease finally decreased to a value approximately the same as that for pure isobutene at the same partial pressure, as shown in Fig. 3. The length of time elapsing before the rate decrease occurred varied with the amount of nitric oxide initially added. Furthermore, the pressure of non-condensable gas measured at the end of the nitric oxide runs was always less than the vapor pressure of nitric oxide at liquid nitrogen temperatures, indicating that the bulk of the nitric oxide was used up during the reaction.

Light Intensity and Quantum Yield

The results of the uranyl oxalate-oxalic acid actinometric determinations are reported in Table V. Note the agreement between runs A_1 and A_2, in which the percentages decomposition of oxalate ion were 13 and 50 percent, respectively. Runs A_3 and A_4 were made after repairs to the reaction system had been made between runs 77 and 79. Run A_5 served to calibrate

a sulfidized copper gauze placed between the lamp and the reaction cell.

With the sulfidized copper gauze in place reducing the light intensity to 0.30 of its unreduced value, the results tabulated in Table VI were obtained. (Values of normal rates were obtained from Fig. 2 by interpolation, when necessary.)

The quantum yield of isobutene consumption, calculated from the data of Tables III and V, is of the order of 0.03.

One one-hour run was made in which the lamp was shuttered for 1 minute after each 10 minutes of exposure. The pressure increased slightly each time that the cell was exposed to the light, and decreased immediately after each shuttering of the lamp. Neglecting these phenomena, the graph of pressure decrease against time of exposure was linear, and the rate of pressure decrease determined from the graph was the same as that for a normal continuous-exposure run made at the same initial pressure.

Effect of Surface

The rate of pressure decrease measured for an initial pressure of about 10 mm when the cell was coated with potassium chloride was about 5 percent lower than the rate observed for the same initial pressure in the uncoated cell.

DISCUSSION

The decrease in rate of consumption of isobutene with increasing initial pressure, paralleled by the decrease in rate of pressure decrease, can best be explained by postulating the formation of an activated isobutene molecule as the product of the initial quenching process. On this basis the initial steps would be the following:

$$i\text{-}C_4H_8 + Hg(^3P_1) \rightarrow i\text{-}C_4H_8^* + Hg(^1S_0) \quad (1)$$

$$i\text{-}C_4H_8^* + i\text{-}C_4H_8 \rightarrow 2i\text{-}C_4H_8 \quad (2)$$

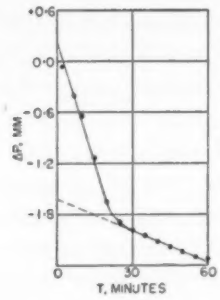

FIG. 3. Pressure decrease *vs.* time for a static run with 1.3 vol. percent of nitric oxide. (Initial isobutene pressure 11 mm.)

with $i\text{-}C_4H_8^*$ leading to reaction if not deactivated.

Both the rate of isobutene consumption and the rate of pressure decrease appear to approach a constant value for initial pressures of the order of 180 mm and higher. Furthermore, in this initial pressure region, the ratio of these respective rates is approximately 2. This suggests that the chief reaction in this region of complete deactivation is dimerization, i.e., that simultaneous with reaction (2) there is a reaction of the type

$$i\text{-}C_4H_8^* + i\text{-}C_4H_8 \rightarrow C_8H_{16}^*. \quad (3)$$

While the dimer thus formed would be "hot," its large number of degrees of freedom should permit it a long enough life that the excess energy would be removed by collisions. The presence among the single-pass products of a liquid in the C_7–C_8 vapor pressure range certainly tends to support the suggestion of dimer formation. However, establishment of this proposed dimerization step and postulation of other steps of the mechanism must await the results of the investigation now being initiated using purer initial reactant, in which more accurate analytical data on the reaction products, including up to the C_8 fraction, will be sought.

TABLE V.

Run No.	Percent decomposition	Intensity einsteins/min. $\times 10^6$
A_1	13	1.6
A_2	50	1.59
A_3	50	1.64
A_4	53	1.70
A_5	32	0.51

TABLE VI.

Run No.	P_0 mm	$-dP/dt$ mm/min. $\times 10^2$	Rate at reduced intensity / Rate at full intensity
83	8.1	0.70	0.31
81	11.7	0.69	0.32
79	11.7	0.78	0.36
82	29.5	0.495	0.27
80	57	0.399	0.26

The absence of acetylene from the major products found in this observation suggests that in Gunning and Steacie's investigation,[5] either an acetylene-generating impurity was present, or acetylene itself was present as an undetected impurity. Their rate of pressure decrease, reduced to a system volume of 280 ml, was about three times that observed in the present investigation, whereas their light intensity, based on the mercury photosensitized reactions of ethylene and corrected in accordance with recent data on the ethylene reaction,[14] was 0.55 times the intensity used in the present investigation. Assuming the rate of pressure decrease to be directly proportional to light intensity, Gunning and Steacie's observed rate was greater than that found by the authors by a factor of 5.5. Results of the present investigation show that added acetylene increases the observed rate of pressure decrease (see Table IV), which supports the suggestion that acetylene may have been present as an impurity in the original gas used by Gunning and Steacie.

The increase in rate when propylene is added to the reacting isobutene indicates that the rates determined by Gunning and Steacie[5] and by the authors may be inaccurate, since propylene was present in the original isobutene to the extent of 1 percent and 1.5 percent, respectively. An investigation using much purer isobutene is under way in these laboratories.

The increase in reaction rate in the presence of added nitric oxide, together with the consumption of the nitric oxide in the course of the reaction, suggests that a mercury photosensitized reaction of nitric oxide with isobutene occurs, similar to that suggested in the case of butadiene.[2]

[14] G. A. Allen and H. E. Gunning, J. Chem. Phys. **16**, 634 (1948).

For our purpose, therefore, these results are irrelevant.

The identification of the apparent induction period with a real pressure increase very closely equal to the pressure decrease observed on shuttering the lamp suggests that these phenomena are due to some physical cause similar to the Budde effect[15] and the Draper effect.[16]

CONCLUSIONS

The results of the present investigation show that isobutene forms an activated molecule in the initial quenching process, although simultaneous alternative processes cannot be eliminated on the basis of these results. Nevertheless isobutene has now been shown to quench in an analogous manner to the other olefins which have been previously investigated—ethylene,[1] butadiene,[2] propylene,[3] isoprene,[3] 1-butene,[4] and 2-butene.[4]

Proposal of a detailed mechanism for the reaction must await investigation of the reaction using a purer initial reactant than heretofore and more accurate analyses of the products formed. Such an investigation might also conceivably shed some light on the low value of quantum yield found in the present investigation.

ACKNOWLEDGMENTS

It is a great pleasure to acknowledge our indebtedness to the Sun Oil Company and to Dr. W. H. Barcus of their Development Laboratory for their kindness in performing the mass spectrometric analyses reported in this paper.

Our thanks are also extended to Mr. Burton E. Dearing for his assistance in making infra-red absorption measurements.

[15] E. Budde, J. prakt. Chem. **7**, 376 (1873).
[16] J. Draper, Phil. Mag. **26**, 476 (1845).

THE JOURNAL OF CHEMICAL PHYSICS VOLUME 16, NUMBER 12 DECEMBER, 1948

The Effect of Electric Fields on the Decomposition of Nitrous Oxide by Alpha-Rays

NELSON T. WILLIAMS* AND HARRY ESSEX
Department of Chemistry, Syracuse University, Syracuse, New York
(Received July 26, 1948)

Combination of oppositely charged ions plays no part in initiating the decomposition of nitrous oxide by alpha-rays at 10 cm and at 20 cm pressure. The decomposition in the absence of a field is evidently largely initiated by the splitting of molecules on electron collision. The application of electric fields above those required to attain half-saturation increases the ion yield because of the acceleration of free electrons by the fields. At higher field strengths the ion yield attains a value which remains unchanged on further increase in field strength. When the ion yield has this final constant value all electrons are attached to form negative atomic or molecular ions before reaching the electrode. Assuming the same reactions occur on electron collision as in the photo-chemical reaction the increase in ion yield as a result of the effect of the field involves a *minimum* of 1.2 molecules of nitrous oxide split without attachment of the electron for each molecule split with attachment.

IN radiation chemistry, ion yields (the number of molecules reacting or produced per ion pair) and their variation on changing conditions have proved useful in the elucidation of mechanism. For gaseous alpha-ray reactions, studies of the effects on ion yields of electric fields across the reaction mixtures have proved particularly indicative as to mechanism. For instance, from the effect of electric fields, the fraction of the reaction initiated by combination of oppositely charged ions may be calculated. Also the extent to which the reaction is initiated by molecule splitting on electron collision may be estimated. In some of the alpha-ray reactions which we have studied, at 20 cm pressure, none of the reaction is initiated by combination of oppositely charged ions but all of them appear to be largely initiated by the second mechanism. In such a molecular split the electron may be left attached to one of the fragments, e.g., $NH_3+e^-\rightarrow NH_2^-+H$. But also it is possible that the electron remain unattached, e.g., $NH_3+e^-\rightarrow NH_2+H+e^-$ and so be left over to repeat the process. From the effect of the field strength on the ion yield we have calculated, apparently for the first time, the relative probability of molecule splitting by electrons, with and without attachment. In the cases which have been studied in this laboratory, splitting without attachment is the more probable process.

This paper presents the data on the decomposition by alpha-rays, of nitrous oxide at 20 cm and at 10 cm pressure. The effect of electric fields on the ion yields at these low pressures is markedly different from the effect at one atmosphere.[1]

The experimental procedure was practically identical with that described in earlier work,[1,2,3,4] from this laboratory, the number of ion pairs produced in unit time being measured by the saturation current and the amount of decomposition calculated from measurements of the pressure of the gaseous products formed which were not condensed by liquid oxygen.

EXPERIMENTAL

The reaction system is shown in Fig. 1. Copper shields were affixed outside to the ends of the reaction vessel by means of a conducting cement made of silver filings in Du Pont nitrocellulose cement in order to eliminate the possibility of sparking between the platinum electrodes and the glass walls, which though invisible may cause considerable ionization. The shield at the high +potential end was connected to the electrode lead, the shield at the low potential end was grounded and provided with a central hole through which passed the lead to the electrode. The reaction system was found to be free from leaks when left evacuated with the mercury *U* seal closed. The radioactive material was placed

* Du Pont Fellow 1946–7.

[1] A. D. Kolumban and H. Essex, J. Chem. Phys. **8**, 450 (1940).
[2] D. FitzGerald and H. Essex, J. Am. Chem. Soc. **56**, 65 (1934).
[3] C. Smith and H. Essex, J. Chem. Phys. **6**, 188 (1938).
[4] M. J. McGuinness, Jr. and H. Essex, J. Am. Chem. Soc. **64**, 1908 (1942).

in a small depression in the bottom of the reaction vessel.

The nitrous oxide was obtained from a cylinder supplied by the Ohio Chemical Company and had a nitrous oxide content of 99.5 percent or more. The gas was further purified by passage over soda lime and barium oxide and condensed in the trap, Fig. 1, by liquid oxygen. After closing the mercury seal the nitrous oxide was vaporized. The nitrous oxide was again condensed, the uncondensed gases evacuated and the process repeated until the pressure of uncondensed gas was at a small fraction of its original value. This sample was used for the run. The saturation current was measured immediately after vaporizing the nitrous oxide at the start of each run and at periods of twenty-four hours or more thereafter during the course of the run and immediately before the end of a run. These values of the saturation current were plotted against time and the average saturation current calculated for the run. The number of ion pairs was calculated from the product of this average saturation current and the duration of the run. At the end of the run the pressure of noncondensed gas was measured one-half hour after condensation and again one-half hour later and, if the pressure appeared to be essentially constant, the average of these values was taken. In a few cases a third reading one-half hour later was required and this was averaged with the preceding reading. Three or four readings at different points on the McLeod gauge were taken for each pressure measurement. The reaction vessel was enclosed in an air bath kept at 30°C. The volume of the reaction system had been determined so the number of molecules of uncondensed gas produced could be calculated from the change in pressure of uncondensed gas. By means of a thermocouple fastened at a particular height on the trap the level of the liquid oxygen was kept at the same height during a pressure measurement and the volume of the system was corrected to take account of the fact that a small portion of the gas was at liquid oxygen temperature.

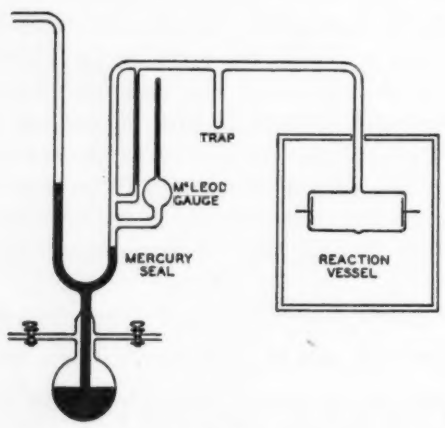

FIG. 1.

The results are presented in Table I. Two series of measurements were carried out. They are designated in the table as Series I and Series II. In Series I the cylindrical reaction vessel was 11 cm long and 6 cm in diameter. The total volume of the system was 565 ml and the factor by which the tabulated pressures must be multiplied to correct for the fact that a portion of the system during the pressure measurements was at liquid oxygen temperature and another portion at room temperature is 1.075. The reaction vessel in Series II measurements was 13.5 cm long and 7.5 cm in diameter, with a total volume of the system of 820 ml and a pressure correction factor of 1.04. The exact amounts of radioactive material used in the decomposition were not determined, since the number of ion pairs produced was calculated directly from the measured value of the saturation current. A mesothorium salt containing a small amount of radium was used in experimental Series I, the total being equivalent to about 0.3 mg of radium. About 0.4 mg of radium as radium bromide was the source of high energy particles in experimental Series II. Ion yields are expressed in molecules of noncondensed gas per ion pair.

The average ion yields *versus* X/p are plotted in Fig. 2, in which X is the field strength in volts per centimeter and p is the pressure of nitrous oxide in mm X/p is a measure of the energy attained by the ions in the gas as a result of the electric field. Half-saturation values of X/p are indicated by solid square and circle. Figure 2 also shows characteristic current—potential curves at both 20 cm pressure and 10 cm pressure from which it is apparent that there is no increase in ionization because of the field at the highest fields employed.

DISCUSSION

With no field applied across the reaction vessel the ions present in the gas become neutralized by combination in the gas or by neutralization at the walls. A field sufficiently strong to produce half-saturation, i.e., to neutralize one-half of the ions at the electrodes, should result in reducing the amount of combination of oppositely charged ions in the gas phase. With nitrous oxide at 20 cm pressure the ion yields at no field and at half-saturation are 4.2 and 4.3 respectively, which agree within the experimental error. At 10 cm pressure the average values in both cases are identical, 3.9. The fact that the application of a field sufficient to produce half-saturation does not change the ion yield at these pressures indicates that none of the reaction is initiated by combination of ions. At the higher pressures of Kolumban and Essex[1] 9 percent of the reaction was found to be initiated by combination of ions.

Increase of the electric field above the value for half-saturation gave increased ion yields at both pressures studied. Such an increase was also observed by Kolumban and Essex[1] at higher pressures. Townsend[5] has shown that in gases at not too low pressures the molecular ions are not accelerated by applied fields to energies much greater than the thermal energies, whereas free electrons are accelerated to energies greatly above thermal, to values determined by X/p. The increase in the ion yield which occurs as the field is increased above half-saturation can be attributed to the splitting of nitrous oxide molecules on electron collision. According to measurements of Bradbury and Tatel[6] nitrous oxide itself has no electron affinity but electrons in nitrous oxide form molecular ions at X/p of 2 corresponding closely with the value of X/p at which in these experiments an increase in ion yield is first observed. According to Bradbury and Tatel[6] the reaction beginning at $X/p=2$ is

$$e^-+N_2O\rightarrow N_2+O^-.$$

Finally further increase of the electric field is found to give no change in the ion yield, a constant value of 8.4 being obtained at 20 cm and 7.5 at 10 cm pressure. The authors believe that at these higher values of X/p, all of the free electrons eventually become attached and form massive ions which then are not appreciably accelerated by the field and cause no further decomposition. Calculations based on the probabilities of electron attachment in nitrous oxide at X/p of 6 and greater as determined by Bradbury and Tatel[6] and by Bailey and Rudd[7] support the assumption that, in these experiments, all of the electrons become attached before reaching the electrodes. The energy of electrons in nitrous oxide as a function of X/p is not well known and it is possible that at these higher values of X/p splitting of nitrous oxide may occur in the manner

$$e^-+N_2O\rightarrow N+NO^-$$

as well as by the Bradbury and Tatel reaction.

However molecular splits without attachment, e.g.,

$$e^-+N_2O\rightarrow N_2+O+e^- \quad \Delta E=1.8 \text{ ev}^8$$
$$e^-+N_2O\rightarrow N+NO+e^- \quad \Delta E=3.7 \text{ ev}^8$$

TABLE I. N_2O decomposition.

Experimental series	X/p	Duration of run in hours	Increase in pressure of noncondensed gases in mm	Saturation current amp. $\times 10^7$	Ion yield
Ion yields at 20 cm pressure and 30°C					
I	0	344.6	0.3302	2.07	4.00
I	0	178.7	0.1925	2.07	4.49
II	0	161.0	0.1651	3.10	4.01
II	0	137.8	0.1456	3.07	4.18
II	0	140.8	0.1539	3.13	4.23
				average	4.2
I	0.6*	279.8	0.2926	2.07	4.37
II	0.6*	132.8	0.1431	3.09	4.23
II	0.6*	158.0	0.1738	3.11	4.28
				average	4.3
II	2.0	164.8	0.2211	3.15	5.18
I	7.5	176.2	0.3539	2.07	8.38
I	9.8	160.8	0.3182	2.08	8.21
I	12.0	139.9	0.2834	2.09	8.37
I	12.0	142.5	0.3065	2.09	8.89
				average	8.6
Ion yields at 10 cm pressure and 30°C					
II	0	140.3	0.0674	1.55	3.76
II	0	139.8	0.0720	1.57	3.97
				average	3.9
II	0.25*	141.0	0.0698	1.57	3.82
II	0.25*	139.8	0.0707	1.57	3.90
				average	3.9
II	4.0	134.0	0.1217	1.57	7.03
II	7.5	139.0	0.1363	1.58	7.51
II	12.0	139.9	0.1413	1.59	7.72

* X/p values at half-saturation current.

[5] J. S. Townsend, *Electricity in Gases* (Clarendon Press, Oxford, 1915), p. 183.

[6] N. E. Bradbury and H. Tatel, J. Chem. Phys. **2**, 835 (1934).

[7] V. A. Bailey and J. B. Rudd, Phil. Mag. (7) **14**, 1044 (1932).

[8] W. A. Noyes, Jr., J. Chem. Phys. **5**, 807 (1937).

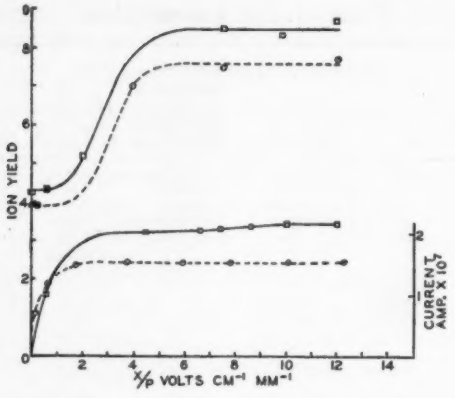

FIG. 2. The two upper curves show the variations in ion yield with X/p, the solid curve at 20 cm, the dashed curve at 10 cm pressure. Values of ion yields at fields sufficient to give half-saturation currents are indicated by the solid square and circle. The two lower curves are typical current *vs.* X/p curves at 20 cm (solid line) and 10 cm (dashed line) respectively.

are possible and must be postulated to explain the magnitude of the increase in ion yield at high field strengths. Evidence for or against electron reactions of this latter type is of course not obtainable from mass-spectrographic studies. The constancy in ion yield at high field strength requires that the ratio of the cross sections of nitrous oxide for splitting without and with electron attachment be independent of field strength.

The pressures used in this work are comparable to those used by Noyes[8] in his photo-chemical studies and the products are substantially the same. Noyes reports the overall reaction in the absence of mercury vapor as

$$4N_2O \rightarrow 2.8N_2 + 2.5NO + 0.7O_2$$

and Wourtzel[9] reports for the alpha-ray decomposition in the presence of mercury vapor that the products include nitrogen, oxygen and oxides of nitrogen. In the photo-chemical decomposition the primary processes are believed to be

$$N_2O + h\nu \rightarrow N_2 + O \quad \text{and} \quad N_2O + h\nu \rightarrow NO + N.$$

Possible subsequent reactions are:

$$\begin{aligned} N + N_2O &\rightarrow N_2 + NO \\ O + N_2O &\rightarrow N_2 + O_2 \quad \text{or} \quad 2NO \\ O + O + M &\rightarrow O_2 + M \\ N + O + M &\rightarrow NO + M \\ N + N + M &\rightarrow N_2 + M \\ O + NO(+M) &\rightarrow NO_2(+M) \\ O_2 + 2NO &\rightarrow 2NO_2, \end{aligned}$$

and in the presence of mercury vapor:

$$\begin{aligned} Hg + NO_2 &\rightarrow HgNO_2 \\ HgNO_2 &\rightarrow HgO + NO. \end{aligned}$$

The average quantum yield obtained by Noyes was 1.9 molecules of noncondensed gas produced per quantum in the presence of mercury vapor. In the alpha-ray decomposition, if it is assumed that the electron collisions with nitrous oxide molecules result, on the average, in the production of the same products in the same proportions as in the photo-chemical process, a value for the number of electron collisions with nitrous oxide molecules resulting in decomposition caused by the electric field can be calculated. Thus it is assumed that the average electron collision will, on splitting a nitrous oxide molecule, yield 1.9 molecules of noncondensed gaseous products. The increased ion yield as a result of the field at 20 cm is 8.4 molecules of noncondensed gas obtained at the high field minus the 4.2 molecules obtained at no field or 4.2 molecules caused by the free electrons accelerated by the field. Since the electrons finally become attached, one splitting process which yields 1.9 molecules of noncondensed product, will result in attachment. This leaves $4.2-1.9$ or 2.3 molecules of product yielded by electron collisions which split nitrous oxide molecules without the electron becoming attached to one of the products. Thus the assumption that the products obtained in this work are the same as those in the photo-chemical study of Noyes leads to the conclusion that 2.3/1.9 or 1.2 collisions of electrons accelerated by the field result in splitting without attachment for each collision producing splitting with attachment. In this calculation it has further been assumed that all of the negative ions are electrons, and the figure given for the ratio of the number of collisions giving splitting without attachment to the splittings with attachment will be low to the extent that negative atomic or molecular ions are present in the negative ion stream to the anode. Work is now in progress in this laboratory to determine the fraction of the negative ions which are electrons, using the Loeb electron filter,[10] a grid across the alternate wires of which a high frequency potential is applied to remove electrons from the negative ion stream. The same ratio of splitting without attachment to splitting with

[9] E. Wourtzel, Le Radium **11**, 289, 332 (1919).

[10] A. M. Cravath, Phys. Rev. **34**, 605 (1929).

attachment is obtained from our measurements at 10 cm pressure, assuming the quantum yield in the photo-chemical reaction at this pressure is 1.6, which is plausible from the data of Noyes[8] which indicate decreasing quantum yield with decrease in pressure.

The value given for the relative frequency of splitting without and with electron attachment is of considerable interest even though the value is approximate and minimum as this is apparently the first attempt to experimentally determine the relative frequency of these competing processes.

Since energetic electrons are present in the absence of a field, much of the alpha-ray decomposition under such conditions must be initiated by electron splitting with and without attachment. However, this is not the only primary mechanism operative under these conditions. Mass-spectrograph analysis of the positive ions produced in nitrous oxide on electron bombardment shows the presence of O^+, N_2^+, NO^+ and N^+.[11]

The ion yields at 10 cm pressure at each X/p are lower than the ion yield at the corresponding X/p at 20 cm pressure. A similar effect of pressure on the quantum yield in the photochemical reaction has been observed.[8] The walls may preferentially catalyze the combination of oxygen and nitrogen atoms relative to the reactions of these atoms with nitrous oxide.

[11] H. D. Smyth and E. C. G. Stueckelberg, Phys. Rev. 36, 478 (1930).

THE JOURNAL OF CHEMICAL PHYSICS VOLUME 16, NUMBER 12 DECEMBER, 1948

Infra-Red Christiansen Filter Effect in Slurries of Organic Crystals

W. C. PRICE*
Ryerson Physical Laboratory, University of Chicago, Chicago, Illinois
AND
K. S. TETLOW
Imperial Chemical Industries, Limited, Nobel Division, Nobel House, Stevenston, Ayrshire, Scotland

(Received July 22, 1948)

The Christiansen filter effect in slurries of organic crystals is reported for the first time, in the infra-red. The main difference between the effect in molecular and in ionic crystals is that the Christiansen (transmission) peak and the "Reststrahlen" (reflection) peaks are much closer together for organic crystals since they are produced by a single frequency instead of a wide band of lattice frequencies. The Christiansen effect is much more selective in organic crystals since it occurs for some bands but not for others. This is thought to be due to the nature of the coupling between the particular vibration and the atoms or groups in the molecule which make major contributions to the polarizability.

THE high transmission of a finely ground suspension of particles in a liquid medium for light for which the particles and the medium have the same refractive index is well known. It was first observed by Christiansen[1] with visible light. It has been made use of both in the ultraviolet[2] and the infra-red[3] as a selective filter for radiation. No description of the effect in slurries of organic crystals has yet been published, as far as the authors are aware. The effect is of considerable interest both from the theoretical and practical points of view, as will become evident from the following considerations.

The changes of refractive index which give rise to the effect are due to absorption bands in the material. The effect can occur at wavelengths far removed from the absorption band as a result of the gradual crossing of the dispersion curve of the particles and that of the medium.

* This work was in part assisted by the Office of Naval Research under Task Order IX of Contract N6-ori 20 with the University of Chicago.

[1] Christiansen, Wied. Ann. (1884).

[2] A. G. Gaydon and G. J. Minkoff, Nature 158, 788, 1946; R. L. Sinsheirner and J. P. Leofbourow, Nature 160, 674 (1947).

[3] R. B. Barnes and L. G. Bonner, J. Opt. Soc. Am. 37, 713 (1947).

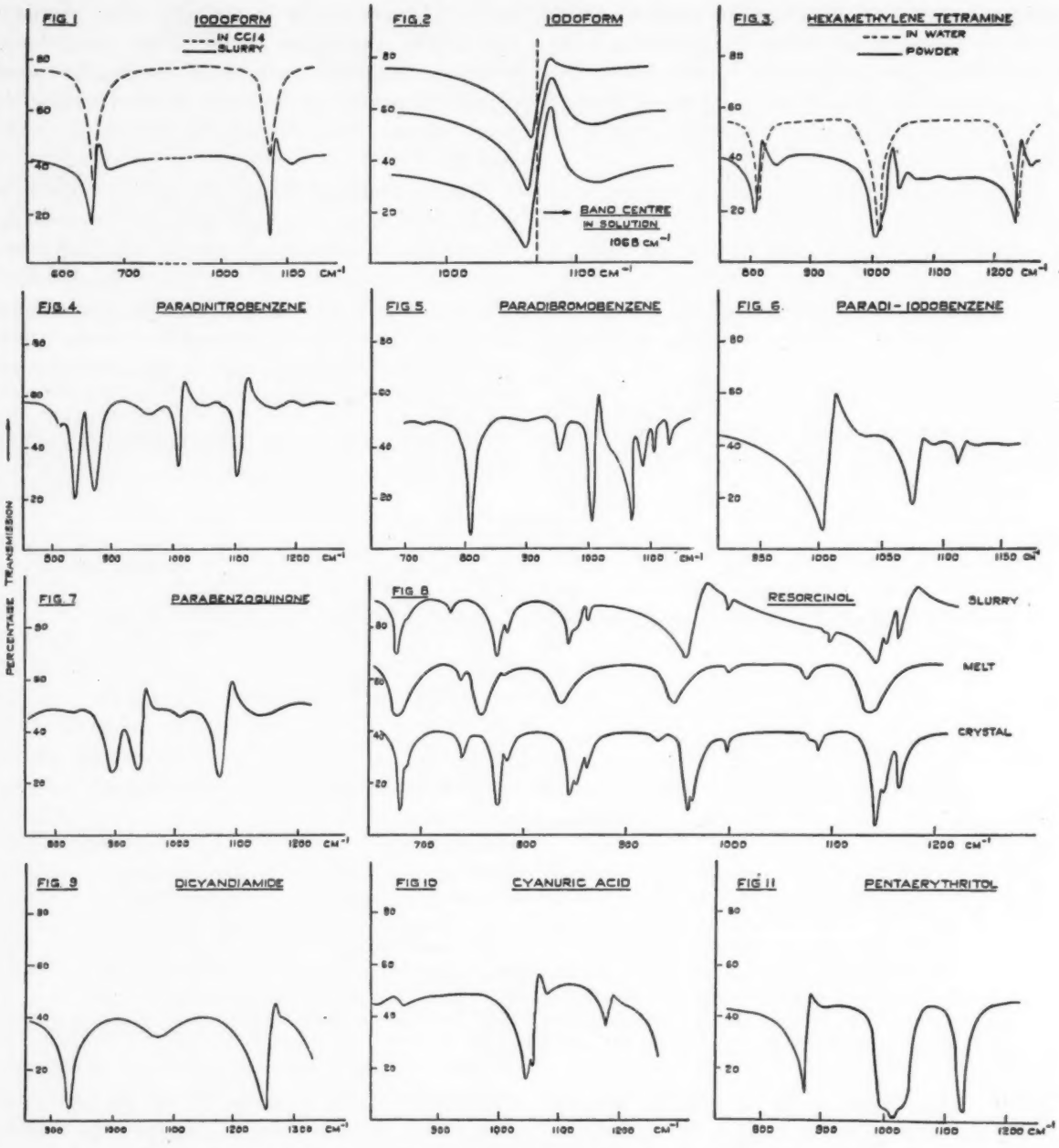

FIGS. 1–11. Infra-red spectra of slurries of substances showing the Christiansen effect.

However, we shall be concerned in what follows only with the effects, in the immediate vicinity of an absorption band, which result from the rapid changes in refractive index (i.e., anomalous dispersion) associated with that band. It is well known that as we approach a band from the long wave side the refractive index increases until it reaches a maximum. This makes for high reflectivity and is, of course, associated with the "Reststrahlen" peaks of ionic crystals. In a finely ground powder or suspension this would greatly increase the scatter and tend to make the powder or suspension opaque on the low frequency side of the band. Passing through the band the refractive index suddenly falls so that losses by scatter are reduced, though losses by absorption may be considerable. On coming out on the high frequency side, reflection losses are

greatly reduced and the powder begins to transmit. This transmission reaches a peak and then is reduced again as the wave-length moves out of the range in which the absorption band has a large effect on the refractive index of the powder. Thus powders of alkali halide crystals have Christiansen transmission peaks just on the high frequency side of their absorption bands[3] as a result of the refractive index being reduced to unity by the negative contribution of the band on its high frequency side. The bands of such crystals are strong, and their effect on the refractive index is large by virtue of the ionic nature of the crystal. They are broad because the absorption corresponds to a group of lattice vibrations, the crystal itself being a macromolecule and linked throughout by strong bonds. In contrast to ionic crystals, the molecules in organic crystals preserve most of their individual character as they are held in the lattice only by Van der Waals and weak polar forces. The absorption bands are sharp and differ little from those of the single molecule.[4] As the binding is mainly covalent, the polarities developed by the vibrations are not nearly so great as in ionic crystals and consequently the bands are weaker and have a smaller effect on the refractive index. Thus the Christiansen-"Reststrahlen" effect would be expected to be much weaker and to be largely confined to the immediate neighborhood of the band. This, in fact, is what has been found.

As quite a large volume of work has been done on slurries of organic crystals without the effect being noticed, it might be suspected that the refractive index of the crystalline particles is little affected by the infra-red absorption bands of these compounds, or possibly that the powders used were ground so finely that the particle size was much less than the wave-length of the light used so that no scattering was produced.** However, the substances reported below show the effect quite well and bring out the somewhat surprising fact that only certain specific infra-red bands of the molecule show the Christiansen effect. This may only be a matter of degree, but it is quite clear from the results to be reported that the effect exerted on the refractivity of the molecule by some bands is of a different order of magnitude from that associated with other bands of comparable intensity. The reason for this selective behavior appears to be that vibrations in groups of atoms which make a major contribution to the molecular refractivity are closely coupled to the electronic polarizability of these atoms (or groups). This is especially so if the vibrations involve appreciable relative displacements of these highly polarizable atoms. Vibrations in other parts of the molecule between atoms making minor contributions to the molecular refractivity will, presumably, not have such a great effect upon the refractive index. Another factor which seems to be important is whether the direction of the vibrating dipole associated with the infra-red band lies along the direction of minimum or maximum electronic polarizability in the molecule.

THE SPECTRA OF SUBSTANCES SHOWING ANOMALOUS TRANSMISSION

Iodoform

The simplest molecule in which the effect has been observed is iodoform. Transmission curves of iodoform, (a) in solution in carbon tetrachloride, and (b) ground into a slurry with liquid paraffin, are shown in Fig. 1. It is clear that the slurry shows an effect similar to anomalous dispersion, the refractive index changes showing themselves in the abnormally high absorption on the low frequency side of the band and abnormally high transmission on the high frequency side of the band. It might be expected

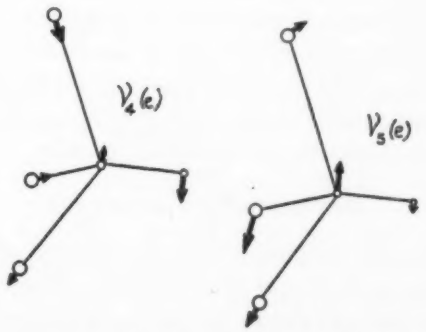

FIG. 12. Normal vibrational modes of iodoform corresponding to $\nu_4(e)$ and $\nu_5(e)$.

[4] T. A. Kletz and W. C. Price, J. Chem. Soc., 644 (1947).

** Since this was written, Barnes *et al.* (Anal. Chem. 20, 402 (1948)) have published an infra-red absorption trace of a slurry of 5-bromo thiophene 2-carboxylic acid. This substance appears to show the Christiansen effect at the 981-cm^{-1} band.

that the point at which the transmission curve crosses the average transmission value for the slurry outside the absorption band should be slightly to the high frequency side of the true position of the absorption band as it would have been observed in an iodoform crystal. Actually, it appears to be coincident with the center of the absorption band in carbon tetrachloride solution. Possibly the solution band is slightly to the high frequency side of the solid band. Figure 2 shows the effect of increasing the amount of slurry in the beam. The dip below normal which the transmission curve takes on the high frequency side of the Christiansen peak is, of course, due to the spread of the absorption band. On the low frequency side the absorption only serves to enhance the loss by multiple reflection and thereby to depress the transmission. It is doubtful whether the refractive index ever falls as low as that of the medium (liquid paraffin). If it did fall appreciably lower, then the transmission peak on the high frequency side of the band might be expected to be a narrow doublet. It is possible that the resolution of the spectrometer would be inadequate to show this.

Both the 1068-cm^{-1} $-\nu_4(e)$ and the 645-cm^{-1} $-\nu_5(e)$ bands show the effect while the $\nu_1(a)$ band does not. It was, of course, not possible to observe the effect at 3030 cm^{-1} because of the strong absorption of the liquid paraffin at this frequency, but no trace of the effect was found with fine powders which gave the effect with the other bands. The two vibrations ν_4 and ν_5 which show the effect are both of the same symmetry species "*e*." They are illustrated in Fig. 12. In both cases the vibrating electric moment is perpendicular to the symmetry axis. The ν_4 vibration is mainly one of CH deformation, but it does involve motion of the iodine atoms along the valence bonds in such a way as to distort the CI_3 symmetry. In ν_5 the iodine atoms move perpendicularly to the CI bonds again in such a way as to distort the CI_3 symmetry.

Hexamethylene Tetramine

The Christiansen effect is very marked in powders and slurries of hexamethylene tetramine (hexamine), as shown in Fig. 3. The powder was deposited on a rocksalt plate by evaporation of a hot solution in ethyl alcohol. In this case bands near 810, 1010, and 1240 cm^{-1} each show a strong marked anomalous transmission. The three bands which show the effect are most probably connected with vibration modes of the N_4 tetrahedron. The dotted curve corresponds to a layer of aqueous solution of hexamine (saturated at 20°C) about ten microns thick between silver chloride plates. The band centers are not always at the same positions relative to the transmission curves. This is probably due to differences between crystal spectra and solution spectra. These arise from small shifts inherent in the crystal spectra caused by the operation of intermolecular forces, or shifts in the solution spectra caused by the association with the solvent. It would be necessary to observe the spectra in thin single crystals to draw any conclusions in this connection (see later discussion of resorcinol).

Para-Substituted Aromatics

The para disubstituted benzenes seem to show the effect more strongly than the ortho and meta isomers, though this is not always the case, e.g., resorcinol seems to show the effect better than hydroquinone. Marked anomalous transmission is exhibited by slurries of di-iodobenzene; however, the relatively similar magnitude of the Christiansen effect in the di-iodo, dibromo, and dinitrobenzenes would not suggest the polarizability of the substituent as the main governing factor. On the contrary it appears more likely that the magnitude of the effect depends on the product of the polarizability and the displacement of the atoms.

All the parasubstituted bodies have a band at wave-lengths just above 1000 cm^{-1}, which shows anomalous transmission in the slurry. This band is probably analogous to the $\nu_{14}(E_{1u})$ [5] mode in benzene which is really a vibration of the H_6 ring against the C_6 ring, the motion taking place in the C_6H_6 plane parallel to one pair of opposite CC bonds. This probably means that there is relative motion of the ring and the substituent and consequently displacement of the π-electrons of the ring relative to the π-electrons of the substituent, with which they are conjugated. Such relative motion of the two groups of elec-

[5] G. Herzberg, *Infra-Red and Raman Spectra of Polyatomic Molecules* (D. Van Nostrand Company, Inc., New York, 1945).

trons which are making major contributions to the refractivity of the molecule may be important in making the band Christiansen active. Another band in the neighborhood of 1100 cm^{-1} is also strongly active for these substituted benzenes.

Resorcinol

A comparison of the spectra of resorcinol in the crystalline form, in the melt, and in the slurry is interesting as it illustrates the variety of information that can be obtained about the origin of the bands by examining the substance in these three physical conditions. In general, the spectrum of the slurry is the same as that of the solid except where the former exhibits the Christiansen effect. Both of these differ from the spectrum of the melt in a manner which has been found general for alkyl phenol crystals.[4] Briefly the differences are that many bands in the crystal are sharper, deeper, and resolved into components relative to the melt. Also they are often shifted appreciably (10–20 cm^{-1}) to higher frequencies. These changes are attributed to effects such as the increased order in the crystal, the action of intermolecular binding forces, the existence of more than one mode in which a molecule can be bound into the lattice, etc. From Fig. 8 it can be seen that the bands in the neighborhood 650–850 cm^{-1} show no Christiansen effect but are sharper than the bands of the melt, shifted to higher frequencies, and split up into two or more components. The bands in this region are probably the bending vibrations of the CH bonds perpendicular to the plane of the ring.[6] The packing of the molecule into the crystal lattice probably restricts their movement and increases their frequency. Bands in the 950–1200-cm^{-1} range show a similar effect but also show the Christiansen effect in the slurry. These bands are probably associated with deformation vibrations of the CH bonds in the plane of the ring (possibly also with OH deformation). For this reason (as has already been pointed out in discussing the parasubstituted bodies) they give rise to first-order displacements of the carbon atoms relative to one another and to substituted groupings, involving relative motions of the π-ring electrons and those of the substituted groups. This leads to strong coupling between the "refracting" electrons and these particular modes of vibration of the molecule, making them Christiansen active.

[6] D. H. Whiffen and H. W. Thompson, J. Chem. Soc. 268 (1945).

Other Compounds

Figures 9–11 give three other examples of the effect. Pentaerythritol $C(CH_2OH)_4$ has a band about 880 cm^{-1} which shows the effect. The (C)OH deformation band at *ca.* 1025 cm^{-1} does not show the effect. Dicyandiamide

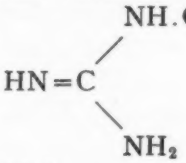

has an active band around 1255 cm^{-1} which is presumably caused by $=C-N$ valence vibration.[7] In cyanuric acid $(HCNO)_n$ an active band occurs at *ca.* 1055 cm^{-1}, possibly associated with $N-O$ valence vibration.

DISCUSSION

It would appear, as far as can be seen from the evidence at present available, that the Christiansen effect is a widespread effect in slurries of organic substances when these are examined in the infra-red. This has been confirmed by Dr. Thompson[8] who has found the effect to occur sporadically throughout the spectra of slurries of carcinogenic hydrocarbons. The strength of the effect appears to depend upon the polarizabilities of the atoms in the molecule and the nature of the vibration in which these are involved.

Our knowledge of the magnitude of the effect of infra-red absorption bands on the refractive index of molecules is rather scanty. For the cases which have been investigated in detail, serious quantitative discrepancies are found with the simple classical theory. The classical formula for the refractive index is

$$n^2-1=N\sum_i e_i^2/\pi m_i(\nu_i^2-\nu^2)+N\sum_j e_j^2/3\pi m_j(\nu_j^2-\nu^2), \quad (1)$$

where ν_i refers to the natural electronic frequencies of the molecule and ν_j to the infra-red interatomic ones; "e" and "m" are the effective charges and masses of the electrons and nuclei.

[7] H. W. Thompson, J. Chem. Soc. 328 (1948).
[8] H. W. Thompson, private communication.

It can be shown from this that

$$4\pi N\alpha-(n_\infty{}^2-1)=\frac{Ne_{eff}{}^2}{3\pi m_{eff}\nu_{vib}{}^2}, \qquad (2)$$

where "α" is the polarizability and "n_∞" the refractive index extrapolated to infinite wavelength. The term $4\pi N\alpha$ in the static dielectric constant should exceed $(n_\infty{}^2-1)$ by a small amount which is a measure of the contribution of the infra-red vibration to the static dielectric constant. The degree with which (2) is satisfied in practice can be regarded as a criterion of the accuracy with which (1) represents the influence of the infra-red frequencies on refractive index. Measurements on hydrogen chloride quoted by Van Vleck[9] give 1.7×10^{-4} for the left side of (2), whereas the right side is calculated as 1.5×10^{-6}, e_{eff} being obtained from measurements of the intensity of the infra-red absorption. The difference though of the correct sign is out in magnitude by a factor of 100. It is not possible with any reasonable value for e_{eff} to make the right side of (2) of the same order of magnitude as the left.

The expression (1) is also unsatisfactory from the point of view of the effects which have been described in this paper, since it does not contain any term which is selective with respect to the character of the vibration. All infra-red bands according to this formula should exhibit the Christiansen effect in a degree proportional to the strength of the band. It is possible that there is a single explanation for both these anomalies. The infra-red term as it is written in (1) holds only for the case of rigid ions. That is, it is assumed that the atoms plus the associated electrons which take part in the vibration —the electrons moving with the nuclei with which they are mainly associated—vibrate as rigid ions of fractional electronic charge. In general, however, this term will also depend to a second order upon (a) the deformability of the ion and (b) effects depending upon the overtones and combination tones of the elastic spectrum which is produced by embedding a molecule in a crystal. The deformability of the ion depends upon the tightness of the binding of the electrons to the nuclei and this is directly connected with the electronic frequencies of the molecule. It is thought possible, therefore, that the formula for the refractive index should contain a cross term of the form

$$\sum_i \sum_j A_j/(\nu_i{}^2-\nu^2)^{\frac{1}{2}}(\nu_j{}^2-\nu^2)^{\frac{1}{2}} \qquad (3)$$

to be added to the right side of (1). 'A' is presumably a factor dependent amongst other things upon the nature of the relative displacements of the atoms in the particular vibration mode being considered. It is thus possible that for particular vibrations this cross term may make a bigger contribution to the refractive index than the atom polarizability itself, and thus resolve some of the difficulties which have been referred to above.

It is difficult at present to assess the influence of (b). In organic crystals, where the molecules are held in the lattice merely by weak Van der Waals forces or hydrogen bonds, the coupling of the molecular vibrations throughout the lattice is only weak. The infra-red spectra of organic crystals in the crystalline and molten state do not indicate large modifications in the molecular vibrations due to the influence of the lattice.[4]

In the above discussion the changes in reflectivity which give rise to the Christiansen effect are taken as evidence of change in refractivity. Professor M. Born kindly reminded the authors in correspondence that the reflectivity 'R' is a complicated function of 'n^2' and depends also upon the absorption coefficient 'k'. The nature of the function $R(n,k)$ is such as to give rise to appreciable displacement of the center of the "Rest-strahl" from the center of absorption in the case of ionic crystals. However it is certain that there is relatively little shift in the cases reported here. This is presumably because the infra-red absorption coefficients of organic crystals are in general much smaller than those of ionic ones.

In conclusion we should like to thank the U. S. Office of Naval Research and Imperial Chemical Industries for sponsoring the work which has been reported in this paper. We are also indebted to Professors M. Born and R. S. Mulliken for valuable discussion. It should be recorded, however, that neither of them considers that there is adequate evidence for expression (3).

[9] J. H. Van Vleck, *Theory of Electric and Magnetic Susceptibilities* (Oxford University Press, New York, 1932), p. 47.

Letters to the Editor

THIS section will accept reports of new work, provided these are terse and contain few figures, and espeically few halftone cuts. The Editorial Board will not hold itself responsible for opinions expressed by the correspondents. Contributions to this section should not exceed 600 words in length and must reach the office of the Managing Editor not later than the first of the month preceding that of the issue in which the letter is to appear. No proof will be sent to the authors. The usual publication charge ($4.00 per page) will not be made and no reprints will be furnished free.

Raman Spectra of Certain Phosphoric Acids and Their Salts

P. HOFFMAN AND T. J. HANWICK
Department of Physics, New York University, New York, New York
September 20, 1948

IN investigating the Raman spectra of certain phosphoric acids and their salts several new lines were found. The wave number displacements were measured from the 4358-angstrom line and are tabulated as follows:

For tripotassium phosphate

Simon and Schultze:[1] 420, 562, 937, 1022.
Hoffman and Hanwick: 420, 573, 704, 936, 1014, 2385.

For dibasic sodium phosphate

Ventakeswaren:[2] 886, 971, 1085.
Hoffman and Hanwick: 381, 527, 860, 992.

Among compounds not previously investigated we have found the following:

For metaphosphoric acid

359, 494, 719, 887, 1081

For potassium pyrophosphate

328, 473, 698, 1014

This work is being extended, and depolarization measurements are in progress.

[1] Simon and Schultze, Zeits. f. anorg. allgem. Chemie **242**, 313–369 (1939).
[2] C. S. Ventakeswaran, Proc. Ind. Acad. Sci. **3A**, 25 (1936).

Effect of Temperature on the Absorption Spectrum of Ozone: Chappuis Bands

A. VASSY AND E. VASSY
Physique de l'Atmosphere, Sorbonne, Paris
September 27, 1948

IN 1882 Chappuis[1] observed, while examining through a spectroscope the ozone bands which he had discovered two years previously, that these bands became more visible when the gas was cooled to about −50°C. Mme. Lefebvre,[2] in 1935, found no appreciable effect of temperature on the same bands.

In 1937 one of the present authors (E.V.)[3] confirmed Chappuis' results and published a graph giving a quantitative estimate of the change in the absorption coefficients for different temperatures. Unfortunately, an error in the wave-lengths appeared in this graph, and the proper correction was made later in two different publications.[4,5]

Recently, G. L. Humphrey and R. M. Badger[6] reinvestigated the phenomenon of absorption in ozone and did not find, within the limit of photometric errors, any change when the temperature was decreased.

Because of the discrepancies in these results and the importance of ozone in the field of atmospheric optics, we have undertaken new computations on the plates obtained in 1937. At that time these spectrograms were only a secondary result in an extensive program, occasioned by the opportunity given by an experimental device which was convenient for checking this point of contention, but as the plates were photographed under strictly correct photometric conditions, they deserve a more detailed study. Moreover, we have now designed a more accurate microphotometer[7] which offers the advantage of constant precision for all densities.

The results definitely show the effect of temperature. The records of spectra of the same quantity of ozone at 20°C and at lower temperatures to −105°C show a perfect coincidence in the blue region where ozone is a weak absorber; they are markedly different in the region of the strong bands (6010 and 5734A).

Table I gives the absorption coefficient for different temperatures; those in column 2 were determined by one of the authors (A.V.) in 1938.[8] It should be emphasized that the secondary maxima corresponding to Chappuis bands (Numbers 5, 6, and 8) are more prominent at low temperatures, as was reported by Chappuis. It has been suggested that the effect of temperature could be related to high concentrations of ozone. In fact G. L. Humphrey and R. M. Badger, and also Mme. Lefebvre, used low concentrations (6 percent), while we used a far higher one (between 60 and 75 percent). In Chappuis' experiments the concentration was low, about 5 percent. For this reason, the argument does not seem valid.

TABLE I.

Wave-length A.U.	+18°C	−42°C	−80°C	−105°C
6010	0.068	0.072	0.078	0.083
5872	0.0575	0.595	0.067	0.0695
5730	0.062	0.067	0.075	0.0775
5600	0.052	0.056	0.0625	0.067
5400	0.038	0.042	0.0485	0.051
5056	0.021	0.0225	0.0265	0.0265
4800	0.0095	0.011	0.0115	0.0115
4500	0.0014	0.0015	0.0015	0.0015

Concerning the atmosphere, Arnulf, Dejardin, and Falgon,[9] investigating the spectrum of atmospheric ozone, brought forward a very good verification of our numerical data. They first determined the ozone thickness and mean temperature in Huggins' bands using Ny and Choong's[10]

coefficients and the method proposed by one of the authors (E.V.). They found 0.290 cm and −35°C; next, with our temperature data and absorption coefficients (brought into agreement with Ny and Choong's) in Chappuis bands, they found 0.296 cm, pointing out that only this procedure gives a good agreement with the ultraviolet result.

We consider these comparative computations as a convincing proof of the influence of temperature on Chappuis bands in atmospheric ozone.

The conclusions resulting from the work of G. L. Humphrey and R. M. Badger raise another question. The measurements made at Mont Blanc by Arnulf, Dejardin, and Falgon are correct, because there is little or no more water vapor above this height. The situation is quite different at low altitudes, where the ozone bands are superimposed on the δ-band and rain bands of water vapor, and also on the α-oxygen band. The water-vapor bands are the more troublesome, and we gave numerical data concerning their contribution in our investigation of atmospheric absorption made in Morocco in 1938.[11]

[1] Chappuis, Ann. Ecole Norm. Sup. **11**, 137 (1882).
[2] L. Lefebvre, Comptes Rendus **200**, 653 (1935).
[3] E. Vassy, Ann. de physique **8**, 679–778 (1937).
[4] A. Vassy and E. Vassy, J. de phys. et rad. **10**, 408 (1939).
[5] E. Vassy, Ann. Astrophys., 5eme annee, No. 2, 82 (April, 1942).
[6] L. Humphrey and R. M. Badger, J. Chem. Phys. **15**, 794 (1947).
[7] A. Vassy and E. Vassy, Sci. et Ind. Photo. **19**, 56 (1948); **16**, 1, 65 (1945).
[8] A. Vassy, Comptes Rendus **206**, 1638 (1938).
[9] A. Arnulf, G. Dejardin, and Falgon, Comptes Rendus **205**, 1086 (1937).
[10] Tsi-Ze Ny and Shin-Piaw Choong, Comptes Rendus **195**, 309 (1932); **196**, 916 (1933).
[11] A. Vassy and E. Vassy, J. de phys. et rad. **10**, 75, 403, 459 (1939).

Nuclear Magnetism in Studies of Molecular Structure and Rotation in Solids: Ammonium Salts

H. S. GUTOWSKY* AND G. E. PAKE†,**
Harvard University, Cambridge, Massachusetts
September 30, 1948

USING apparatus previously described,[1] we have carried out a series of measurements on the width and structure of nuclear resonance absorption lines in various types of solids at temperatures ranging from 90°K to room temperature. In crystal powders of certain ammonium salts,[2] the line width is found to undergo a relatively sharp transition at temperatures 100° or more below the well-known specific heat anomalies for these substances. Figure 1, which plots against temperature the width of the proton line in NH_4Cl, illustrates such a transition.

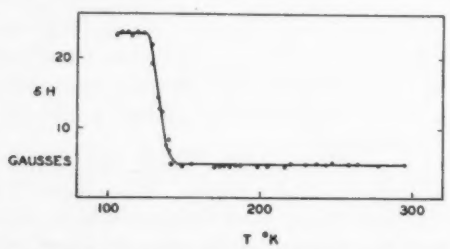

FIG. 1. Line width *versus* temperature for the proton resonance absorption line in NH_4Cl crystal powder.

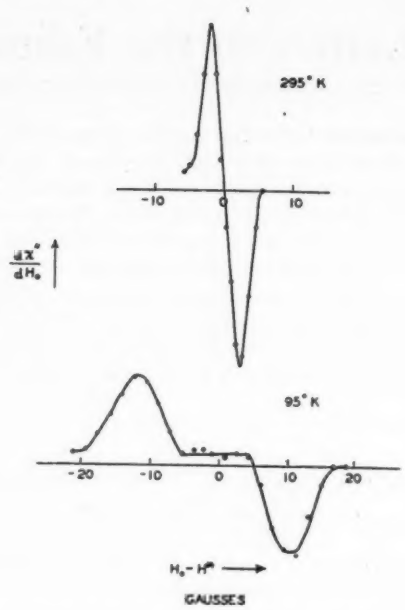

FIG. 2. Derivatives of the proton resonance absorption line in NH_4Cl crystal powder at 95°K and 295°K. H^* was approximately 6820 gauss.

In these experiments, "line width," denoted δH, is taken to be the width in gauss between points of maximum and minimum slope on the absorption curve, and is to be distinguished from the root-second-moment of the line, $\Delta H_2 = \langle (\Delta H)^2 \rangle_{Av}^{\frac{1}{2}}$. The proton line was observed at 29.0 megacycles/sec. for all salts investigated.

Of eleven ammonium salt powders investigated, NH_4Cl, NH_4Br, NH_4IO_3, and NH_4CNS were found to have proton line widths of approximately 20 gauss at our lowest attainable temperature of 90°K to 95°K. At higher temperatures, the line in each of these four salts undergoes transition, within a temperature interval usually smaller than 20°, to a narrower line of width from 3.5 to 5.3 gauss which remains essentially unchanged through the specific heat anomaly and up to room temperature. Line widths of the other ammonium salts fell between 2.6 and 6.6 gauss, staying nearly constant for a given salt over the entire accessible temperature range. Table I tabulates the values of the temperature T_w at the center of the line-width transition and the length of the temperature interval ΔT in which the transition takes place. For comparison, temperatures of the known specific heat anomalies are also given.

Figure 2 presents experimental absorption curves for the proton line in NH_4Cl crystal powder at 95°K and 295°K. The root-second-moment[3] computed from the curve for 95°K is $\Delta H_2 = 7.55$ gauss. Using the theory developed by Van Vleck,[4] and assuming that at temperatures below the line-width transition the ammonium tetrahedra are stationary with respect to the crystal lattice, one finds that a theoretical root-second-moment in agreement with experiment corresponds to an N−H interatomic distance in the tetrahedron of 1.01±0.01A. Since this is close to the N−H distance in the ammonia (NH_3) molecule, it appears that the broad lines indeed correspond to a crystal lattice in

TABLE I.

Compound	Temperature T_w of line-width transition	Width ΔT of transition	Specific heat anomaly
NH_4Cl	133°K	16°	242.8°K
NH_4Br	108	16	235.2
NH_4I	<95	—	230.7
NH_4IO_3	120	7	—
NH_4CNS	100	20	—
NH_4NO_3	<95	—	212.8
$(NH_4)_2SO_4$	<95	—	223.4

which the ammonium tetrahedra may be considered stationary. It has therefore been assumed in Table I that at sufficiently low temperatures the other ammonium salts will undergo similar line-width transitions.

It can be shown[5] that the critical frequency above which relative nuclear motions should begin to narrow the absorption line is near the width, expressed as a frequency, of the broad line corresponding to the stationary nuclear configuration. We can account for the line width at temperatures just above the transition region by assuming hindered rotation or quantum-mechanical tunneling of the NH_4 tetrahedra at frequencies of the order of 100 kilocycles. Such a frequency will contribute negligibly to the specific heat.

The second-moment formula of Van Vleck has been used to investigate the nature of the rotation or tunneling of the ammonium tetrahedra above the line-width transition, and the results will be discussed in a more detailed account to be submitted to this journal.

In addition, the same theoretical considerations have been used in the interpretation of line-width transitions observed for the proton lines in a number of the simpler organic compounds. Also, the relation between the second-moment and interatomic distances in a stationary lattice has been used to determine molecular structure in several cases, including diborane, for which the experimental data support the ethylene-bridge structure. Reports of these experiments and findings are also in preparation.

* Now at the University of Illinois, Urbana, Illinois.
† Predoctoral Fellow of the National Research Council.
** Now at Washington University, St. Louis, Missouri.
[1] G. E. Pake and H. S. Gutowsky, Phys. Rev. **74**, 979 (1948).
[2] F. Bitter and co-workers [Phys. Rev. **71**, 738 (1947)] have reported a qualitative observation that the proton line in NH_4Cl is slightly broader at low temperatures than at room temperature, but is consistently broad as is characteristic of normal solids.
[3] G. E. Pake and E. M. Purcell, Phys. Rev. **74**, 1184 (1948).
[4] J. H. Van Vleck, Phys. Rev. **74**, 1168 (1948).
[5] N. Bloembergen, E. M. Purcell, and R. V. Pound [Phys. Rev. **73**, 679 (1948)] give, on page 704, the general nature of the relation.

An Equation of State for Gases at High Pressures and Temperatures from the Hydrodynamic Theory of Detonation

MELVIN A. COOK
Department of Metallurgy, University of Utah, Salt Lake City, Utah
September 13, 1948

IN regard to the criticisms of my paper[1,2] by Dr. Stewart Paterson[3,4] I find, after looking more carefully into my method (a) solution of the equations of the hydrodynamic theory, that Dr. Paterson is correct in pointing out that method (a) is an unsatisfactory solution. In carrying out the solutions by method (a), I was including, rather naively, a step which had been introduced as a convenient short cut in earlier studies by method (b) which, although I failed to realize it, actually did depend on the nature of the solutions of method (b). The data reported in my paper,[1] while calculated by the procedure in question (although not as described in reference 1) are actually identical with those which would be obtained by the direct application of method (b). The slight difference between the two curves of Fig. 1 of my paper was due to the use of slightly different detonation velocities. This was, in fact, mentioned in the paper of reference 1. As far as I am concerned, Dr. Paterson and I are now in agreement on all essential points of discussion. As a matter of fact, the recent work of Paterson[5] together with the arguments in reference 1, I believe, present strong evidence for the validity of the equation of state

$$pv = nRT + \alpha(v)p$$

for gases under the conditions encountered in the detonation of solid and liquid explosives.

[1] Melvin A. Cook, J. Chem. Phys. **15**, 518 (1947).
[2] Melvin A. Cook, J. Chem. Phys. **16**, 554 (1948).
[3] Stewart Paterson, J. Chem. Phys. **16**, 159 (1948).
[4] Stewart Paterson, J. Chem. Phys. **16**, 847 (1948).
[5] Stewart Paterson, Research **1**, 221 (1948).

The Vapor Pressure and Melting Point of Graphite

LEO BREWER
Chemistry Department, University of California, Berkeley, California
September 24, 1948

IN a letter to this Journal, L. H. Long has listed four types of experimental data which he believes will not admit a value of 170 kilocalories for the heat of sublimation of graphite. Careful examination of these data indicate that they are not capable of contradicting a heat of sublimation of 170 kilocalories, an atmospheric sublimation point of around 4600°K, or a melting point of over 5000°K.

(*i*) At temperatures above 3400°K where the carbon partial pressure is above 1 mm, the smoke due to carbon gas condensing in the cooler portions of an apparatus invalidates direct observations of the temperature by an optical pyrometer. Thus the temperatures given by Ribaud and Begue,[1] Basset,[2] and others who have worked in this high temperature range are much too low. In addition, their degassing procedures were poor. Both these effects produce results which make carbon seem more volatile than it really is.

(*ii*) Long lists various values for the melting point of carbon. However, Steinle[3] has clearly shown that these previous workers had not actually reached the melting point. The pressure work of Basset[2] and Steinle[3] show that the triple point of carbon occurs above 100 atmospheres. From the vapor pressures given by Brewer, Gilles, and Jenkins,[4] this must mean that carbon melts above 5000°K.

Carbon can be melted in contact with tantalum carbide at temperatures above 3300°C, but this is due to the eutec-

tic between C and TaC as shown by Ellinger.[5] A melting point over 5000°K for carbon is consistent with Steinle's work which showed that there was a large temperature gradient from the interior of the carbon rods, where melting took place, to the exterior where a lower temperature was read.

(*iii*) At 4000°K, the partial pressure of carbon is almost 0.1 atmosphere which should be sufficient to maintain an arc.

(*iv*) The work of Mott[6] only demonstrates that carbon is more volatile than tungsten. This is consistent with the boiling point of around 6000°K for tungsten which is given by Kelley.[7] The volatization which limited the thin carbon tube used by Brewer, Gilles, and Jenkins[4] to a top temperature of 3000°K is consistent with the partial pressure of around 0.03 mm. As a result of faster vaporization from the hottest sections, these sections become thinner, which increases the electrical resistance and thus increases the temperature of these hot rings still further. Thus temperatures above 3000°K are reached, and these hot rings lose carbon rapidly enough to cause breaking of the tube at the weak ring which results after loss of a fraction of a mm thickness of carbon. These results are quite consistent with the vapor pressures given by Brewer, Gilles, and Jenkins.

The data discussed above and other data which present direct evidence on the vapor pressure of graphite have been carefully examined, and no experiments have been found that are capable of excluding 170 kilocalories as the heat of sublimation of graphite.

[1] G. Ribaud and J. Begue, Comptes Rendus **221**, 73 (1945).
[2] J. Basset, Brennstoff-Chemie **23**, 127 (1942).
[3] H. Steinle, Zeits. f. angew. Mineral. **2**, 28, 344 (1940).
[4] L. Brewer, P. W. Gilles, and F. A. Jenkins, J. Chem. Phys. **16**, 797 (1948).
[5] F. H. Ellinger, Trans. Am. Soc. Metals **31**, 89 (1943).
[6] W. R. Mott, Trans. Am. Electrochem. Soc. **34**, 255 (1918).
[7] K. K. Kelley, Bur. of Mines Bull. 383 (1935).

Notes on the Properties of Synthetic Rutile Single Crystals

S. Zerfoss and R. G. Stokes
Crystal Section, Naval Research Laboratory, Washington, D. C.
and
C. H. Moore, Jr.
Research Laboratory, Titanium Division, National Lead Company, South Amboy, New Jersey
July 19, 1948

THE synthesis of large single crystals of rutile by the Titanium Division, National Lead Company, was announced recently.[1] It appears desirable to call attention to the exceptionally high dielectric constants which can be obtained in these crystals by proper treatment.

The color of the crystals is opaque black after they come from the furnace. This opaque black color can be changed gradually to transparent blue and finally to yellow by treatment in an oxygen atmosphere at 1000°C. The color differences presumably are related to the titanium/oxygen ratio; the yellow variety corresponds to Ti/O value of $\frac{1}{2}$. A reversal of the color changes can be effected by treatment in hydrogen at 600° to 800°C.

In order to determine the effect on the electrical properties caused by varying oxygen proportions in the lattice of rutile, a series of dielectric constant and resistivity measurements were made on the single crystal material.

A General Radio 716B capacity bridge was used with a simple crystal holder to measure the dielectric constant. The bridge was driven by a 1000-cycle oscillator, and all values of the dielectric constant are 1000-cycle values.

The resistivity of the specimens was measured using the voltage-current method. For the high resistivities an electrometer and high voltage supply were used; for the low resistivities a simple ohmmeter sufficed.

An oriented sample, 0.26×0.155×0.185 cm, in the completely oxidized condition was measured in the three principal crystallographic directions with the following results:

Crystallographic direction	Dielectric constant
X	89
Y	92
Z	180

Two unoriented rectangular samples, 0.6×0.8×0.25 cm and 0.9×0.5×0.19 cm, were completely oxidized and then subjected to a series of treatments in hydrogen for short periods. Measurements of the dielectric constant and resistivity were made after each reduction treatment. Typical data are given in Table I.

Table I.

Reduction exposure	Temp. °C	Time of treatment	Color	Dielectric constant	Resistivity (ohm cm)
First	600	5 min.	faint blue	2.34×10^4	4.73×10^5
Second	600	5 min.	faint blue	3.01×10^4	7.12×10^5
Third	600	5 min.	faint blue	2.22×10^4	9.5×10^5
Sixth	600	5 min.	faint blue	1.79×10^4	9.5×10^5

Subsequent treatment at 800°C for 30 minutes yielded a material of metallic luster having a blue color but also opaque when resistivity was low. The dielectric constants for the principal directions in the crystal initially increase proportionally upon reduction, but finally approach a common value in the well reduced material. The properties of the black original furnace material are apparently identical with the well reduced blue material. (Exploratory experiments show that the reduced material is not ferroelectric.)

A reasonable explanation of the observed effects might be based on the idea that the reduced material can be regarded as an irregular sandwich of a conducting surface region and a dielectric interior with indefinite boundaries. In this case the existence of a space charge polarization would account for the major portion of the observed change in properties.[2] Such regions could also account for the variation of the dielectric constant and resistivity of the basal plane.

These data are preliminary in character, but are considered of sufficient novelty to be presented pending a more thorough study of the electrical and photo-conductive properties.

[1] Science News Letter, October 1947.
[2] Table of Dielectric Materials, Report V, Contract OEMsr-191 NDRC, Laboratory for Insulation Research, MIT, p. 18 (1944).

Viscosity-Composition-Temperature Relations in the System Na_2O-SiO_2

STEPHEN W. BARBER
Department of Chemistry, University of Toledo, Toledo, Ohio
October 1, 1948

A CAREFUL examination of viscosity data for the soda-silica system from Heidtkamp and Endell[1] and from Lillie[2] shows that it is very well represented for high temperatures by an equation of the form

$$\log\eta = A + BS_0 + [(C + DS_0)/2.303RT], \qquad (1)$$

wherein a different set of constants is required for each of the following ranges in the value of the silicon-oxygen ratio, S_0,

above 0.435
from 0.435 to 0.400
from 0.400 to 0.345
below 0.345.

These are the critical values for S_0 used by Huggins and Sun[3] in their density calculations.

A very helpful picture of the log viscosity-reciprocal T curve was derived from a study of the analogous relation for log resistivity, Babcock[4] has given us the relation,

$$\log\eta = \beta \log\rho, \qquad (2)$$

where β is constant for a given composition. This relation is interpretated to mean that that viscosity depends on the mobility of the sodium ion in this system.

It was found that log resistivity[4,5] could be well represented by an equation of the form

$$\log\rho = [\log A - c + (E/2.303RT)]f(T) + c, \qquad (3)$$

where A and E are the characteristic values for $f(T) = 1$ at high temperatures and c is a small constant not affected by $f(T)$. It appears that $f(T)$ must describe a transformation from ionic binding above about 1600°K to ionic-covalent binding which is essentially complete below 700°K. The increase in E is about fifty-five percent of its value below 700°K. This agrees well with an estimate of percent covalent binding from Pauling.[6]

Derivation of a relation for log viscosity from the Maxwell-Boltzmann energy-distribution law, with appropriate considerations for the nature of the transformation, led to an exactly similar equation,

$$\log\eta = [\log A + \log N_0 + (E/2.303RT)]f(T) - \log N_0. \qquad (4)$$

From the derivation

$$A = C(1/N_0),$$

where N_0 is a probability at infinite temperature and C is an effect factor relating N_0 to viscosity. It appears that $f(T)$ must apply to $\log C$ as well as to E. Obviously any change in E, the bond strength, must change the effect of each bond. It is clear too that, in the absence of associations or dissociations, N_0 must not be affected by $f(T)$.

Inasmuch as a suitable relation was derived considering N_0 constant, it appears that the effect of the transformation described by $f(T)$ is not a change in aggregation but simply a tightening of the structure with decreasing temperature.

It appears that $\log N_0$ is simply related to composition. Reasoning from this, and from the nature of C, we are led to the form of Eq. (1) for a composition relation, wherein the critical values of S_0 approximate the compositions where the ratios of silicon atoms to sodium atoms are small integers. This ratio is thought of as the number of sites each sodium atom must visit to permit flow thrqugh one interatomic distance.

A detailed presentation is planned for publication as soon as these relations can be further verified and the form of $f(T)$ can be studied more at length.

[1] G. Heidtkamp and K. Endell, Glastech. Ber. **14**, 89 (1936).
[2] H. R. Lillie, J. Am. Ceram. Soc. **22**, 367 (1939).
[3] M. L. Huggins and K. Sun, J. Am. Ceram. Soc. **26**, 4 (1943).
[4] C. L. Babcock, J. Am. Ceram. Soc. **17**, 329 (1934).
[5] E. Seddon, E. J. Tippett, and W. E. S. Turner, J. Soc. Glass Tech. **16**, 450 (1936).
[6] L. Pauling, *Nature of the Chemical Bond* (Cornell University Press, Ithaca, New York, 1942).

The Hydrogen Fluoride Dipole Moment and the Structure of the Dimer*

R. A. ORIANI AND C. P. SMYTH
Princeton University, Princeton, New Jersey
September 30, 1948

QUANTUM mechanics leads to the equation[1]

$$\mu = [9kTP_m/4\pi N(1 - (h^2)/(24\pi^2 IkT))]^{\frac{1}{2}},$$

for the relation between the molar orientation polarization P_m, and the intrinsic dipole moment μ of a diatomic molecule. In this equation k is the Boltzmann constant, h, the Planck constant, N, the Avogadro number, T, the absolute temperature, and I, the moment of inertia. The divergence from classical mechanics is given by the second term within the parentheses in the denominator and becomes appreciable only for molecules of very small moment of inertia. Monomeric hydrogen fluoride, with a moment of inertia of 1.32×10^{-40} c.g.s. unit,[2] is a molecule whose dipole moment should be computed by means of the above equation rather than by the classical expression. When this is done, using the data of Hannay and Smyth[3] and of Oriani and Smyth,[4] one obtains 1.98×10^{-18} as the dipole moment of the HF molecule instead of the previously published value of 1.91×10^{-18} given by the classical equation.

In a recent article Evans and Glockler[5] carried out calculations based on electrostatics for the configuration and potential energy of the hydrogen fluoride dimer. They were led to the conclusions, also reached by Briegleb,[6,7] that an antiparallel arrangement of dipoles represented the structure of minimum potential energy, and that the energy of each of the two hydrogen bonds in the dimer was 11.9 kcal./mole. This configuration, however, fails to explain the large increase in dielectric polarization of hydrogen fluoride vapor observed by the writers[4] as the temperature is decreased and pressure increased, for such an antiparallel arrangement of HF units would have zero dipole moment. These polarization data, together with the electron diffraction studies of Bauer, Beach, and Simons[8] and the vapor density work of Long, Hildebrand, and Morrell,[9] indicate structures for the polymers consisting of chains, some of

which link up to form rings. Furthermore, Tanford[10] has computed a hydrogen bond energy of 6.3 kcal./mole for the one hydrogen bond in the dimer structure based on the zig-zag model given by electron diffraction, from which the entropy of the dimer is calculated. He uses Briegleb's equilibrium constant k for $2HF \rightleftharpoons (HF)_2$, the large error in which introduces but a small error into the bond energy calculation because $\log K$ is used. Thus, the zig-zag model, deduced from electron diffraction experiments and having the polarity necessary to explain the polarization measurements, also leads to a reasonable value for the energy of the hydrogen bond.

The semi-empirical quantum-mechanical treatment also accorded by Evans and Glockler[5] to the hydrogen fluoride dimer indicates a linear configuration, and hence is in qualitative agreement with polarization data. However, the crudeness of the approximations necessary in evaluating the London equation leads to an admittedly unreliable result.

* This research was carried out with the support of the Office of Naval Research.

[1] P. Debye, *Polar Molecules* (Dover Publications, New York, 1945).
[2] D. E. Kirkpatrick and E. O. Salant, Phys. Rev. **48**, 945 (1935).
[3] Hannay and Smyth, J. Am. Chem. Soc. **68**, 171 (1946).
[4] R. A. Oriani and C. P. Smyth, J. Am. Chem. Soc. **70**, 125 (1948).
[5] G. E. Evans and G. Glockler, J. Chem. Phys. **16**, 324 (1948).
[6] Briegleb, Zeits. f. physik. Chemie **B51**, 9 (1941).
[7] Briegleb, Zeits. f. physik. Chemie **B52**, 368 (1942).
[8] Bauer, Beach, and Simons, J. Am. Chem. Soc. **61**, 19 (1939).
[9] Long, Hildebrand, and Morrell, J. Am. Chem. Soc. **65**, 182 (1943).
[10] C. Tanford, unpublished calculations.

The Ultimate Liquid Transmission Limit?

H. B. KLEVENS
Division of Agricultural Biochemistry, University of Minnesota, St. Paul, Minnesota
AND
J. R. PLATT
Department of Physics, University of Chicago, Chicago, Illinois
September 30, 1948

IN a recent paper,[1] the far ultraviolet transmission limits of n-heptane and of two perfluorocarbons were determined as shown in rows 1–3 of Table I. The markedly poorer transmission of the fluorocarbons was surprising, for the extremely low refractive indices of perfluoro compounds had indicated that their transmission limits might lie at shorter wave-lengths than those of the corresponding hydrocarbons. Moreover, the M→V transition in perfluorotoluene is at 1780A,[2] compared with its location in toluene at 1885A.[3] Recently, a carefully fractionated n-perfluorooctane was made available.[4] It transmits to 1592A in an 0.5-mm cell, to 1565A in an 0.03-cm cell, and to 1780–1830A in a 1-cm cell. The cut-offs are very sharp, as indicated by the change of only 30A with a 20-fold change in cell thickness.

The energy at the extreme transmission limit of the perfluorooctane is about 64,000 cm^{-1}. This extends the region of the ultraviolet available for solution studies some 5000 cm^{-1} from the previous hydrocarbon limit of 58,500 cm^{-1}, which is itself some 10,000 cm^{-1} above the usual quartz spectrograph ultraviolet limit. This extension from the quartz region is one and one-half times the total frequency spread in the visible between 4000–7000A, and

TABLE I. Transmission limits.

Compound	Source	Purification	Cell thickness	Limit
1. n-C_7H_{16}	Westvaco	sulf. acid and/or silica gel	0.13 mm	1700A*
2. n-C_7F_{16}	du Pont	no treatment	0.5	1800*
3. n-C_9F_{20}	du Pont	no treatment	0.5	1830*
4. n-C_8F_{18}	see reference 4	repeated fractionation b.p. 104.5°C; $n_D^{20}=1.268$	0.03 0.5	1565 1592
5. CF_3-cycloC_6F_{11}	du Pont	no treatment sulf. acid	0.5 0.5	1860 1850
6. $(CF_3)_2$-cycloC_6F_{11}	du Pont	no treatment	0.5	1960

* See reference 1.

offers correspondingly large opportunities for characterization of complex molecules and studies of their electronic behavior.

We may consider whether this limit of 1565A will be the ultimate transmission limit for practical solvents in absorption spectrophotometry. Fluorides transmit better than corresponding hydrides or other compounds because of the high ionization potential of fluorine, higher than that of any other combining element. Similarly, molecules made from second-row elements will transmit better than their heavier analogs. Price[5] and others have pointed out these relations between ionization potentials and spectra. Now second-row fluorides with one central atom, BeF_2, BF_3, CF_4, etc., are either solids or gases. They can be used as solvents only at low temperatures (with decreased solubility) and/or high pressures, or at high temperatures, with possible decomposition of complex solute molecules. Evidently, for a solvent, we need a larger fluoride molecule, with a skeleton of several other atoms such as −C−C−C−, −B−B−B−, −B−N−B−, forming a long enough chain to be liquid at room temperatures. Chains containing O, Si, or S would not be feasible because of their known absorption about 2000A.

The transmission properties of the liquid 8-carbon fluoride chain we have seen here. As for boron chains, BF_3 is formed instead of B_2F_6, and pure fluoroboron chains are probably not possible. If they could exist, or if mixed hydride-fluoride-boron chains existed, they would probably not be transparent below 1700A because of their unsaturation characteristics (conjugated?) as shown by the recently reported maximum of about 1350A for the bridge-like diborane,[6] and as indicated by the absorption of B_5H_9 near 2000A.[7]

As for −B−N−B− chains, we may reason from the unsaturated rings of this type to the little-studied saturated chains. The N→V transition of benzene is at 1835A, of borazole at 1720A, and of perfluorobenzene at 1740A (estimated from perfluorotoluene[2]). For perfluoroborazole, this transition might lie as low as 1625A. Then a saturated −B−N−B− hydride chain might transmit to about 1600A and the fluoride analog to about 1475A. A polymer of BH_2NH_2 is known which is a solid.[8] Its ultraviolet transmission is not known. A similar polymer $(BF_2NF_2)_x$, with $x=3$ or 4, might be a suitable solvent to extend the transmission limit if such a compound could be prepared.

It seems, therefore, that the liquids promising to be more transparent than fluorocarbons are at present largely hypo-

thetical. Even if one were found and prepared in suitable quantity and purity, there would still remain questions of its stability, reaction with window materials, and potency as a solvent (especially of complex organic compounds). The *n*-perfluoroparaffins promise to be satisfactory on all these counts.

[1] H. B. Klevens and J. R. Platt, J. Am. Chem. Soc. **69**, 3055 (1947).
[2] Unpublished results of the authors.
[3] J. R. Platt and H. B. Klevens, Chem. Rev. **41**, 301 (1947).
[4] Through the courtesy of Drs. H. M. Scholberg and W. H. Pearlson, Research Laboratories, Minnesota Mining and Manufacturing Company, St. Paul, Minnesota.
[5] W. C. Price, Chem. Rev. **41**, 257 (1947).
[6] W. C. Price, J. Chem. Phys. **15**, 614 (1947).
[7] J. R. Platt, H. B. Klevens, and G. W. Schaeffer, J. Chem. Phys. **15**, 598 (1947).
[8] H. I. Schlesinger, D. M. Ritter, and A. B. Burg, J. Am. Chem. Soc. **60**, 2297 (1938); and R. E. Moore, M. S. Thesis, University of Chicago, June, 1948.

The Average Boundaries of Statistical Chains

C. A. HOLLINGSWORTH
Department of Chemistry, University of Pittsburgh, Pittsburgh, Pennsylvania
September 17, 1948

THIS is to acknowledge my discovery that a problem which I solved as an example in a recent paper[1] had already been solved by W. Kuhn and H. Kuhn.[2] These authors give a result that differs from mine by only 5 percent. They also give values of various other parameters of branched as well as unbranched chains.

[1] C. A. Hollingsworth, J. Chem. Phys. **16**, 544 (1948).
[2] W. Kuhn and H. Kuhn, Helv. Chim. Acta. **30**, 1233 (1947).

On the Classification of Symmetry Coordinates*

WILLIAM J. TAYLOR
Cryogenic Laboratory, Department of Chemistry, Ohio State University, Columbus, Ohio
October 6, 1948

THE symmetry type or irreducible representations of the $3n-6$ vibrations of an n-atomic symmetrical molecule may be found by group theoretical methods which will be restated briefly. The atoms may be divided into sets equivalent under the point group of the molecule; the permutation matrices for any given set of equivalent atoms then form a reducible representation of the group, which may be reduced to a "sum" of irreducible representations by the standard orthogonality relation for group characters. The direct product of this sum by the sum of irreducible representations for translation yields the total contribution of this set of equivalent atoms. Summing the representations thus obtained over all sets of equivalent atoms in the molecule, and subtracting finally the representations for translation and rotation, yields the representations for the vibrations (with the sum of the dimensions equal to $3n-6$).

A similar procedure may be used to find *separately* the irreducible representations of the symmetry coordinates formed from equivalent internal coordinates, which are commonly taken as a starting point for normal coordinate analyses. It is a considerable advantage to be able to enumerate the irreducible representations of the symmetry coordinates without, or before, actually setting up the analytical expressions for these coordinates. Comparison of the representations for the sets of symmetry coordinates taken separately with the sum of representations for the $3n-6$ vibrations is usually sufficient to identify the redundant coordinates. In making frequency assignments, even when a normal coordinate analysis is not contemplated, a knowledge of the representations of the symmetry coordinates is useful in indicating the physical nature of the vibrations allowed in the spectra, and therefore in estimating probable frequencies. As is well known, each normal mode is formed only from symmetry coordinates belonging to the same representation.

In this communication the general principles of the method for symmetry coordinates are described. A paper now in preparation will give a fuller account and will contain tables by means of which the irreducible representations of most sets of equivalent internal coordinates may be obtained by inspection.

A set of equivalent internal coordinates may be divided into (equal) subsets such that each subset is associated with one point of an equivalent set of points, in the sense that the subsets permute among themselves in the same way as the points under the operations of the point group. The permutation matrices for this set of equivalent points form a reducible representation of the group, which may be reduced as discussed in the first paragraph. Those operations of the point group which do not permute a particular point of the set form a subgroup of the group. The operations of this subgroup will transform in some manner the members of the subset associated with this point; the introduction of subsets is necessary because, in general, the transformations of a subset under the subgroup cannot be represented by the permutations of a set of points. The case of most interest is that in which the coordinates of the subset belong to a single irreducible representation of the subgroup, the number of coordinates in the subset being equal to the dimension of the representation. In the case of the cyclic and dihedral groups the subgroup can contain only non-degenerate or one-dimensional representations, and each subset only one coordinate, unless the point lies on the principal symmetry axis and the latter is threefold or higher. In the latter case, and also in the case of tetrahedral and octahedral groups, when the point lies on a three- or fourfold axis, the subgroup will contain one or more two-dimensional representations, and the subset may contain one or two equivalent internal coordinates. There is also the relatively unimportant case in which the single point of the set lies at the origin, in which case three-dimensional representations occur for the tetrahedral and octahedral groups. There are, in addition, some cases of interest in which the subset lies in more than one representation of the subgroup. It should be noted that when the representation of the subset in the subgroup is one-dimensional, it may still not be totally symmetric.

The representation of the subset in the subgroup (the same for all subsets) may be obtained by inspection by considering the transformations under the subgroup of the $\mathbf{s}$-vectors associated with the coordinates of the subset

which have been defined by Wilson.[1] One or more of the representations of the complete group (or, in a few cases, a linear combination of representations) will have characters identical with those of this representation of the subgroup, for those classes which contain operations in the subgroup. The direct product of any one of these representations (or combinations of representations) of the complete group with the sum of representations for the permutation matrices (of the set of equivalent points) will yield the required sum of irreducible representations for the complete set of equivalent internal coordinates. (If the subset lies in more than one representation of the subgroup, the contributions obtained for each taken separately are added.)

As a simple example, the torsions about the carbon-carbon single bonds in benzene (point group D_{6h}) will be considered. The six torsions permute in the same way as the set of six midpoints of the sides of the carbon hexagon. The representation of the permutations is $A_{1g}+B_{2u}+E_{1u}+E_{2g}$. The subgroup at a point of the set is C_{2v}, and the representation of the torsion in the subgroup is A_2 (corresponding to a rotation about the C_2 axis). The corresponding representations of D_{6h} are A_{1u} and B_{2g}. The direct product of either of these with the representation of the permutations yields $A_{1u}+B_{2g}+E_{1g}+E_{2u}$ as the representation of the set of six equivalent torsions.

* This work was carried out under contract between ONR and The Ohio State University Research Foundation.

[1] E. B. Wilson, Jr., J. Chem. Phys. 9, 76 (1941), Eq. (2). The s-vectors are the coefficients in the linear functions connecting the internal coordinates with the vector displacements of the atoms. The only non-vanishing s-vectors for a given internal coordinate are those attached to the few atoms whose relative motion changes the coordinate. The orientation of the s-vectors with respect to the symmetry elements may be obtained by inspection by noting that the s-vector for a given internal coordinate attached to a given atom lies in the direction in which this atom must move, all other atoms remaining fixed, to produce the maximum positive rate of change of the coordinate per linear distance traveled. For the present purpose the magnitudes of the s-vectors are not important, but only the equality or inequality of the magnitudes, which is obvious from symmetry considerations.

Note on the Energy of a Rotating Molecule

ROBERT KARPLUS*
Mallinckrodt Chemical Laboratories, Harvard University, Cambridge, Massachusetts
August 27, 1948

THE quantum-mechanical problem of the energy levels of a molecule has been attacked by Born and Oppenheimer,[1] who expanded the accurate Hamiltonian operator about the equilibrium configuration of the nuclei in powers of k; $K^4=m/M\approx10^{-4}$, the ratio of the electronic mass to a nuclear mass. They show that the energy can be decomposed into contributions from the electronic, the vibrational, and the rotational motion, which first enter in the zeroth-, second-, and fourth-order corrections, respectively. In higher orders of approximation, which these authors did not examine in detail, the three types of motion interact. Wilson and Howard,[2] and Nielsen,[3] and Darling and Dennison[4] have investigated the interaction of rotational and vibratory motion. They conclude that the rotational energy levels are those of an effective asymmetric rotor, appropriate to a given vibrational state, and differing somewhat from the equilibrium rotor; a small term that can be described as centrifugal distortion perturbs the motion of this rotor. These authors do not make clear the magnitude of the corrections to be expected. The recent interest in pure rotational spectra which are observed in the microwave region has made it imperative that the higher order terms in the Hamiltonian be examined from a consistent point of view. With this in mind, the procedure of Born and Oppenheimer[1] has been continued.[5]

The results of the perturbation calculation will now be briefly summarized. The Hamiltonian operator which determines rotational fine structure of a given non-degenerate electronic and vibrational state can be written

$$H_R=H_R^{(4)}+H_R^{(6)}+H_R^{(8)}+\cdots,$$

where the superscripts describe the magnitude of a term in powers of k relative to the electronic energies. H_R is a function of angular momentum operators P which can act only on a rotational wave function. Electronic and vibrational labels on these operators are understood.

The leading term, $H_R^{(4)}$, is the Hamiltonian of a rigid rotator whose moments of inertia are those of the equilibrium configuration of the nuclei (electronic masses not included). In a system of principal axes it is

$$H_R^{(4)}=\Sigma_\alpha \mu_{\alpha\alpha}^0 P_\alpha^2, \quad \alpha=x, y, z$$

$$1/\mu_{\alpha\alpha}^0=I_\alpha=\text{equilibrium moment of inertia},$$

$H_R^{(4)}$ is independent of vibrational and electronic properties.

The largest correction, $H_R^{(6)}$, is also a homogeneous quadratic polynomial in the angular momentum operators. It therefore merely introduces corrections to the equilibrium rotational constants. By insertion of the appropriate quantities, the results of Nielsen's calculation, contained in the corrections $x_{s\sigma}$, $y_{s\sigma}$, $z_{s\sigma}$, reference 3, Eqs. (27) and (28), have been verified exactly. They contain the quadratic and cubic potential constants, but are independent of the electronic structure.

The next correction, $H_R^{(8)}$, considerably complicates the description of the system, because it is the sum of a homogeneous quadratic and a homogeneous quartic polynomial in the operators P. The latter is the centrifugal distortion which has been discussed by several authors.[2-4,6] The former provides further corrections to the rotational constants; it depends on quadratic, cubic, quartic, and quintic potential constants, and also includes terms that depend on the electronic structure. These are given by

$$\mu_{\alpha\alpha}^0 P_\alpha^2 \sum_{n'} (\mu_{\alpha\alpha}^0 (P_\alpha)_{nn'}(P_\alpha)_{n'n})/(E_n-E_{n'}),$$

(n, n' are electronic quantum numbers). They may very simply be shown to appear when the electronic wave equation is solved in a rotating coordinate system.[7,8]

In conclusion, it should be mentioned that the expansion which has been discussed is reliable only when the energy differences between electronic or vibrational states are of the same magnitude as the energies themselves. If the differences are much smaller (near-degeneracy), some corrections to the energy will be larger than their place in the series in the first equation would indicate.

The author wishes to express his appreciation to Pro-

fessor E. Bright Wilson, Jr., who suggested this problem, for many helpful discussions.

* This work was carried out with the aid of a U. S. Rubber Company predoctoral fellowship.

[1] M. Born and R. Oppenheimer, Ann. d. Physik. IV **84**, 457 (1927).
[2] E. B. Wilson, Jr. and J. B. Howard, J. Chem. Phys. **4**, 260 (1936).
[3] H. H. Nielsen, Phys. Rev. **60**, 794 (1941).
[4] B. T. Darling and D. M. Dennison, Phys. Rev. **57**, 128 (1940).
[5] R. Karplus, Ph.D. Thesis (Harvard, 1948).
[6] E. B. Wilson, Jr., J. Chem. Phys. **5**, 617 (1937).
[7] G. C. Wick, Phys. Rev. **73**, 51 (1948).
[8] The detailed derivation of these terms is contained in a Ph.D. thesis submitted by the author to Harvard University in June 1948.

Chemical Kinetics of Bromine Following Neutron Capture*

WILLIAM H. HAMILL AND RUSSELL R. WILLIAMS, JR.
University of Notre Dame, Notre Dame, Indiana
October 13, 1948

THE problem of determining the extent to which a direct correlation exists between photo-chemistry and hot-atom chemistry is one of considerable practical and theoretical interest. Suess[1] initiated a very promising study for the case of $Br^{79}(\eta, \gamma)Br^{80}$ by following the distribution of Br^{80} (18 min.) between addition to C_2H_2 and exchange with HBr in the gas phase. Both C_2H_5Br and HBr were used as targets with variable amounts of C_2H_2. The $C_2H_3Br^*$ and HBr^* were separated by water extraction. Upon the basis of the postulated kinetic Eqs. (1)–(5), and with certain approximations, he showed that the usual steady-state treatment gave

$$\text{organic Br*/inorganic Br*} = a(C_2H_2)/b + c(C_2H_2),$$

in approximate agreement with his experimental results. He also concluded that there was no evidence of failure to rupture the HBr bond, which he had expected from a consideration of recoil energy and momentum transfer. On the other hand, the C—Br bond, with a more favorable mass ratio, would always rupture as a result of the η, γ-process.

Since either qualitative or quantitative interpretation of Suess' results is uncertain because of low precision, unavoidable with a weak neutron source, it seemed desirable to repeat this work with a stronger source. Our experimental procedures approximate his; we have, however, used ethylene instead of acetylene. In addition to Suess' mechanism Eqs. (1)–(5), where A represents either C_2H_2 or C_2H_4,

$$HBr + Br^* \xrightarrow{k_1} HBr^* + Br, \tag{1}$$

$$A + Br^* \underset{k_3}{\overset{k_2}{\rightleftharpoons}} ABr^*, \tag{2, 3}$$

$$ABr^* + HBr \xrightarrow{k_4} AHBr^*, \tag{4}$$

$$ABr^* + HBr \xrightarrow{k_5} ABr + HBr^*, \tag{5}$$

we also formally introduce the η, γ-process, Eqs. (6) and (7), for HBr as target and assume $k_6 = 0$ for C_2H_5Br as target.

$$HBr + n \xrightarrow{k_6} HBr^*, \tag{6}$$

$$\xrightarrow{k_7} H + Br^*. \tag{7}$$

This mechanism leads, without approximation, and assuming (Br*) and (ABr*) constant, to

$$\begin{aligned}(A)/(\text{organic Br*/inorganic Br*}) &= [(k_1k_3/k_2k_4) + (k_1(k_4+k_6)(HBr)/k_2k_4)][1 + (k_6/k_7)] \\ &\quad + [(k_5/k_4) + (k_6/k_7) + (k_5k_6/k_4k_7)](A). \end{aligned} \tag{8}$$

The left-hand side (A/R) is expressed in Fig. 1 as a function of ethylene pressure at constant (HBr); pressures are expressed in millimeters. Our present experimental results, preliminary in character and somewhat lacking in precision, are consistent with this treatment for Br^{80} (18 min.). It also appears that $k_6/k_7 \approx 0.08$; this ratio probably exceeds zero by more than experimental error.

The non-equality of k_6/k_7 to zero can also be tested by comparing the Br^{80} (18 min.)/Br^{80} (4.5 hr.) ratios for the water-soluble and water-insoluble activities. Unless the k_6/k_7 ratio happens to be the same for both these η, γ-processes, there should be different activity ratios in the two phases because of chemical discrimination between HBr* and Br*. Quite different kinetics for Br^{80} (18 min.) arising from η, γ and isomeric transition could confuse the result, but Suess[1b] found substantially similar behavior for the two cases. We find, for one-hour neutron bombardment of gaseous HBr with added C_2H_4 and carrier C_2H_5Br, that the ratio of activities Br^{80} (18 min.)/Br^{80} (4.5 hr.) differs between the phases and corresponds, approximately, to $k_6/k_7 = 0$ for Br^{80} (4.5 hr.).

We are preparing to study rather fully, with improved apparatus and better precision, the gas kinetics of nuclear processes involving Br^{80} (18 min.), Br^{80} (4.5 hr.), and Br^{82} to determine what special effects, if any, are associated

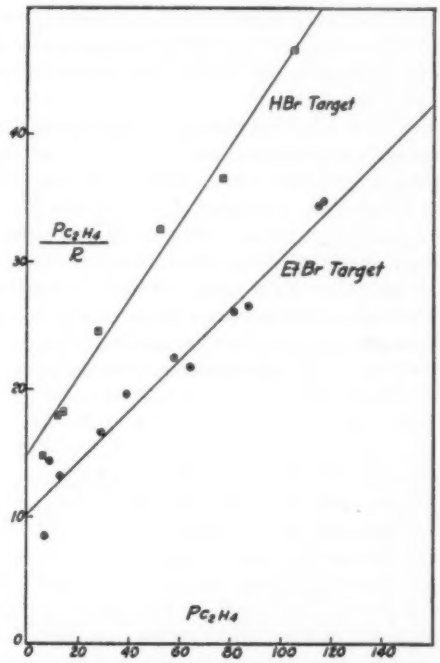

FIG. 1. Test of Eq. (8) for $Br^{79}(\eta, \gamma)Br^{80}$ (18 min.).

with high recoil energy from the η, γ-process and with electric charge from the internal conversion which accompanies isomeric transition. We also plan to study eventually the corresponding kinetics for chlorine and iodine.

* The work reported here was supported under ONR Contract N6ori 165, T.O. II.

[1a] H. Suess, Zeits. f. physik. Chemie **B45**, 297 (1939); [b] *ibid.*, **B45**, 312 (1939).

Linear Atomic Chain and the Metallic State

T. A. Hoffmann and A. Kónya
Physical Institute of the University for Technical and Economic Sciences, Budapest, Hungary

July 8, 1948

It is known in the quantum mechanics of molecules that from the molecular orbital method and the valence bond method the former one is more adapted to describe larger molecules, especially if unlocalized bonds are present. The electrons forming such bonds have just the properties that they cannot be fixed on individual atoms or between any two neighboring atoms, but they show their effect practically distributed to the whole molecule. So they show great analogy with the valence electrons of the metals. We now proceed to apply the M.O. method in the LCAO approximation to some problems concerning metals.[1] This method is here adapted to treat a linear arrangement of similar atoms. Even this very simple model shows typically the development of the metallic properties. We restrict ourselves to the treatment of atoms with only one valence electron, arranged at equal distances from one another.

The molecular orbitals can be written $\psi_m=\sum_{i=1}^{n} c_{mi}\varphi_i$, where $\varphi_1, \varphi_2, \cdots, \varphi_n$ are the normalized eigenfunctions of the valence electrons of each of the n atoms constituting the chain. The φ_i-s are here identical eigenfunctions, i denoting the nucleus to which they are related. The coefficients c_{mi} and the energy E_m can be determined by the usual degenerate first-order perturbation method. Taking the simplified assumption that only neighboring atomic orbitals interact, the other interactions being negligible, we form the integral $\beta=\int \varphi_i^* H \varphi_{i+1} dv$, where H is the Hamiltonian of the whole system, which can be replaced, in the approximation used, by the Hamiltonian of the diatomic molecule consisting of the atoms i and $i+1$. Similarly, we neglect overlap integrals except those of two neighboring orbitals, i.e., $S=\int \varphi_i^* \varphi_{i+1} dv$. The integrations are to be extended to the whole space. The secular equation of this problem will be now

$$\begin{vmatrix} W & \beta' & 0 & \cdots & 0 & 0 & 0 \\ \beta' & W & \beta' & \cdots & 0 & 0 & 0 \\ 0 & \beta' & W & \cdots & 0 & 0 & 0 \\ \cdots & \cdots & \cdots & \cdots & \cdots & \cdots & \cdots \\ 0 & 0 & 0 & \cdots & W & \beta' & 0 \\ 0 & 0 & 0 & \cdots & \beta' & W & \beta' \\ 0 & 0 & 0 & \cdots & 0 & \beta' & W \end{vmatrix}_{n} = 0. \qquad (1)$$

Here is $W=Q-E$, where $Q=\int \varphi_i^* H \varphi_i dv$ is the Coulombic energy of the electron in the valence orbital of the ith atom; E denotes the required energy of the molecular orbital—further, we have used $\beta'=\beta-ES$. The eigenvalues E can be determined from Eq. (1), which is of grade n in E. One can easily see that the solutions of (1) are

$$E_m=Q-2\beta\cos(\pi m/n+1)/1-2S\cos(\pi m/n+1), \qquad (m=1, 2, \cdots, n). \qquad (2)$$

The possible energy terms are consequently in an energy band, the bottom of which we get by taking $m=n$, and the top of which by taking $m=1$, since Q and β are negative; further, we have $QS>\beta$ practically always.

The orbitals belonging to these terms must be populated by the n electrons available according to the Pauli principle; i.e., at absolute zero temperature each of the $n/2$ deepest terms of (2) must be occupied by two electrons if n is even, or each of the $n-1/2$ deepest terms of (2) by two electrons and the next higher term by one electron if n is odd. If $n\to\infty$, the two cases yield the same limit, so we can restrict ourselves to the case of even n. The eigenvalues of (2) belonging to the $n/2$ lowest states are those with $m=n$, $n-1, \cdots, n/2+1$.

One can show, generally, that the average energy of the electrons lies lower than that of the electron in the atom, moreover, lower than that of the electrons in the diatomic molecule. The calculation will be extremely simple if we neglect S. In this case we get the average electronic energy

$$\bar{E}=(2/n)\sum_{m=(n/2)+1}^{n} E_m$$

$$=Q-(4\beta/n)\sum_{m=(n/2)+1}^{n}\cos(\pi m/n+1)$$

$$=Q-(2\beta/n)+(2\beta/n\sin(\pi/2(n+1))). \qquad (3)$$

One can show that Eq. (3) decreases steadily with n, so that any new atom which lengthens the chain makes the average energy deeper. In the case of $n\to\infty$ we get

$$\bar{E}=Q+(4/\pi)\beta=Q+1.27\beta, \qquad (4)$$

which shows that our infinite chain is stable against dissociation into atoms by 1.27β and against dissociation into molecules by 0.27β. If we do not neglect S, we have for $n\to\infty$, if $|S|<\frac{1}{2}$,

$$\bar{E}=(\beta/S)+(2(QS-\beta)/\pi S(1-4S^2)^{\frac{1}{2}})\arccos(-2S). \qquad (5)$$

The next step is the determination of Q, β, and S. If we treat atoms for which we know the valence orbitals, we can calculate these quantities as functions of the lattice constant and minimize (5) with respect to this parameter. So we can calculate the values of the lattice constant, the total energy, the sublimation energy, and the band width by the formulas given above. So, for instance, we get by this rough calculation with Li eigenfunctions given by Duncanson and Coulson[2] for the lattice constant 3.7A, for the total energy per electron 6.23 ev, for the sublimation energy 0.64 ev, and for the width of the energy band at this lattice distance 8.19 ev. These results should not be seriously compared to the experimental results of a real metal—first of all because the latter has a space configura-

tion. In this case the degeneracy would be even greater, and so we can expect stronger bond.

A mathematical difficulty arises if we treat the plane or the space lattice in a similar way, but we hope these difficulties are not insurmountable. In spite of the difference between a real metal and our linear lattice, we can use the latter in some problems, especially those concerning end effects, etc., in the following way. We can construct the total electron density as a function of the distance from one end of the chain. The results show that though the electrons are distributed almost uniformly in the whole chain, there is some deviation near its free end. So we are able to calculate the dipole moment caused by this irregularity. We can take the surface of a metal as if it were built up of the ends of linear chains. Taking into account the crystal structure of the metal, we can make statements about the behavior of the free ends, i.e., the dipole moments of these chains, which determine the dipole moment of the surface, the adsorption on the surface, the work function, etc.

By this method we can treat also the effect of strange atoms built in the lattice at random or systematically (alloys).

Here we can mention that the viewpoint of Pauling in a recent paper,[3] taking into account, among the resonating structures, ionic states also, can be compared with ours presented above, since the M.O. method automatically takes into account ionic states.

Detailed calculations will be published in a forthcoming paper.

[1] This is just the reverse of what Bayliss has done, having constructed a "metallic" model for the conjugated polyenes on the basis of the analogy mentioned above (N. S. Bayliss, J. Chem. Phys. **16**, 287 (1948)). The authors take this opportunity to thank the Board of Editors for calling their attention to this paper.

[2] W. E. Duncanson and C. A. Coulson, Proc. Roy. Soc. Edinburgh **62A**, 37 (1944).

[3] L. Pauling, Nature **161**, 1019 (1948).

Structure and Conductivity in the VI_B Group of the Periodic System

F. DE BOER
Philips Research Laboratories, N. V. Philips' Gloeilampenfabrieken, Eindhoven, Netherlands

October 15, 1948

UNDER the title quoted above a paper was recently published in your journal by A. von Hippel.[1] In connection with this paper I should like to mention some results in a study on the same subject, carried out during the period 1940–45.

The trigonal forms of selenium and tellurium exhibit a curious abnormality: the coefficient of thermal expansion parallel to the *c* axis is negative. This may be explained as follows.

The attraction forces between the spiral chains—which lie parallel to the *c* axis—increase the valence angles and cause the spirals to lengthen if they approach each other.[2]

I tried to calculate whether the forces between the spirals would be sufficient to explain this abnormality, if a lattice

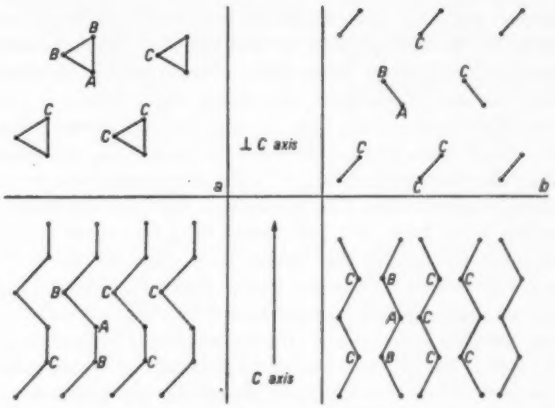

FIG. 1. Comparison of the two lattices. (a) The trigonal spiral chain lattice; the distances are those of the selenium lattice. (b) The hypothetical zigzag chain lattice. Valence angles and atomic radii are the same as in (a). The covalent-bound neighbors of atoms *A* are indicated by *B*, the next nearest atoms—van der Waals bound—by *C*.

were assumed, in which the bonds in the chains were purely covalent, and the bonds between atoms of different chains were of the van der Waals type. The results made it seem probable that the forces between the chains were greater than could be explained by the formulas for the van der Waals-London forces.

This result was caused essentially by the abnormal value of the "van der Waals radius" in the trigonal selenium lattice. The value of this is 1.74A, whereas the normal value may be considered to be 2.0A.[3]

The existence of electrical conductivity made it seem plausible that metallic forces were active here.

Because of war conditions these results had not been published. Meanwhile, the discovery of the cubic form of polonium[4] added an important indication that forces of the metallic type could determine the form of the selenium and tellurium lattices, as was worked out in von Hippel's paper.[1]

Von Hippel chooses for the metallic lattice the simple cubic lattice found in β-polonium. For the covalent type a lattice is assumed which is very similar to the trigonal selenium lattice.

I should like to make a few remarks concerning this latter choice, which may be considered as a further argument in favor of von Hippel's theory. It is possible to construct a lattice, built up from long chains of atoms, which has a larger lattice energy than the spiral chain lattice. If the valence angles, the covalent, and the van der Waals radii are the same in both lattices, the contributions of the van der Waals-London forces will essentially determine the energy difference.

The hypothetical lattice mentioned is the polyethylene type of lattice[5] and is built up from zigzag chains instead of spiral chains. In Fig. 1 the hypothetical lattice and the lattice actually found are drawn, using the covalent and van der Waals radii known from the trigonal form of selenium, 1.16 and 1.74A, respectively, for both lattices. From this figure the number of nearest neighbors belonging to different chains may be seen. For the zigzag chains lattice this number is 8, instead of 4 in the spiral chain

lattice, and this number determines the most important term in the contribution to the van der Waals-London energy. For a given value of the valence angles, covalent, and van der Waals radii, the zigzag chain lattice is thus the more stable of the two. To explain why, nevertheless, the spiral chain lattice is found actually, one has to assume that the abnormal radius of 1.74A could not exist in the zigzag chain lattice. The decrease of the "van der Waals" radius from 2.0A to 1.74A would thus be caused by the metallic forces and the existence of these forces in the trigonal form of selenium would make the spiral chain lattice the more stable of the two. From this point of view the peculiar structure of trigonal selenium and tellurium as well as the abnormal value of the van der Waals radius are indications that a simple picture for the lattice forces is not sufficient to describe the situation in these lattices, and a contribution of forces of the metallic type must be taken into account.

[1] A. von Hippel, J. Chem. Phys. **16**, 372 (1948).
[2] F. de Boer, Rec. Trav. Chim. **62**, 151 (1943).
[3] Linus Carl Pauling, *The Nature of the Chemical Bond* (Cornell University Press, Ithaca, 1940), p. 176.
[4] W. Beamer and C. R. Maxwell, J. Chem. Phys. **14**, 569 (1946).
[5] Maurice L. Huggins, J. Chem. Phys. **23**, 37 (1945).

The Calculation of Interaction Potentials from Collision Cross-Section Measurements

M. C. KELLS
Department of Chemistry, Massachusetts Institute of Technology, Cambridge, Massachusetts
October 8, 1948

A METHOD for calculating interaction potentials from collision cross-section measurements has been presented by J. H. Simons, C. M. Fontana, E. E. Muschlitz, Jr., and S. R. Jackson,[1] and J. H. Simons, E. E. Muschlitz, Jr., and L. G. Unger.[2] Their method consists essentially of using classical theory and of integrating the collision cross section along the scattering path. They have developed the theory for an interaction potential of the form $V(r)=-K/r^n$, where r is the distance of separation of the centers of mass of the interacting particles. In the present article their method for calculating a correct value of K is shown to be unnecessary; a consistent approximate treatment presented here is entirely satisfactory for the determination of K.

The symbols which will be used are defined as follows:

l = length of the scattering path,
a = radius of the receiver,
b = perpendicular distance from the scattering molecule to the original line of approach of the beam particle,
x = a variable representing distance measured along the scattering path,
r_0 = distance of closest approach of the interacting particles,
m_1 = mass of the beam particle,
m_2 = mass of the scattering particle,
W = kinetic energy of the beam particle,
$\mu=m_1m_2/(m_1+m_2)$,
ϕ = scattering angle in apparatus coordinates,
K_e = potential constant K obtained from an exact treatment,
K_a = potential constant K obtained from the above authors' approximate treatment,
K_a' = potential constant K obtained by consistent use of small angle assumptions,
$C=\pi^{\frac{1}{2}}\Gamma(\frac{1}{2}n+\frac{1}{2})/\Gamma(\frac{1}{2}n)$,
$f_c=K_e/K_a$ = the factor by which K_a (determined graphically from the experimental measurements by using the method of the above authors) is multiplied to obtain the correct value of $K=K_e$,
$f_c'=K_e/K_a'$ = the correction factor for obtaining K_e from K_a' which may be determined graphically in the same manner as K_a.

TABLE I. The correction factors f_c' and f_c.

m_1/m_2	½					1				
l/a	5	10	13.89	21.11	63.53	5	10	13.89	28.12	84.71
f_c'	1.000	0.988	0.988	0.994	0.997	1.039	1.003	0.997	0.995	0.997
f_c	0.524	0.697	0.764	0.836	0.939	0.456	0.637	0.712	0.837	0.940

The values of $f_c=K_e/K_a$ reported by the above authors are valid only for a value of l/a of 13.89 which corresponds to the geometry of their particular apparatus.[3] The factor f_c is obtained from the appropriate integrals in the manner shown below.

The classical treatment of the scattering problem for two point masses, involving conservation of angular momentum and total energy, yields the following general relation:

$$\int_0^l b^2dx=\int_0^l r_0^2dx+(K/W)(m_1/\mu)\int_0^l r_0^{2-n}dx. \quad (1)$$

The exact treatment for the case $n=4$ (the deviation of f_c from unity increases for a given m_1/m_2 and l/a as n increases, and $n=4$ is the largest n value investigated by the above authors) then gives, with $dx=-ad\cot\phi$ and Sn defined as $S_n=(K/W)(m_1/\mu r_0^n)$:

$$\int_0^l b^2dx=a(K_em_1/W\mu)^{\frac{1}{4}}\times\left[\int_0^{l/a}S_4^{-\frac{1}{4}}d\cot\phi+\int_0^{l/a}S_4^{+\frac{1}{4}}d\cot\phi\right]$$
$$=a(K_em_1/W\mu)^{\frac{1}{4}}(A+B). \quad (2)$$

The integrals A and B are evaluated graphically.

The above authors' approximate treatment overlooks the r_0^{2-n} integral of Eq. (1) and assumes all collisions to result in small angle scattering. This gives for the case $n=4$

$$\int_0^l b^2dx=\int_0^l r_0^2dx=l^{\frac{3}{4}}(\pi K_a/3aW)^{\frac{1}{4}}. \quad (3)$$

Then by equating the values of the integral, $\int_0^l b^2dx$, from Eqs. (2) and (3), the above authors' factor f_c is obtained in the form

$$f_c=K_e/K_a=[\pi/3][(l/a)^3][\mu/m_1][(A+B)^{-2}]. \quad (4)$$

However, if the r_0^{2-n} integral is not omitted in an approximate treatment, a completely satisfactory value of K, determined graphically from the experimental data, may be obtained directly. The approximate treatment carried con-

sistently through with small angle assumptions gives

$$\int_0^l b^2dx=[n/(n+2)]l^{1+2/n}(K_a'C/aW)^{2/n}+[anm_1/2\mu]C^{(2/n)-1}(K_a'l/Wa)^{2/n}. \quad (5)$$

For $n=4$ the factor f_c' is then obtained in the form

$$f_c'=K_c/K_a'=\{[\pi/3][(l/a)^3][\mu/m_1]+[8/3][(l/a)^2]+[16/3\pi][m_1/\mu][(l/a)]\}(A+B)^{-2}. \quad (6)$$

The dependence of f_c' and f_c on l/a was investigated for the cases $m_1/m_2=\frac{1}{2}$ and $m_1/m_2=1$. In Table I the results are shown.

It is of interest to note that f_c' is within about one percent of unity for l/a greater than about 10. In general, as l/a increases above the values shown, the deviation of f_c' and f_c from unity will decrease.

For the case $n=2$ the above authors' values are used for $f(f\cong f_c)$ and f_c' is calculated from the relation

$$f_c'\cong f+(1/D)(\mu/m_1)(l/a), \quad (7)$$

where D corresponds to $A+B$ with one small angle approximation. The D values are obtained from the factor f since

$$f=[\pi/4D][(\mu/m_1)(l/a)]^2. \quad (8)$$

For $m_1/m_2=\frac{1}{2}$, $l/a=13.89$, $f=0.882$, $f_c'=1.003$, for $m_1/m_2=1$, $l/a=13.89$, $f=0.843$, $f_c'=0.998$, and for $m_1/m_2=\frac{3}{2}$, $l/a=13.89$, $f=0.806$, $f_c'=0.991$. In a similar manner for $n=4$, $m_1/m_2=\frac{3}{2}$, $l/a=13.89$, $f_c=0.658$, $f_c'=0.994$.

For values of l/a greater than about 10 then the small angle assumption treatment will give values of K accurate to within present experimental error for $m_1/m_2\leq\frac{3}{2}$ and $n\leq 4$. For sufficiently large values of l/a, accurate values of K may undoubtedly be attained by the small angle treatment for values of $m_1/m_2>\frac{3}{2}$ and $n>4$.

[1] Simons, Fontana, Muschlitz, Jr., and Jackson, J. Chem. Phys. 11, 307 (1943).
[2] Simons, Muschlitz, Jr., and Unger, J. Chem. Phys. 11, 322 (1943).
[3] Simons, Francis, Fontana, and Jackson, Rev. Sci. Inst. 13, 419 (1942).

The Role of the Carbides of Iron in the Fischer-Tropsch Synthesis

S. C. SCHUMAN
Hydrocarbon Research, Inc., Trenton, New Jersey
October 14, 1948

RECENTLY Kummer, Browning, and Emmett[1] have indicated from thermodynamic considerations that "the direct reduction by hydrogen of either form of Fe_2C cannot account for the synthesis of normal 1-monoolefins or of higher paraffins from carbon monoxide and hydrogen over the temperature and pressure range commonly employed in the Fischer-Tropsch synthesis." However, it should not be implied that this conclusion represents conclusive or even substantial evidence that thermodynamic data preclude the carbide being intermediate in the synthesis. For example, we have calculated the equilibrium constants for the reactions

TABLE I. Equilibrium constants for formation of hydrocarbons from Fe_2C, CO, and H_2.

Reaction	n	Temp. °K	$K_{atmos.}$
(1)	2	500	1.00
(1)	8	500	3×10^{23}
(1)	2	600	9.1×10^{-3}
(1)	8	600	6.6×10^{4}
(2)	2	500	8.3×10^{7}
(2)	8	500	6×10^{29}
(2)	2	600	2.6×10^{3}
(2)	8	600	6.2×10^{8}

$$Fe_2C+(2n-1)H_2+(n-1)CO=C_nH_{2n}+Fe+(n-1)H_2O, \quad (1)$$

and

$$Fe_2C+2nH_2+(n-1)CO=C_nH_{2n+2}+Fe+(n-1)H_2O, \quad (2)$$

by which hydrocarbons are produced with each hydrocarbon molecule containing one carbon atom derived from an Fe_2C intermediate, using the free energy data for Fe_2C given by Kummer, Browning, and Emmett, and the data for CO, H_2O, and hydrocarbons of Rossini.[2] Table I gives the equilibrium constants for both reactions at 227°C and 327°C for $n=2$ and $n=8$. These data indicate that the formation of hydrocarbons from Fe_2C is thermodynamically possible under the conditions employed in the Fischer-Tropsch synthesis. While no claim is being made here that reactions (1) and (2) represent the chemical process responsible for the formation of Fischer-Tropsch hydrocarbons, they are at least as compatible with the experimental synthesis data as the reactions considered by Kummer, Browning, and Emmett.

[1] Kummer, Browning, and Emmett, J. Chem. Phys. 16, 739 (1948).
[2] Rossini *et al.*, J. Research Nat. Bur. of Stand. 34, 143, 403 (1945); 36, 559 (1946).

A New Method of Determining X-Ray Intensities*

N. C. BAENZIGER
Institute for Atomic Research, Iowa State College, Ames, Iowa
October 12, 1948

A NEW solution to the problem of determining integrated intensities of x-ray reflections recorded on film has been found which involves the radioactive toning of the photographic film. Because of the presently available radioactive isotopes suitable for this purpose, the best reagents are the mercuric chloride intensifier and the cobalt ferrocyanide toner. Only the latter has been examined.

The cobalt isotope, Co^{60} (half-life = 5.3 years, 1.1- and 1.3-Mev γ, and 0.31-Mev β), may be obtained in specific activities up to 100 millicuries per gram.

The toning process takes place in a bleaching,

$$4\,Ag+[Fe(CN)_6]^{=}\rightarrow Ag_4Fe(CN)_6,$$

and a toning step.

$$Ag_4Fe(CN)_6+CoX_2\rightarrow 4\,AgX+Co_2Fe(CN)_6.$$

A bleach solution which has been found to be suitable is a 5 percent $K_3Fe(CN)_6$ solution with approximately ten

TABLE I. Counting rate *vs.* exposure relationship.*

Exposure	Optical density	Counting rate ($c/m \div 64$)	Linear response
	Experiment 1 <space		
Background	0.10	10.00	
1		3.37	2.76
2		5.56	5.52
4		11.37	11.04
8		21.91	22.08
16		42.84	44.16
32	1.88	78.55	88.32
64	>3.0	132.44	176.6
128	>3.0	191.28	
	Experiment 2 <		
Background	0.10	9.76	
1		6.10	6.72
2		13.36	13.44
4		26.99	26.88
8	1.4	53.58	53.76
16	2.38	96.34	107.5

* Each measurement is an average of two counts >10,000 counts Counting rates have been corrected for background and dead time Punch size =0.018 cm²; spot area =0.008 cm².

drops of concentrated NH_4OH added. The radioactive toning solution was prepared by dissolving the metallic pellets of cobalt, from the Oak Ridge National Laboratory, in nitric acid and converting to the bromide by evaporating to near dryness repeatedly with HBr. The final 100-ml solution of cobalt bromide contained 0.04 gram of cobalt and approximately 1.2 millicurie of activity.

The toning process was carried out as follows: the x-ray negative was soaked in water for 30 minutes, placed in the bleaching solution for a minimum of 30 minutes, rinsed in running water for one hour, placed in the cobalt toner for a minimum of 30 minutes, and the occluded activity on the film diluted by placing the films first in 100 ml of water for one hour, followed by another dilution in two liters of water for another hour; finally, the film was rinsed one hour in running water and dried. The toning experiments were carried out at 25° and in ordinary light, except that the bleached film was handled in subdued light before toning.

The samples were counted using a thin-window (3 mg/cm²) Victoreen Geiger-Müller counting tube and standard scaling circuit. Because of the gamma-rays, the spots were removed from the film with a punch. The punchings were mounted below the counting tube window on a lead disk. The error due to geometry was much less than the statistical counting error in all measurements.

A linear relation between optical density and exposure up to an optical density of two, reported for double-coated, non-screen x-ray film by Bell,[1] has been confirmed for Eastman non-screen film by counting the activity of eight standard spots which were printed on the film, using an eight-step sector (Table I). The deviation at the low optical density is due to the error resulting from the subtraction of a high background counting rate caused by silver deposited as chemical fog.

In order to test the method, Weissenberg diagrams of anthracene crystals were prepared, and the intensities of the (00l) reflections were determined by the procedure outlined above. The results of these measurements are compared with those of Robertson[2] and Banerjee[3] in Table II.

TABLE II. Measurement of anthracene (00l) intensities.*

Indices	Ionization (2)	Photometer (2)	Banerjee (3)	Observed
002	192	194	192	192
003	52	59	45	45
004	81	72	75	81
005	32	31	10	31

* One measurement of >13000 counts for each punching. Punching size =0.018 cm²; spot size =0.001 cm², counting time per punching 10–15 minutes.

The counting time and errors caused by the background can be reduced by using cobalt with higher specific activity (100 instead of 30 mc/g) and by reducing the ratio of background to spot counting rates. The latter can be accomplished using smaller punches, larger crystals, larger camera radius, or oscillating the film holder slightly during exposure.

* Work performed under Contract No. W-7405 eng-82.

[1] G. E. Bell, Brit. J. Radiol. **9**, 578 (1936).
[2] J. M. Robertson, Proc. Roy. Soc. **A140**, 79 (1933).
[3] K. Banerjee, Ind. J. Phys. **4**, 557 (1930).

Errata: On the Order-Disorder Transition in Solids. Parts I and II

[J. Chem. Phys. **16**, 519 (1948)]

YOSIO MUTŌ
Maebashi Medical College, Maebashi, Japan

Pages	Line	Error	Correction
521 1	18	(15) and (14)	(15) into (14)
	25	$/\partial \ln G$	$/\partial \ln T$
	27	$G_{TT}' = -zw/2kT$	$G_{TT}' + G_T'' \rho_T = -zw/2kT$
521 r	26	$\lim\theta \rightarrow \rho \rightarrow 0$	$\lim\theta \rightarrow \rho - 0$
522, 523		Z	z
525 1	28	in the gas phase	is the gas phase.

Physics Lib.

THE JOURNAL OF CHEMICAL PHYSICS

VOLUME 16 NUMBER 12

DECEMBER, 1948

Published by the

AMERICAN INSTITUTE OF PHYSICS

Incorporated

LANCASTER, PA., AND NEW YORK, N. Y.

THE JOURNAL OF CHEMICAL PHYSICS

BOARD OF EDITORS

JOSEPH E. MAYER, *Editor*

Associate Editors

Term ending December 31, 1948	*Term ending December 31, 1949*	*Term ending December 31, 1950*
CHARLES D. CORYELL	K. J. MCCALLUM	J. G. ASTON
F. O. RICE	A. L. PATTERSON	TERRELL L. HILL
L. H. THOMAS	HERTHA SPONER	GILBERT W. KING
G. W. WHELAND	GEORGE UHLENBECK	F. LONDON
E. BRIGHT WILSON, JR.	BRUNO H. ZIMM	GLENN T. SEABORG
		NATHAN SUGARMAN

THE JOURNAL OF CHEMICAL PHYSICS is published monthly by the American Institute of Physics. Its purpose is to bridge a gap between journals of physics and journals of chemistry. The artificial boundary between physics and chemistry has now been in actual fact completely eliminated, and a large and active group is engaged in research which is as much the one as the other. It is to this group that the Journal is rendering its principal service and makes its greatest appeal, both as a prompt and efficient medium for publication of research and as a convenient and carefully edited assemblage of pertinent information.

Suggestions for Contributors

Send manuscripts to Joseph E. Mayer, Kent Chemical Laboratory, University of Chicago, Chicago 37, Illinois. Textual material (abstract, body of the paper, tabular material, references, and figure captions) must be in English, typewritten (except mathematical expressions) double spaced with wide margins on a durable, white paper, preferably letter size. The original copy, not the carbon, should be submitted. For general style, spellings, abbreviations, and form, consult recent issues of this journal.

An abstract must accompany each article. It should be adequate as an index and as a summary.

All but the simplest mathematical expressions should be carefully printed in by hand. Be sure to distinguish between capital and small letters. Indicate clearly superscripts and subscripts by inverted carets and carets, respectively. Avoid complicated superscripts and subscripts. Avoid repetition of a complicated expression by representing it by a symbol. Identify in the margin Greek letters and unusual symbols. Use fractional exponents instead of root signs. Use the solidus (/) for fractions wherever its use will save vertical space.

References should appear as footnotes, numbered consecutively.

Tables may be typewritten on sheets separate from the running text. Each table must have a caption which will make the data in the table intelligible without reference to the text. Avoid complicated column headings.

Wherever possible figures should be planned for the width of a column (3 in.). A convenient reduction ratio is about 2:1 or 3:1. Lettering should be large enough on the original that when reduced it shall not be less than about 1/16 in. (~1.5 mm). Line drawings must be in *india ink* on white paper or tracing cloth. Coordinate paper is not desirable but if used must be blue lined and the coordinate lines which are to show must be inked over. Photographs should have maximum black and white contrast. Identify each original drawing or photograph on the back with the author's name and the figure number. Figures should be numbered consecutively. Captions should be typed on a separate sheet of paper.

A limited number of alterations in proof are unavoidable, but the cost of making extensive alterations after the article has been set in type will be charged to the author.

Proof and all correspondence concerning papers in the process of publication should be addressed to the Publication Manager, American Institute of Physics, 57 East 55 Street, New York 22, New York.

Subscription Price

	U. S. AND CANADA	ELSEWHERE
To members and associate members of the American Institute of Physics	$10.00	$11.00
To all others	12.00	13.00

Back Number Prices

Complete set: Vol. 1, 1933—Vol. 15, 1947 (with exception of January and August 1933 issues, out of print) $150.00

Yearly rate: $13.00.

Single copies: $1.25 each.

Subscriptions and orders for single copies should be addressed to Prince and Lemon Streets, Lancaster, Pennsylvania, or to the American Institute of Physics, 57 East 55 Street, New York 22, New York.

Changes of address should be sent to the Business Manager, American Institute of Physics.

The Journal of Chemical Physics is published monthly at Prince and Lemon Streets, Lancaster, Pennsylvania.

Entered as second-class matter December 30, 1933, at the Post Office at Lancaster, Pa., under the Act of August 24, 1912. Acceptance for mailing at special rate of postage, provided for in the Act of February 28, 1925, embodied in paragraph 4, Section 538, P. L. & R.: authorized February 3, 1933.

THE AMERICAN INSTITUTE OF PHYSICS

INCORPORATED

57 East 55 Street New York 22, N.Y.

MEMBER SOCIETIES:

American Physical Society
KARL K. DARROW, *Secretary*, Columbia University, New York 27, New York.

Optical Society of America
ARTHUR C. HARDY, *Secretary*, Massachusetts Institute of Technology, Cambridge 39, Massachusetts.

Acoustical Society of America
WALLACE WATERFALL, *Secretary*, 57 East 55th Street, New York 22, New York.

Society of Rheology
EARL K. FISCHER, *Secretary*, Institute of Textile Technology, Charlottesville, Virginia.

American Association of Physics Teachers
C. J. OVERBECK, *Secretary*, Northwestern University, Evanston, Illinois.

AFFILIATED SOCIETIES:

American Society for X-Ray and Electron Diffraction

Electron Microscope Society of America

Physical Society of Pittsburgh

Physics Club of Chicago

Physics Club of Philadelphia

Cleveland Physics Society

Physics Club of the Lehigh Valley

ASSOCIATES:

Over seventy-five leading industrial enterprises and other institutions which contribute to the support of the Institute.

JOURNALS:

The Physical Review
JOHN T. TATE, *Editor*, University of Minnesota, Minneapolis, Minnesota.

Reviews of Modern Physics
J. W. BUCHTA, *Editor*, University of Minnesota, Minneapolis, Minnesota.

Journal of the Optical Society of America
GEORGE R. HARRISON, *Editor*, Massachusetts Institute of Technology, Cambridge, Massachusetts.

The Journal of the Acoustical Society of America
FLOYD A. FIRESTONE, *Editor*, 3318 Fessenden Street, N.W., Washington, D. C.

American Journal of Physics
THOMAS H. OSGOOD, *Editor*, Michigan State College, East Lansing, Michigan.

The Review of Scientific Instruments
GAYLORD P. HARNWELL, *Editor*, Randal Morgan Laboratory of Physics, University of Pennsylvania, Philadelphia, Pennsylvania.

The Journal of Chemical Physics
JOSEPH E. MAYER, *Editor*, Kent Chemical Laboratory, University of Chicago, Chicago 37, Illinois.

Journal of Applied Physics
ELMER HUTCHISSON, *Editor*, Case Institute of Technology, Cleveland 6, Ohio.

Physics Today
DAVID A. KATCHER, *Editor*, American Institute of Physics, 57 East 55 Street, New York 22, New York.

OFFICERS

GEORGE R. HARRISON, *Chairman*
Massachusetts Institute of Technology

WALLACE WATERFALL, *Secretary*
The Celotex Corporation

GEORGE B. PEGRAM, *Treasurer*
Columbia University

JOHN T. TATE,
Adviser on Publications
University of Minnesota

GOVERNING BOARD

LUIS W. ALVAREZ
ROBERT B. BROOM
E. U. CONDON
A. J. DEMPSTER
W. F. FAIR, JR.
HARVEY FLETCHER
R. C. GIBBS
GEORGE R. HARRISON
W. V. HOUSTON
PAUL E. KLOPSTEG
F. W. LOOMIS
PHILIP M. MORSE
GEORGE B. PEGRAM
A. H. PFUND
JOHN T. TATE
WALLACE WATERFALL
M. W. WHITE
A. G. WORTHING

ADMINISTRATIVE STAFF

HENRY A. BARTON, *Director*
CLEVELAND NORCROSS,
Assistant Director
RUTH F. BRYANS,
Publication Manager
THEODORE VORBURGER,
Business Manager

THE American Institute of Physics was founded in 1931 as a federation of leading societies in the field of Physics. It combines into one operating agency those functions on behalf of physics which can best be done by the Societies jointly. Its purpose is the advancement and diffusion of physics and its applications to human welfare. To this end it publishes for itself or the Societies the nine journals listed on this page; promotes unity and effectiveness of effort among all who are interested in physics; renders numerous direct services to physicists and to the public; and cooperates with government agencies, national associations, educational institutions, technical industries, and others in such manner as to realize the opportunities and fulfill the responsibilities of physics as an important and constructive human activity.

CONTENTS

THE JOURNAL OF CHEMICAL PHYSICS VOL. 16, NO. 12 DECEMBER, 1948

Cation Arrangement in Spinels . . . E. J. W. VERWEY, F. DE BOER, AND J. H. VAN SANTEN 1091

Scattering of Light and the Radial Distribution Function of High Polymer Solutions . . . . . BRUNO H. ZIMM 1093

Apparatus and Methods for Measurement and Interpretation of the Angular Variation of Light Scattering; Preliminary Results on Polystyrene Solutions . . . . . BRUNO H. ZIMM 1099

Entropy, Enthalpy, and Free Energy of the Electrical Double Layer at an Ideal Polarized Electrode. Part I. Thermodynamic Theory . . . . . DAVID C. GRAHAME 1117

Electronic States of Organic Molecules . . . . . WILLIAM T. SIMPSON 1124

Does Ultraviolet Absorption Intensity Increase in Solution? . LOIS E. JACOBS AND JOHN R. PLATT 1137

Mercury Photosensitized Reactions of Isobutene . . . . G. A. ALLEN AND H. E. GUNNING 1146

Effect of Electric Fields on the Decomposition of Nitrous Oxide by Alpha-Rays . . . . . NELSON T. WILLIAMS AND HARRY ESSEX 1153

Infra-Red Christiansen Filter Effect in Slurries of Organic Crystals . . . . . W. C. PRICE AND K. S. TETLOW 1157

Letters to the Editor:

Raman Spectra of Certain Phosphoric Acids and Their Salts . . P. HOFFMAN AND T. J. HANWICK 1163
Effect of Temperature on the Absorption Spectrum of Ozone: Chappuis Bands . . . . . A. VASSY AND E. VASSY 1163
Nuclear Magnetism in Studies of Molecular Structure and Rotation in Solids: Ammonium Salts . . . . . H. S. GUTOWSKY AND G. E. PAKE 1164
Equation of State for Gases at High Pressures and Temperatures from the Hydrodynamic Theory of Detonation . . . . . MELVIN A. COOK 1165
Vapor Pressure and Melting Point of Graphite . . . . . LEO BREWER 1165
Notes on the Properties of Synthetic Rutile Single Crystals . . . . . S. ZERFOSS, R. G. STOKES, AND C. H. MOORE, JR. 1166
Viscosity-Composition-Temperature Relations in the System Na_2O-SiO_2 . . STEPHEN W. BARBER 1167
Hydrogen Fluoride Dipole Moment and the Structure of the Dimer . R. A. ORIANI AND C. P. SMYTH 1167
Ultimate Liquid Transmission Limit? . . . . . H. B. KLEVENS AND J. R. PLATT 1168
Average Boundaries of Statistical Chains . . . . . C. A. HOLLINGSWORTH 1169
On the Classification of Symmetry Coordinates . . . . . WILLIAM J. TAYLOR 1169
Note on the Energy of a Rotating Molecule . . . . . ROBERT KARPLUS 1170
Chemical Kinetics of Bromine Following Neutron Capture . . . . . WILLIAM H. HAMILL AND RUSSELL R. WILLIAMS, JR. 1171
Linear Atomic Chain and the Metallic State . . . . . T. A. HOFFMAN AND A. KÓNYA 1172
Structure and Conductivity in the VI$_B$ Group of the Periodic System . . . . . F. DE BOER 1173
Calculation of Interaction Potentials from Collision Cross-Section Measurements . . M. C. KELLS 1174
Role of the Carbides of Iron in the Fischer-Tropsch Synthesis . . . . . S. C. SCHUMAN 1175
New Method of Determining X-Ray Intensities . . . . . N. C. BAENZIGER 1175
Errata: On the Order-Disorder Transition in Solids. Parts I and II . . . . . YOSIO MUTŌ 1176

Author Index to Volume 16 1177

Analytic Subject Index to Volume 16 1184

Volume Table of Contents iii

LANCASTER PRESS, INC., LANCASTER, PA.